

AD-A155 304

AD

AD-E401 338

(2)  
EAD

TECHNICAL REPORT ARLCD-TR-85007

**FEASIBILITY OF A MICROPROCESSOR CONTROLLED RECOIL MECHANISM  
FOR LARGE CALIBER ARTILLERY WEAPONS**

**GEORGE Y. JUMPER, JR., LTC USAF  
ASSOCIATE PROFESSOR, DEPARTMENT OF ENGINEERING  
UNITED STATES MILITARY ACADEMY**

**STEPHEN G. FLOROFF  
ARDC**

**DTIC  
ELECTE  
JUN 3 1985  
S D  
B**

**MAY 1985**



**U.S. ARMY ARMAMENT RESEARCH AND DEVELOPMENT CENTER**

**LARGE CALIBER WEAPON SYSTEMS LABORATORY**

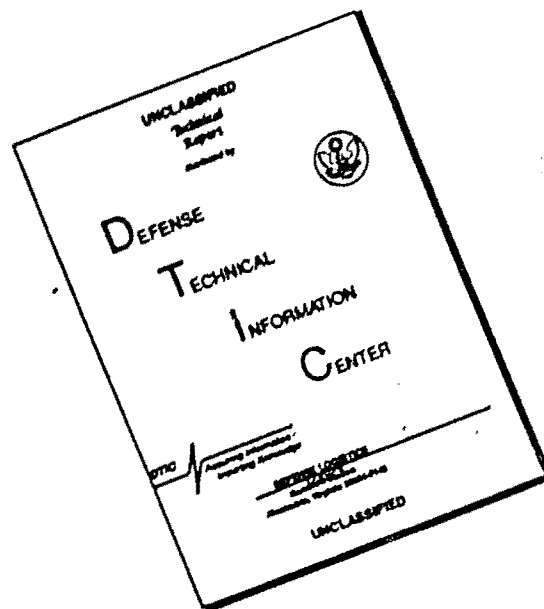
**DOVER, NEW JERSEY**

DTIC FILE COPY

**APPROVED FOR PUBLIC RELEASE; DISTRIBUTION UNLIMITED.**

**85 5 20 010**

# DISCLAIMER NOTICE



THIS DOCUMENT IS BEST QUALITY AVAILABLE. THE COPY FURNISHED TO DTIC CONTAINED A SIGNIFICANT NUMBER OF PAGES WHICH DO NOT REPRODUCE LEGIBLY.

The views, opinions, and/or findings contained in this report are those of the author(s) and should not be construed as an official Department of the Army position, policy, or decision, unless so designated by other documentation.

Destroy this report when no longer needed. Do not return to the originator.

UNCLASSIFIED

SECURITY CLASSIFICATION OF THIS PAGE (When Data Entered)

REPORT DOCUMENTATION PAGE		READ INSTRUCTIONS BEFORE COMPLETING FORM
1. REPORT NUMBER Technical Report ARLCD-TR-85007	2. GOVT ACCESSION NO. AD-A155304	3. RECIPIENT'S CATALOG NUMBER
4. TITLE (and Subtitle) FEASIBILITY OF A MICROPROCESSOR CONTROLLED RECOIL MECHANISM FOR LARGE CALIBER ARTILLERY WEAPONS		5. TYPE OF REPORT & PERIOD COVERED
7. AUTHOR(s) George Y. Jumper, Jr., LTC USAF Stephen G. Floroff, ARDC		6. PERFORMING ORG. REPORT NUMBER
9. PERFORMING ORGANIZATION NAME AND ADDRESS ARDC, LCWSL Weapons Division (SMCAR-LCW-E) Dover, NJ 07801-5001		8. CONTRACT OR GRANT NUMBER(s)
11. CONTROLLING OFFICE NAME AND ADDRESS ARDC, TSD STINFO Div (SMCAR-TSS) Dover, NJ 07801-5001		10. PROGRAM ELEMENT, PROJECT, TASK AREA & WORK UNIT NUMBERS
14. MONITORING AGENCY NAME & ADDRESS (if different from Controlling Office)		12. REPORT DATE May 1985
		13. NUMBER OF PAGES 79
		15. SECURITY CLASS. (of this report) Unclassified
		15a. DECLASSIFICATION/DOWNGRADING SCHEDULE
16. DISTRIBUTION STATEMENT (of this Report)  Approved for public release; distribution is unlimited.		
17. DISTRIBUTION STATEMENT (of the abstract entered in Block 20, if different from Report)		
18. SUPPLEMENTARY NOTES		
19. KEY WORDS (Continue on reverse side if necessary and identify by block number) Recoil mechanism                      Recoil brake Servovalve                                155-mm SP howitzer M109 Closed-loop control                    Large caliber artillery weapons Optimum energy absorption Rodpull		
20. ABSTRACT (Continue on reverse side if necessary and identify by block number)  Artillery recoil mechanisms provide energy absorption by throttling hydraulic oil through a variable orifice. This orifice is a function of the recoil stroke and is mechanically a "fixed" system. Variations in hydraulic oil characteristics, maximum applied impulse, and manufacturing tolerances in throttling orifice construction cause non-optimal energy absorption. This report proposes a closed-loop feedback controlled servovalve to optimize energy dissipation regardless of system variables. Possible control algorithms are presented. (cont)		

DD FORM 1 JAN 73 1473 EDITION OF 1 NOV 65 IS OBSOLETE

UNCLASSIFIED

SECURITY CLASSIFICATION OF THIS PAGE (When Data Entered)

UNCLASSIFIED

SECURITY CLASSIFICATION OF THIS PAGE(When Data Entered)

20. ABSTRACT (cont)

Recoil mechanism computer simulation using servovalve control prove the viability of this approach. Novel applications of electronic recoil control applied to artillery weapons are also discussed.

UNCLASSIFIED

SECURITY CLASSIFICATION OF THIS PAGE(When Data Entered)

**ACKNOWLEDGMENT**

Grateful acknowledgment is given to John Tobak for his assistance in using the SUPER\*SCEPTRE computer program, and to Nancy Mahoney and John VanderWeide for their assistance in generating necessary SUPER\*SCEPTRE computer runs, collating endless amounts of data, and drawing the numerous figures necessary to complete this report. Special thanks are also in order for Aichel Dupont of Rock Island Arsenal for providing powder gymnasticator input impulse profiles and constructive critique of the microprocessor controlled recoil mechanism concept.

**S** DTIC  
ELECTE **D**  
JUN 3 1985  
**B**

Accession For	
NTIS GRA&I	<input checked="" type="checkbox"/>
DTIC TAB	<input type="checkbox"/>
Unannounced	<input type="checkbox"/>
Justification	
By	
Distribution/	
Availability Codes	
Dist	Avail and/or Special
<b>A-1</b>	



## CONTENTS

	Page
Introduction	1
Identification of Forces Applied to an Artillery Recoil Mechanism	1
Description of Forces Applied to the Recoil Mechanism	3
Breech Force	3
Weight Component	4
Recoil Resistance or Rodpull	4
Sliding Friction Force	5
Recoil Mechanism Design Constraints	5
Rodpull Profile	5
Ideal Rodpull Profile	7
Rationale for Microprocessor Controlled Recoil	7
Microprocessor Control Concept	8
Computer Simulation of Recoil Mechanism M178	9
Adequacy of M178 Recoil Mechanism Simulation	12
Powder Gynasticator	16
Control Algorithms	23
Level 1 Control--Maintain a Preset Rodpull	23
Level 2 Control--Compute Rodpull During Recoil	26
Control Simulations	29
Level 1 Control--Smoothed Gynasticator Impulse	29
Level 2 Control--M203 Propelling Charge	30
Level 2 Control--Smoothed Gynasticator Impulse	36
Level 2 Control--Short Recoil Mode (Smoothed Gynasticator Impulse)	36
Future Applications of Microprocessor Recoil Control	40
Conclusions	42
References	43

Appendixes

A	Equivalent Orifice Area Computation	45
B	M178 Recoil Mechanism Model	55
C	St. Chamond Recoil Mechanism Model	61
D	Full Automatic Control Models	65
	SUPER*SCEPTRE Symbols	71
	Distribution List	73

## FIGURES

	Page
1 Forces acting on typical artillery recoil mechanism	2
2 Typical breech force profile	3
3 Typical breech force profile with muzzle brake	4
4 Typical recuperator force curves	5
5 Breech force/rodpull relationship	6
6 Ideal rodpull profile	7
7 Microprocessor recoil control schematic	9
8 Recoil mechanism network for SUPER*SCEPTRE model	10
9 Design input force--M203 charge	13
10 Final area schedule--long recoil	14
11 Final area schedule--short recoil	15
12 Rodpull profile--M178 model	17
13 Ideal and check run velocity profiles	18
14 Recoil motion--M178 model	19
15 Comparison of recoil brake pressure--SUPER*SCEPTRE simulation to live fire data	20
16 Powder gymnasticator schematic	21
17 Breech force profile based on recoil response--powder gymnasticator (M203 equivalent)	22
18 Recoil motion M178 model with gymnasticator input profile	24
19 Rodpull profile M178 model with gymnasticator input profile	25
20 Magnitude of forces in recoil process	28
21 Transition function for calculated rodpull	29
22 St. Chamond switching function	30
23 Recoil motion, St. Chamond--75,000 lb desired rodpull	31

24	Rodpull profile, St. Chamond--75,000 lb desired rodpull	32
25	Desired servovalve area, St. Chamond--75,000 lb desired rodpull	33
26	Actual servovalve area, St. Chamond--75,000 lb desired rodpull	34
27	Rodpull comparison--M203 impulse	35
28	Level 2--control variable relationships	37
29	Level 2--controlled and uncontrolled rodpull gymnasticator impulse	38
30	Level 2--rodpull profile, short stroke mode gymnasticator impulse	39
31	Forces acting on weapon structure	57

## INTRODUCTION

Large caliber artillery recoil mechanisms are comprised of three basic components: a recoil brake, a counter-recoil mechanism, and a counter-recoil buffer. The recoil brake provides a controlled resistance to weapon recoil by throttling hydraulic fluid through a variable orifice. The counter-recoil mechanism, or recuperator, returns the recoiling parts to the initial firing position by storing and releasing a portion of the recoil energy. The counter-recoil buffer reduces counter-recoil velocity of the moving parts to zero through a hydraulic fluid throttling process similar to the recoil brake.

Ideally, the recoil brake should throttle hydraulic oil so that a constant retarding force vs recoil distance curve is obtained. Since the area under this curve represents energy dissipation, a constant force is the lowest retarding force for a given recoil length. This is desirable and results in reduced weight of the weapon supporting structure. In addition, weapon stability is increased.

Traditionally, the design of a throttling orifice is based on the highest impulse the weapon will encounter. Maximum available recoil stroke is used to determine this orifice profile. Thus, maximum recoil stroke should theoretically occur at maximum impulse. In reality, this is not the case.

Variations in maximum impulse due to production tolerances in propellant manufacture, propellant temperature variations due to varying climatic conditions, manufacturing tolerances in the throttling orifice, and variable hydraulic fluid characteristics (i.e., viscosity) all tend to upset the ideal force-stroke relationship. In addition, recoil operation at less than maximum impulse will not utilize the full stroke available, since the orifice profile was not designed for these conditions. This results in a non-optimized force versus stroke profile. Thus, higher than necessary force peaks are applied to the weapon structure.

It is proposed that a microprocessor controlled servovalve be used to optimize energy dissipation in the recoil brake regardless of the system variables mentioned above. The servovalve is envisioned as a constantly variable orifice operated by a closed loop feedback control system. This report describes two control schemes which could be used for a servovalve system. Computer simulation of these schemes applied to a computer generated recoil mechanism model demonstrate the viability of this approach. Novel applications of microprocessor recoil control applied to artillery weapons are then offered for consideration.

## IDENTIFICATION OF FORCES APPLIED TO AN ARTILLERY RECOIL MECHANISM

For a simple, one-dimensional, recoil mechanism, the motion is governed by Newton's second law:

$$\Sigma F = M_r \ddot{X} \quad (1)$$

where

$\Sigma F$  = sum of all forces acting on the recoil mechanism in the direction of motion ( $lb_f$ )

$M_r$  = mass of recoiling parts (slugs)

$\ddot{X}$  = acceleration of recoiling parts ( $ft/sec^2$ )

Figure 1 illustrates a free body diagram of forces acting on a typical artillery recoil mechanism.

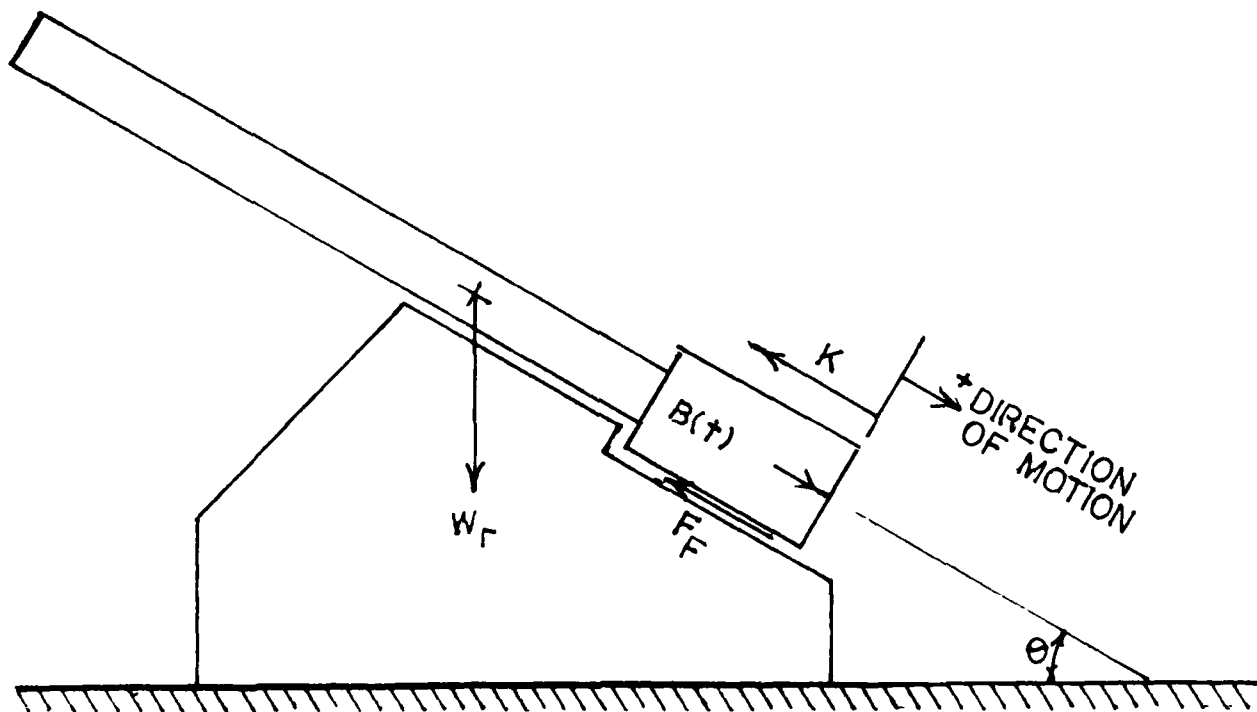


Figure 1. Forces acting on typical artillery recoil mechanism

where

$B(t)$  = propellant gas force as a function of time ( $lb_f$ )

$K$  = recoil system resistance to recoil ( $lb_f$ )

$F_f$  = mechanical friction due to recoil mechanism movement ( $lb_f$ )

$W_r$  = weight of recoiling parts ( $lb_f$ )

$\theta$  = angle of elevation of the weapon (degrees)

Arbitrarily assuming a positive direction as shown in figure 1, equation 1 can be rewritten as

$$M_R \ddot{X} = B(t) + W_R \sin \theta - K - F_F \quad (2)$$

Equation 2 forms the basis for a simple, single degree-of-freedom simulation of a typical artillery recoil mechanism. (The derivation is also presented in reference 1, page 17 and reference 2, page 68).

## DESCRIPTION OF FORCES APPLIED TO THE RECOIL MECHANISM

### Breech Force

Breech force,  $B(t)$ , is described as the input force imparted to the weapon as a result of propellant ignition. This is also known as breech force since propellant gas acts against the weapon breech. This force can exceed one million pounds in large artillery weapons.  $B(t)$  is not constant and is dependent on the burning rate of the propellant. A typical  $B(t)$  profile is illustrated in figure 2.

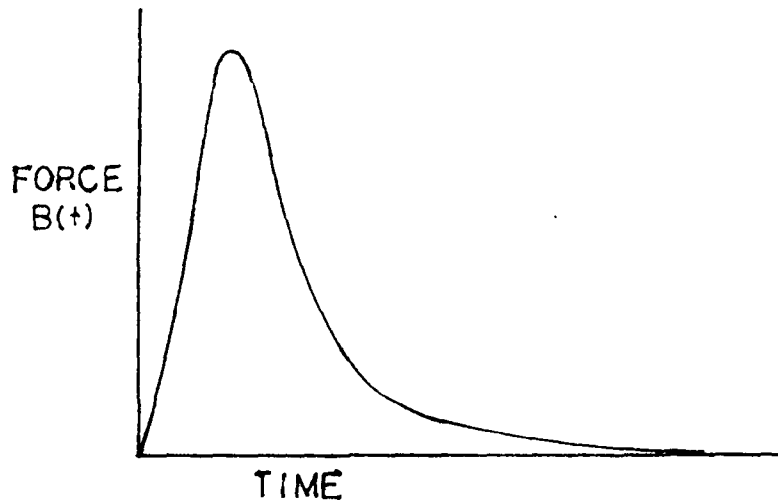


Figure 2. Typical breech force profile

In many instances artillery weapons employ a device known as a muzzle brake to reduce the energy imparted to the weapon structure. The device is placed at the end of the gun tube and re-directs exhaust gases rearward, generating an impulse opposite in direction to recoil momentum. This force is usually incorporated into the breech force function, in which case the  $B(t)$  curve is modified as shown in figure 3.

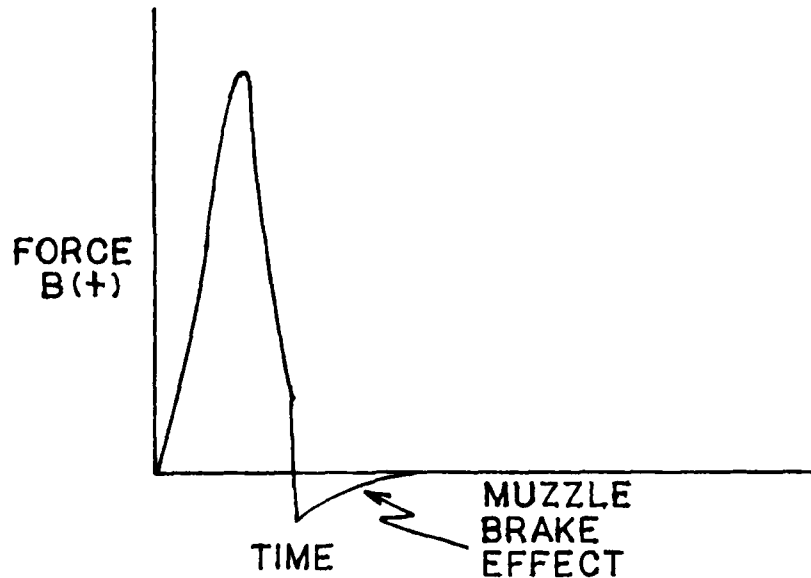


Figure 3. Typical breech force profile with muzzle brake

#### Weight Component

Also included in the equation of motion is the component of the weight of the recoiling parts in the direction of recoil ( $W_r \sin \theta$ )

#### Recoil System Resistance or Rodpull

Recoil system resistance or rodpull, ( $K$ ), is defined as all forces (except mechanical friction) acting in a direction opposite recoil motion. There are three basic constituents of recoil resistance:

1. Recoil Brake ( $F_B$ )--The recoil brake provides a resistive force by throttling hydraulic oil through a variable orifice. This variable orifice is a function of the recoil stroke.

2. Recuperator Force ( $F_R$ )--The recuperator is a counter-recoil mechanism which returns the recoiling parts to the initial firing position by storing, then releasing a portion of recoil energy. Weapon recoil provides energy input to the recuperator. As the recuperator stores energy, increasing resistive force is applied against recoil motion. A recuperator device is either spring or gas operated. Two characteristic curves of resistive force are possible as shown in figure 4.

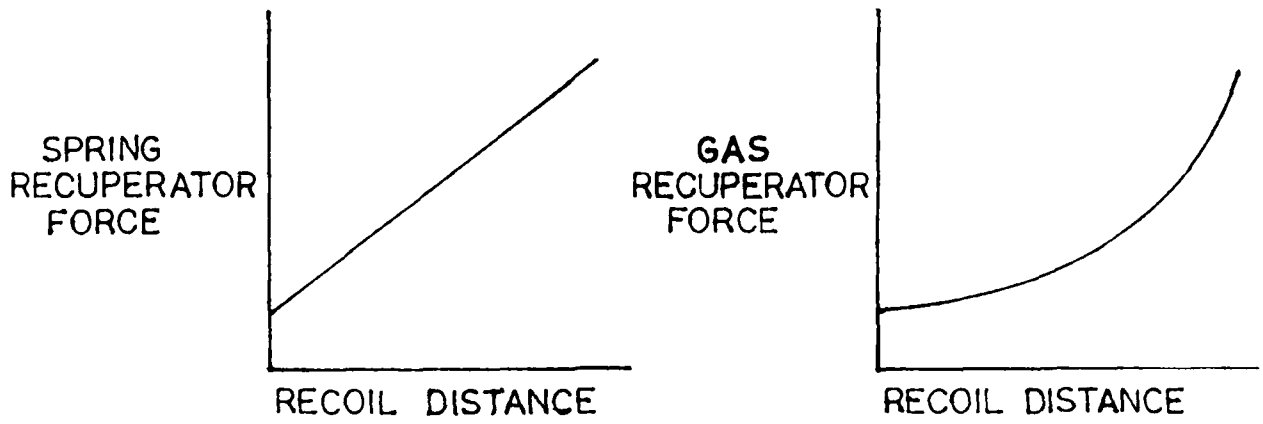


Figure 4. Typical recuperator force curves

An initial force is always present in the recuperator in order to "hold" the recoiling parts in the firing position.

3. Packing Friction ( $F_p$ )--Packing friction is the frictional force resulting from the hydraulic oil seals in the recoil brake and recuperator. It is often assumed to be a constant throughout the recoil stroke.

For many artillery weapons, recoil system resistance is transferred to the weapon supporting structure by a single rod. Hence, the term "rodpull" is traditionally used to define the resisting force offered by the recoil mechanism:

$$\text{Rodpull (K)} = F_B + F_R + F_p \tag{3}$$

**Sliding Friction Force**

Recoiling parts generate mechanical friction due to metal to metal contact. Sliding friction ( $F_f$ ) is a function of friction coefficients, recoil distance, and weapon elevation.

**RECOIL MECHANISM DESIGN CONSTRAINTS**

**Rodpull Profile**

The traditional purpose of a recoil mechanism is to reduce forces imposed on the weapon structure due to firing. Since rodpull is the primary resistance

offered to the imposed breech force, it is necessary to formulate an ideal rod-pull profile in order to design an effective recoil mechanism. Rewriting equation 2, considering only the two primary forces, breech force and recoil resistance, yields:

$$M_r \ddot{X} = B(t) - K \quad (4)$$

Integration of equation 4, with respect to time, leads to the familiar corollary to Newton's Law that the change in momentum of an object is equal to the sum of the impulses delivered to the object

$$M_r v_2 - M_r v_1 = t_1 \int^{t_2} B(t) dt - t_1 \int^{t_2} K dt \quad (5)$$

If  $t_1$  is the time immediately before firing, then  $t = 0$ ; if  $t_2$  is the instant recoil motion stops,  $T$ , then the recoiling mass has zero velocity before and after the recoil stroke and the equation reduces to

$$\int_0^T B(t) dt = \int_0^T K dt \quad (6)$$

Thus, rearward impulse delivered to the recoiling mass from the breech force must be balanced by the impulse from rodpull. Breech force is large in magnitude but short in duration (figs. 2 and 3). Rodpull force generated by the recoil mechanism is, by design, smaller in magnitude but longer in duration. In order to keep the magnitude of  $K$  as low as possible, the ideal shape would be a rectangle. This relationship formed by equation 6 can be graphically depicted in figure 5.

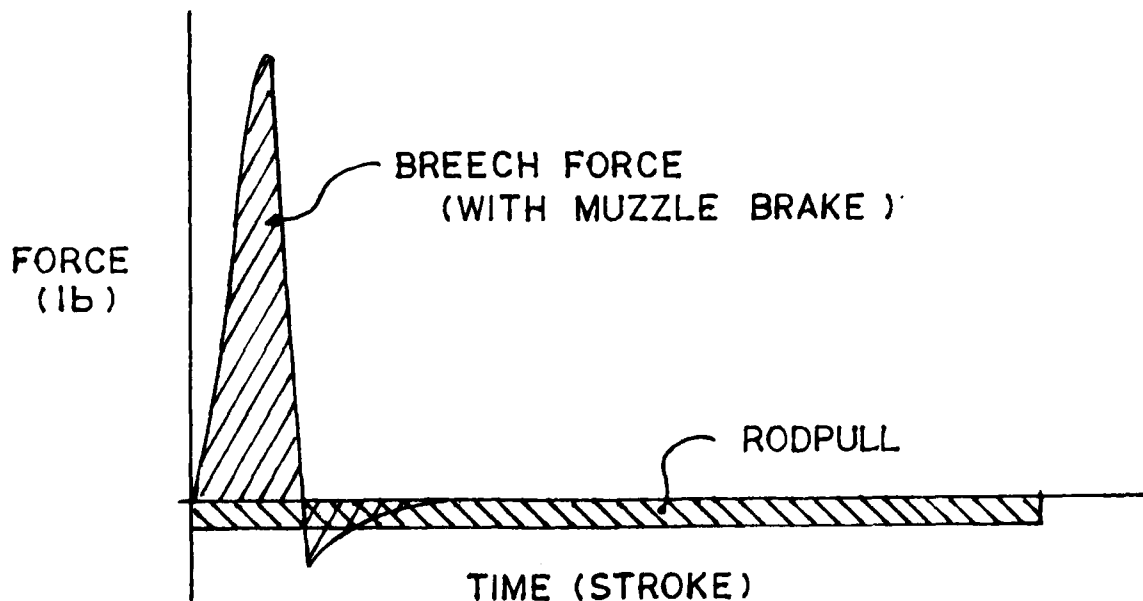


Figure 5. Breech force/rodpull relationship

It is apparent from figure 5 that required rodpull force can be minimized by arranging for the longest possible rodpull duration. This is equivalent to maximizing recoil stroke.

### Ideal Rodpull Profile

Rodpull was previously defined as consisting of three constituent forces: recoil brake, recuperator, and packing friction forces. Since both the recoil brake and the friction forces depend on system motion, only the recuperator force is present prior to and after recoil motion. Taking this fact into account, the rodpull curve graphically depicted in figure 6 is a more practical ideal than the rectangle.

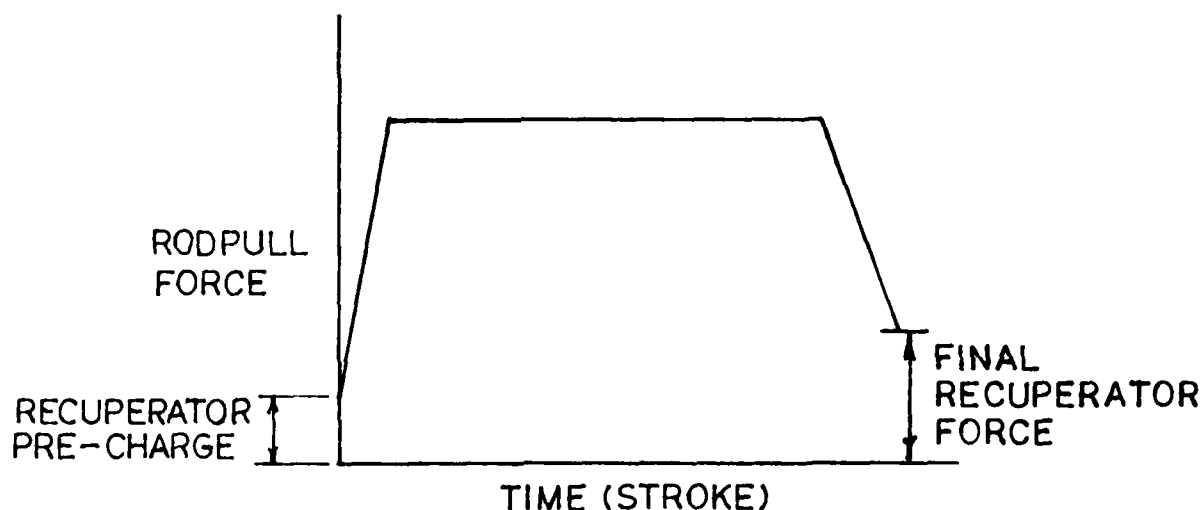


Figure 6. Ideal rodpull profile

Peak rodpull force can be reduced by permitting longer time and, consequently, a long recoil stroke to occur. However, there must be a practical limit to the allowable stroke available for energy dissipation. This limit is based on the configuration of each particular weapon. Large mobile artillery generally provides from 20 to 70 in. of recoil stroke. (By comparison, a tank might be limited to 12 inches.)

### RATIONALE FOR MICROPROCESSOR CONTROLLED RECOIL

The primary constituent of rodpull is the retarding force generated by the recoil brake. The force of the brake is generated by throttling hydraulic oil through a variable orifice. **It is this orifice over which the recoil mechanism designer has ultimate control.** Every attempt is made to design this variable

orifice so that the ideal rodpull curve (fig. 6) is achieved. Unfortunately, this ideal curve is rarely realized due to the following conditions:

1. Variations in hydraulic fluid characteristics. Specifically, temperature induced fluid viscosity changes affect the Reynolds number and, hence, orifice discharge coefficients. Consequently, nonideal rodpull curves result at extreme fluid temperatures.

2. Design impulse is inconsistent due to propellant temperature and manufacturing variations which change the  $B(t)$  curve.

3. Production tolerances used in machining the variable orifice cause nonideal rodpull profiles.

In essence, the recoil brake throttling orifice is an open loop control system designed around ideal parameters which rarely exist. A closed loop, feedback-controlled servovalve, placed parallel to the existing throttling orifice, could adjust for the above conditions and maintain the ideal rodpull profile.

In addition, since orifice area is a function of recoil stroke, it is mechanically a fixed system. Since only one area profile is available, it is designed to handle the highest impulse the weapon will encounter. Recoil operation at less than maximum impulse will cause a nonideal rodpull versus time curve, since the orifice profile was not optimized for this condition. At lower impulse inputs, the recoiling mass stops in a shorter distance than is available. Thus, higher than necessary loads are applied to the weapon. The recoil mechanism does have a finite life and every load is a step to the eventual wear out of the system. If the recoil mechanism can operate in a fashion which will utilize all available stroke, regardless of impulse, longer recoil mechanism life can be expected.

#### MICROPROCESSOR CONTROL CONCEPT

On the basis of the rationale described above, it is desirable to control rodpull with a continuously variable throttling orifice. This could be accomplished with a microprocessor-controlled servovalve plumbed parallel to the existing recoil brake. A schematic of this concept is shown in figure 7.

Assuming rodpull, distance, velocity, and acceleration are continuously available to a microprocessor, a closed loop recoil control scheme could be designed to optimize recoil rodpull regardless of the system variables.

In order to verify this approach to recoil control, a computer simulation of a typical artillery recoil mechanism, augmented with an electronically controlled bypass valve is presented.

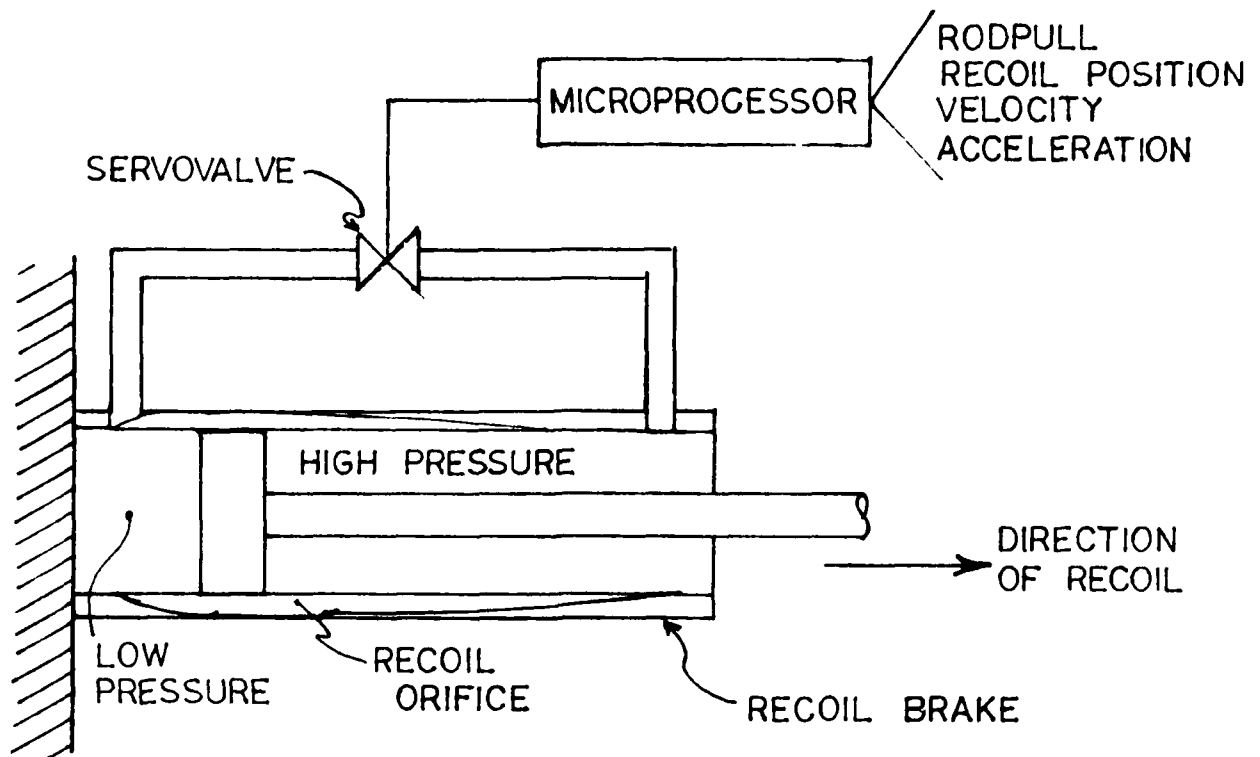


Figure 7. Microprocessor recoil control schematic

#### COMPUTER SIMULATION OF RECOIL MECHANISM M178

The recoil mechanism modeled in this feasibility study is designated M178 and is used on the 155-mm self-propelled howitzer M109. Many of these howitzers are in service, and the recoil system is typical for large artillery pieces. The M178 is designed to produce one of two lengths of recoil at maximum applied impulse. Long recoil (34 to 36 in.) is used at gun tube elevations from 0 to 45 degrees. Short recoil (24 to 26 in.) is used at gun tube elevations from 45 to 70 degrees. This is necessary to prevent the recoiling parts from hitting the vehicle floor at higher firing angles. Two distinct orifice area profiles are available which permit these two recoil strokes to occur. The mechanics of actuating these orifice profiles are discussed in reference 2 beginning on page 155. For the purposes of this report, an equivalent single orifice area is assumed. Furthermore, hydraulic fluid compressibility and unsteady flow are not addressed in this recoil simulation.

The M178 recoil mechanism was modeled on a system analysis program called SUPER\*SCEPTRE (ref 3). The original SCEPTRE program was developed by IBM and sponsored by the Air Force Weapons Laboratory at Kirtland Air Force Base. Originally, the program automatically solved complex nonlinear electrical circuit problems with very simple input data requirements. The Army Research and Development Center (ARDC) sponsored the upgrade of the program, which was carried out

at the University of South Florida, to include mechanical, digital, and control systems. SUPER\*SCEPTRE retains the simple input requirements but is suprisingly powerful. It can solve multidisciplinary problems with complex interactions, but only requires minimal setup times and usually minimal machine time. The implementation at ARDC provides rapid graphical and tabular output.

The first step in the modeling process is to take the recoil mechanism free body diagram (fig. 1) and represent it as a mechanical network (fig. 8). Only four forces are included as primary forces in the network, with rodpull representing the sum of the packing friction, recuperator, and brake forces.

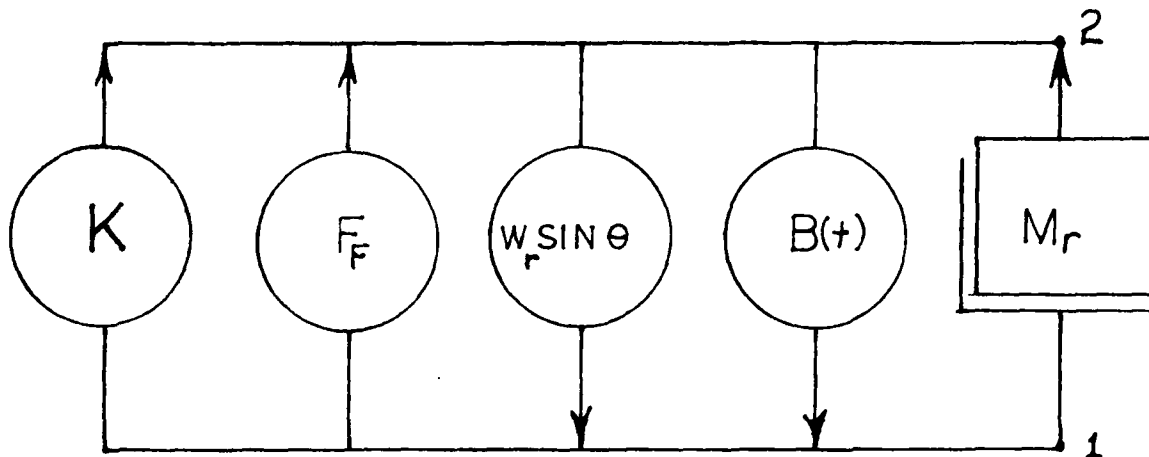


Figure 8. Recoil mechanism network for SUPER\*SCEPTRE model

Arrow direction is determined by visualizing an electrical analogy between force and current. Both  $B(t)$  and  $W_r \sin \theta$  tend to lift the recoiling mass off its inertial frame so they tend to facilitate current flow. Rodpull and  $F_f$  resist this motion, so they are shown impeding the current flow.

The second step is the preparation of the input data list to represent the mechanical network (fig. 8). The following data were used for this list:

- Rodpull (K)--In this case, K represents the sum of packing friction, recuperator force, and recoil brake force.

- Packing Friction--The packing friction used to design the M178 was computed to be 2340 lb (ref 2, page 193). This amount is assumed constant throughout the recoil stroke.

- Recuperator Force--The M178 recuperator uses nitrogen gas as an energy storage medium. This force is modeled as a polytropic compression process (ref 2, page 188):

$$F_R = A_R P_o \left[ \frac{V_o}{V_o - A_R X} \right]^n \quad (7)$$

where

$F_R$  = recuperator force ( $lb_f$ )

$A_R$  = recuperator cylinder cross section ( $in.^2$ ) - 9.724  $in.^2$  for the M178

$P_O$  = initial recuperator gas pressure (psi) - 650 psi for the M178

$V_O$  = initial recuperator gas volume ( $in.^3$ ) - 1,015  $in.^3$  for the M178

$X$  = recoil distance (in.) 36 in. - maximum for the M178

$n$  = polytropic exponent (assume 1.6)

• Brake Force--The primary resistance to recoil is generated by throttling hydraulic fluid through a continuously varying orifice. In reality, this orifice consists of various piston port areas, fluid connecting port areas, and leakage areas in addition to the main control orifices. For purposes of this system level model, the concept of an equivalent orifice area is used. This concept can be visualized as an equivalent single orifice with a discharge coefficient of 1, which provides the same retarding force as the combination of the various actual orifices in the M178 recoil mechanism. The equation for equivalent brake force (ref 2, page 99) is:

$$F_B = \frac{A_B^3 v^2 \omega}{2A_e^2 g} \quad (8)$$

where

$F_B$  = brake force ( $lb_f$ )

$A_B$  = equivalent recoil piston area ( $in.^2$ ) - 32.98  $in.^2$  for the M178

$v$  = recoil velocity (in./s)

$\omega$  = density of hydraulic fluid ( $lb/in.^3$ ) - assume 0.0313  $lb/in.^3$

$A_e$  = equivalent area orifice ( $in.^2$ )

$g$  = gravitational constant ( $in./s^2$ )

• Friction Force ( $F_F$ )--Friction force represents sliding friction of the gun tube on gun tube slides. In the case of the M178, the tube slides through two ring supports. Sliding friction was computed (ref 2, page 190) as:

$$F_F = \mu W_r \cos \theta (67.15 - X)/14.15 \quad (9)$$

where

$F_F$  = friction force ( $lb_f$ )

$\mu$  = coefficient of friction (assume 0.15)

$W_r$  = weight of recoiling parts ( $lb_f$ ) - 4,360  $lb_f$  for the M178

$\theta$  = weapon elevation (degrees)

$X$  = recoil distance (in.)

• Weight Component ( $W_r \sin \theta$ )--The total weight of the recoiling parts for the M178 was determined to be 4,360 lb (ref 2, page 181). Although the M178 can operate at elevation angles which vary from 0 to 75 degrees, the recoil brake control orifices were optimized for the worst case conditions of the weight component which occurs at 45 degrees for long recoil and 75 degrees for short recoil.

• Breech Force [ $B(t)$ ]-- The M203 impulse profile as a function of time (ref 2, page 209) is graphically depicted in figure 9. Negative breech force indicates a muzzle brake is in use.

The recoil simulation was used initially to generate an equivalent orifice area profile. This was accomplished by assigning various constant values of rodpull and observing the amount of force required to stop the recoiling mass within the required distance. By subtraction of recuperator and friction forces, the required brake force was determined. An inverted form of equation 9 was then used to generate an equivalent orifice area as a function of recoil position. The SUPER\*SCEPTRE input deck, necessary to compute an equivalent orifice area profile for both long and short recoil, is listed in appendix A. Appropriate outputs are also listed.

The orifice profile was modified to incorporate a leakage area in the M178 recoil mechanism estimated to be 0.5 in.<sup>2</sup> (ref 2, page 181). This revised orifice profile was put into subsequent recoil simulations in a tabular format. The final orifice profiles and tabulated orifice schedules for both long and short recoil strokes are shown in figures 10 and 11, respectively.

#### ADEQUACY OF M178 RECOIL MECHANISM SIMULATION

After determining the effective orifice area profile, a check run was made to observe results. Using the design breech force curve (M203 charge), assuming a 45 degree weapon elevation, and using the long stroke equivalent orifice area profile, a plot of rodpull and recoil distance was requested. (The appropriate SUPER\*SCEPTRE input deck is listed in appendix B.) The peak rodpull generated

DESIGN INPUT FORCE  
M 203 CHARGE  
FIG. 9

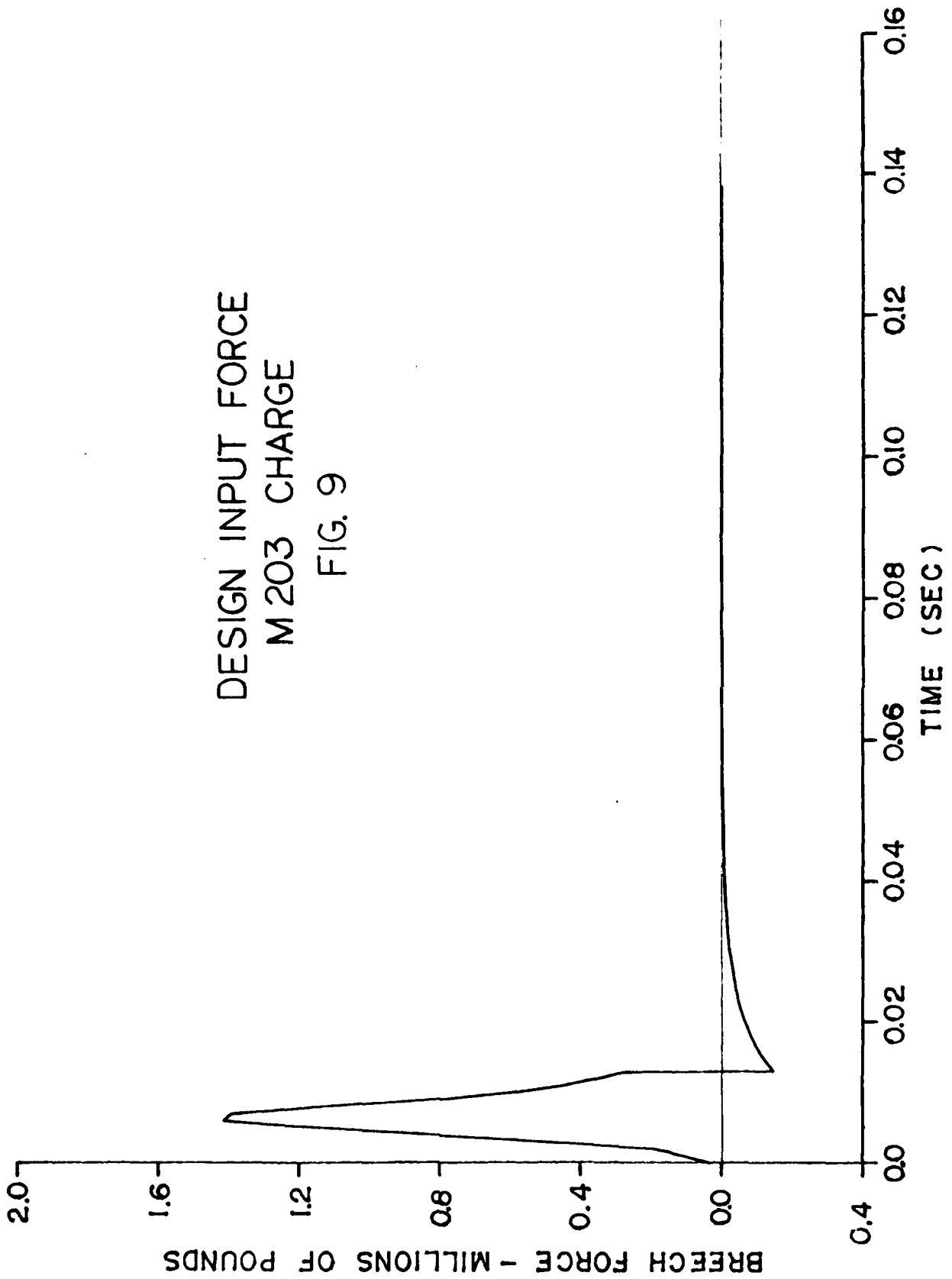


Figure 9. Design input force--M203 charge

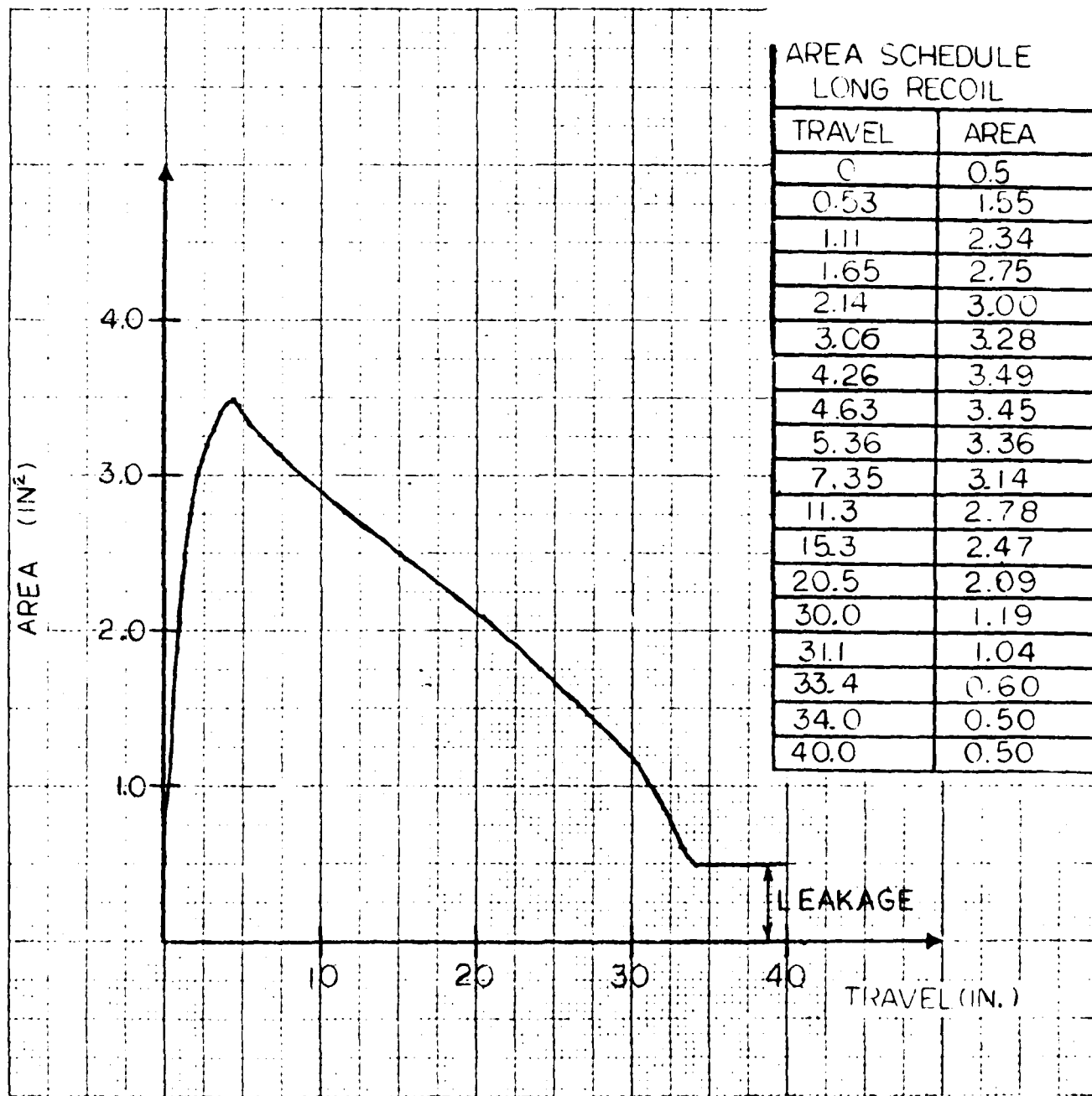


Figure 10. Final area schedule--long recoil

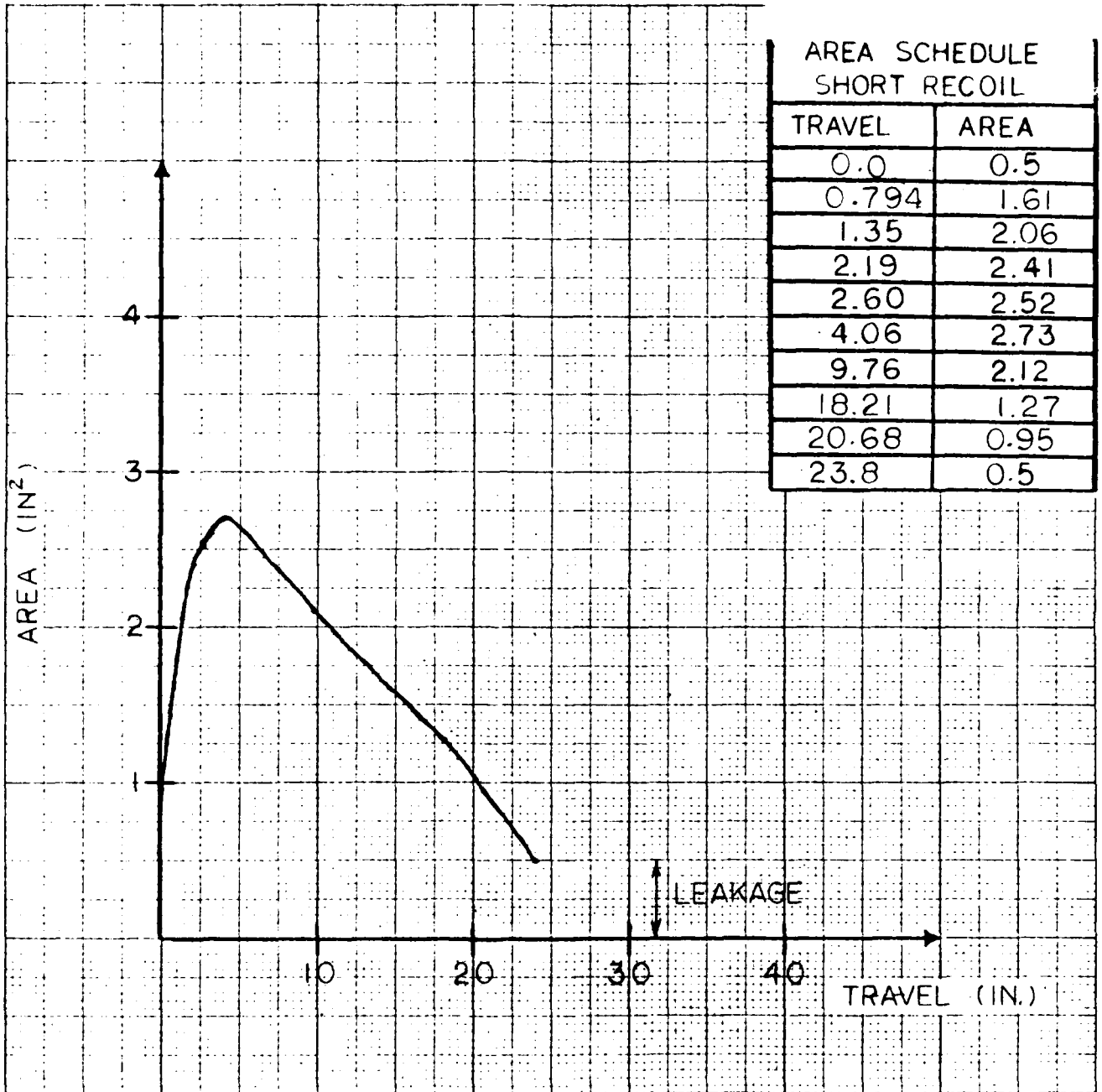


Figure 11. Final area schedule--short recoil

was slightly under 80,000 lb (fig. 12). Since the original rodpull which generated the orifice area profile was 70,000 lb (app A, input deck), a discrepancy is immediately evident. This is due to the leakage area present in the M178 mechanism.

The initial leakage area permits the recoiling mass to gain slightly more recoil velocity than was originally computed in the ideal simulation (fig. 13). This results in a recoil stroke which is within the 36-inch-stroke limit of the M178 (fig. 14). Since brake force is proportional to recoil velocity squared (eq 8), the brake force rises to a higher level. In reality, the rodpull of the production M178 is 15% higher than the design rodpull of 70,500 lb (ref 2, page 217). Therefore, the results of the model appear reasonable.

A difficulty in assessing the adequacy of the model is the scarcity of good live firing data to compare with the predicted values obtained with SUPER\*SCEPTRE. Live-fire testing of the M178 recoil mechanism was accomplished at Aberdeen Proving Ground (APG) intermittently during the period of 8 September 1977 to 22 March 1979 (ref 4). A comparison of the SUPER\*SCEPTRE check run oil pressure output with that of the top left M178 recoil cylinder is shown in figure 15. The live-fire curve exhibits some of the features of the SUPER\*SCEPTRE model. An obvious difference is that the live-fire curve has some large amplitude variations in the initial portion of the pressure profile. Discussions between the authors and cognizant APG personnel uncovered a possible explanation for these oscillations. Since they occur at about the time the muzzle brake activates, the accompanying overpressure in the area surrounding the weapon may have caused noise in the data acquisition equipment. These oscillations are even more pronounced in other firings. **While it has not been clearly established that these oscillations actually exist, electronic recoil control designers should be aware of the potential occurrence of oscillations near 300 Hz.**

It would be possible to adjust the area schedules to more nearly match either a desired ideal rodpull or the pressure traces of the live firing, but it would not be possible to match both. The model, as it stands, is a reasonably accurate representation of the M178 recoil mechanism. It appeared to be adequate to determine the potential of an automatic control system to improve the recoil process of the M178; therefore, it will be used "as is" for the remainder of this study.

#### POWDER GYMNASTICATOR

Any hardware modification to the M178 recoil mechanism would probably undergo initial testing on a device known as a powder gymnasticator. The powder gymnasticator is a mechanism which can exercise or gymnasticate recoil mechanisms without actually firing the weapon. A schematic of the powder gymnasticator is provided in figure 16.

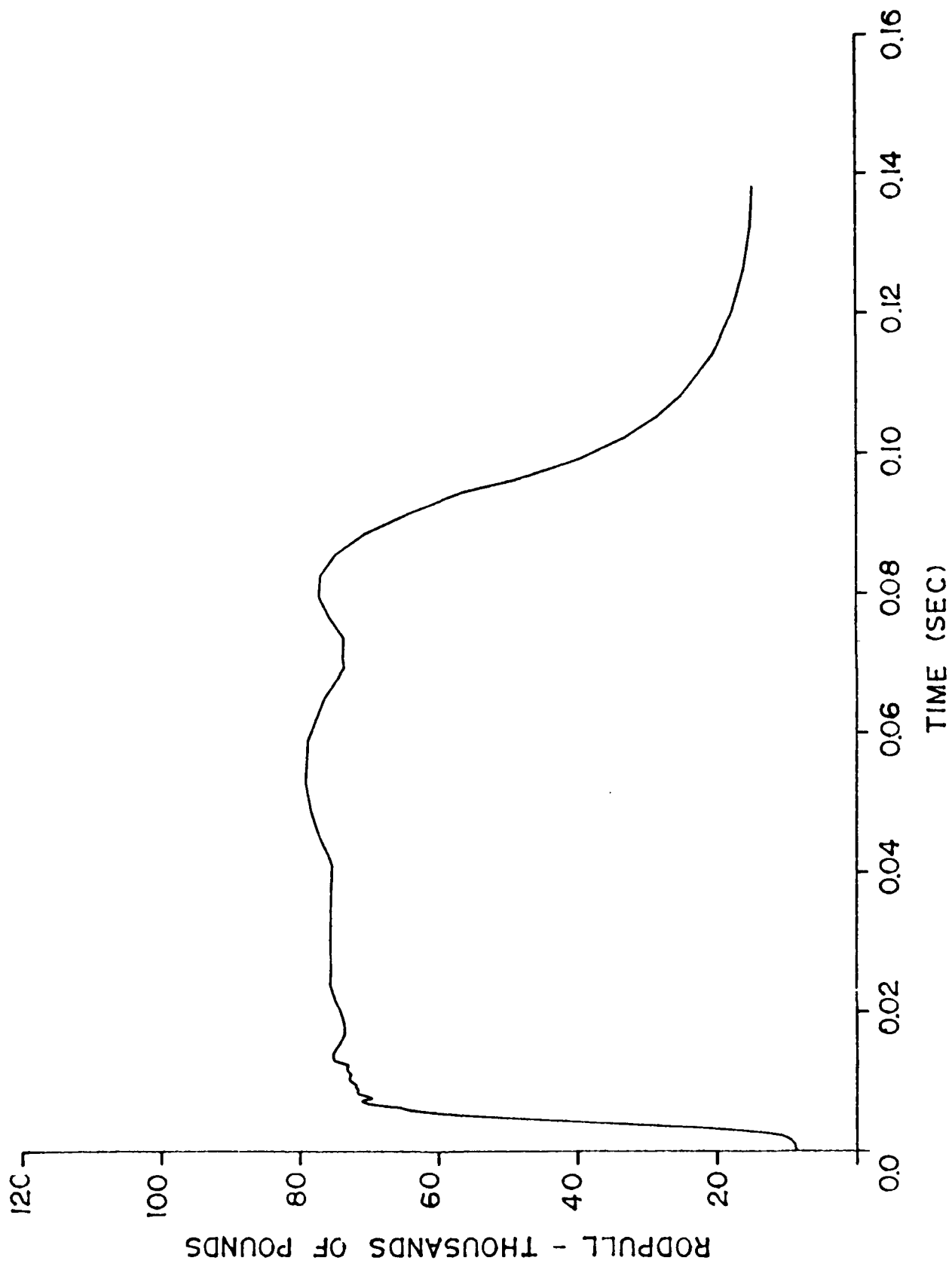


Figure 12. Rodpull profile -- M178 model

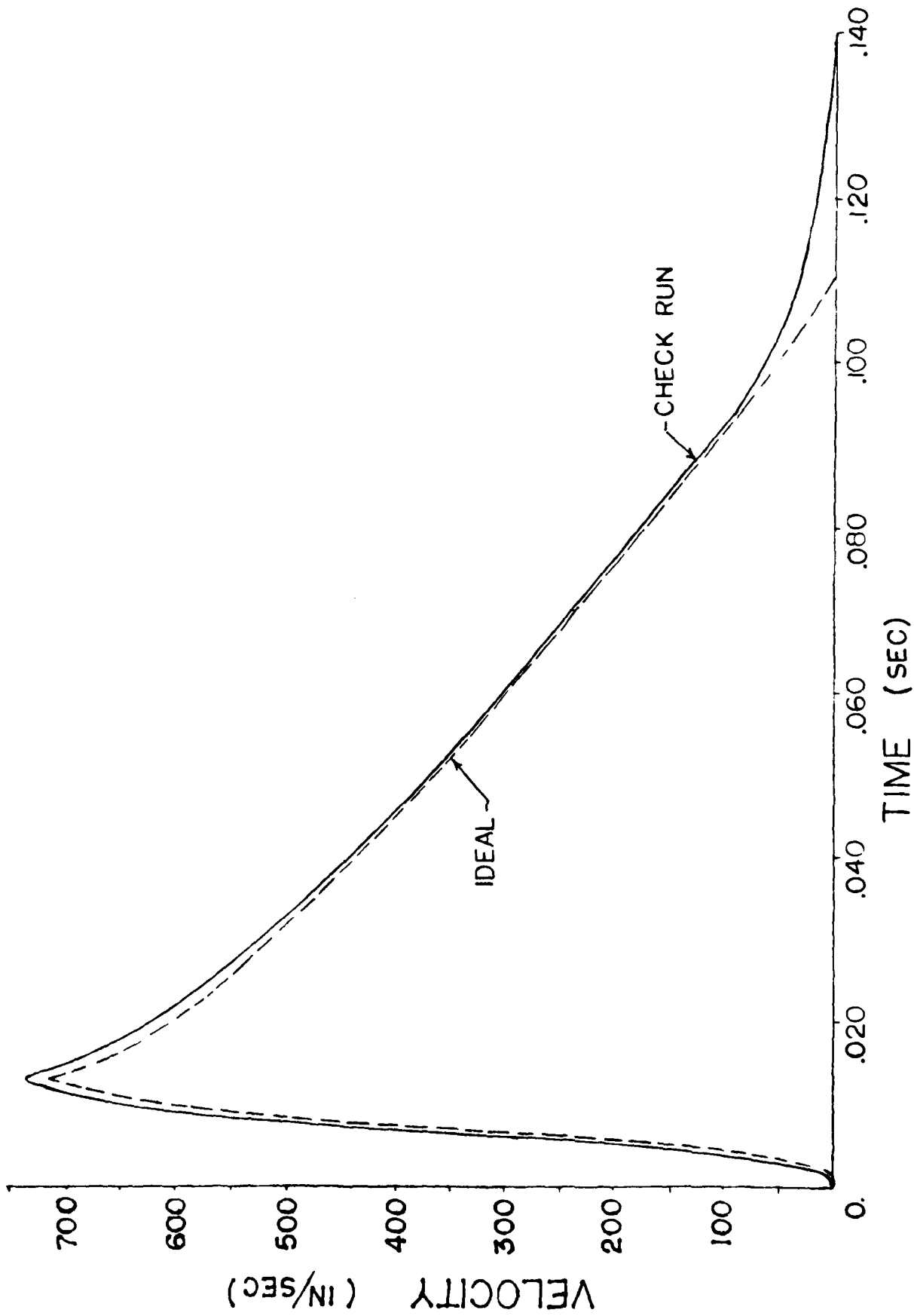


Figure 13. Ideal and check run velocity profiles

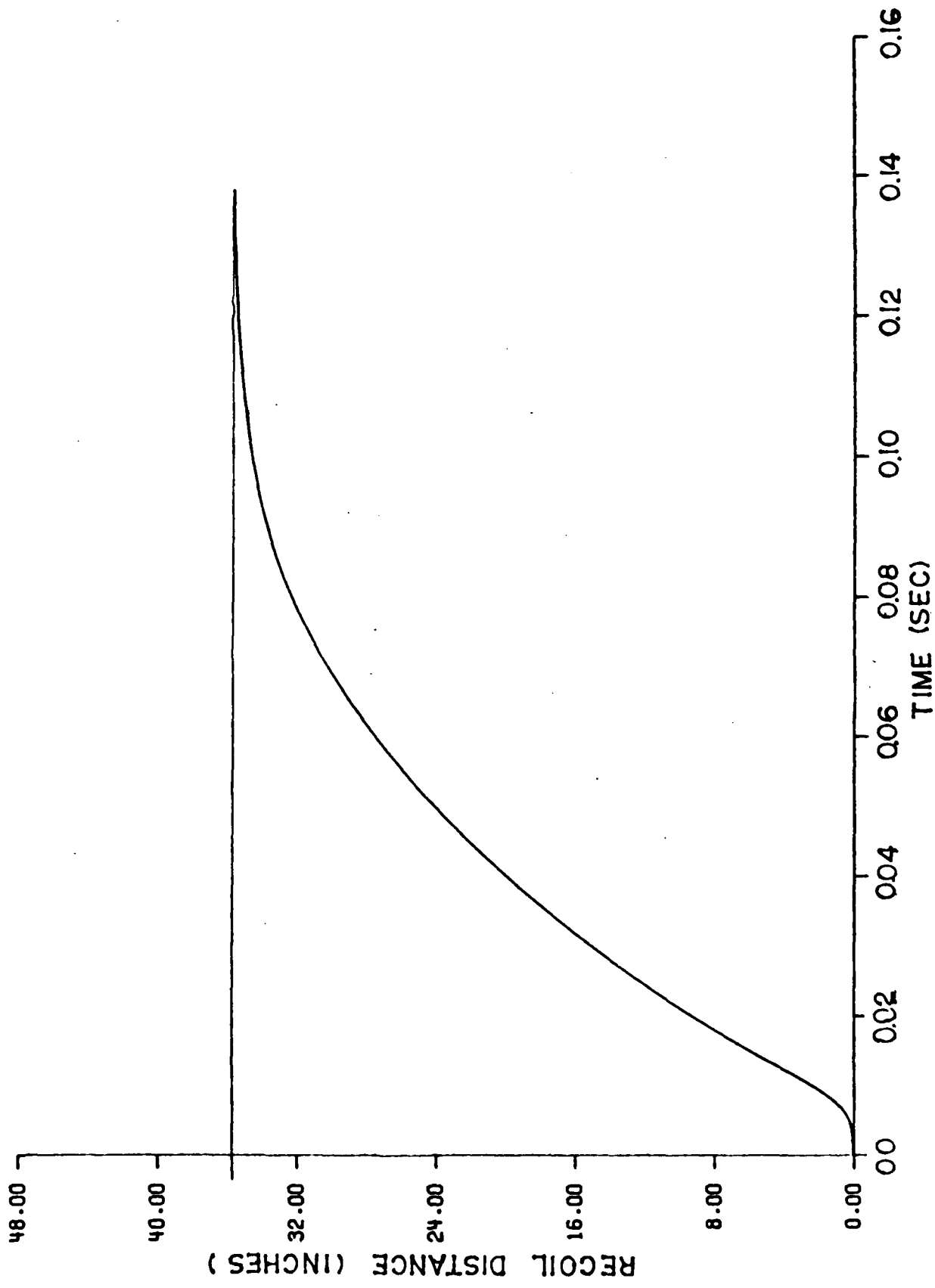


Figure 14. Recoil motion--MI78 model

HOWITZER, SP, M109A1 WITH PROPELLING CHARGE M203  
TOP LEFT RECOIL CYLINDER OIL PRESSURE VS TIME  
ROUND NO.: 28  
Date Fired: 31 Oct 77, QE: 510 mils, Temperature: Ambient

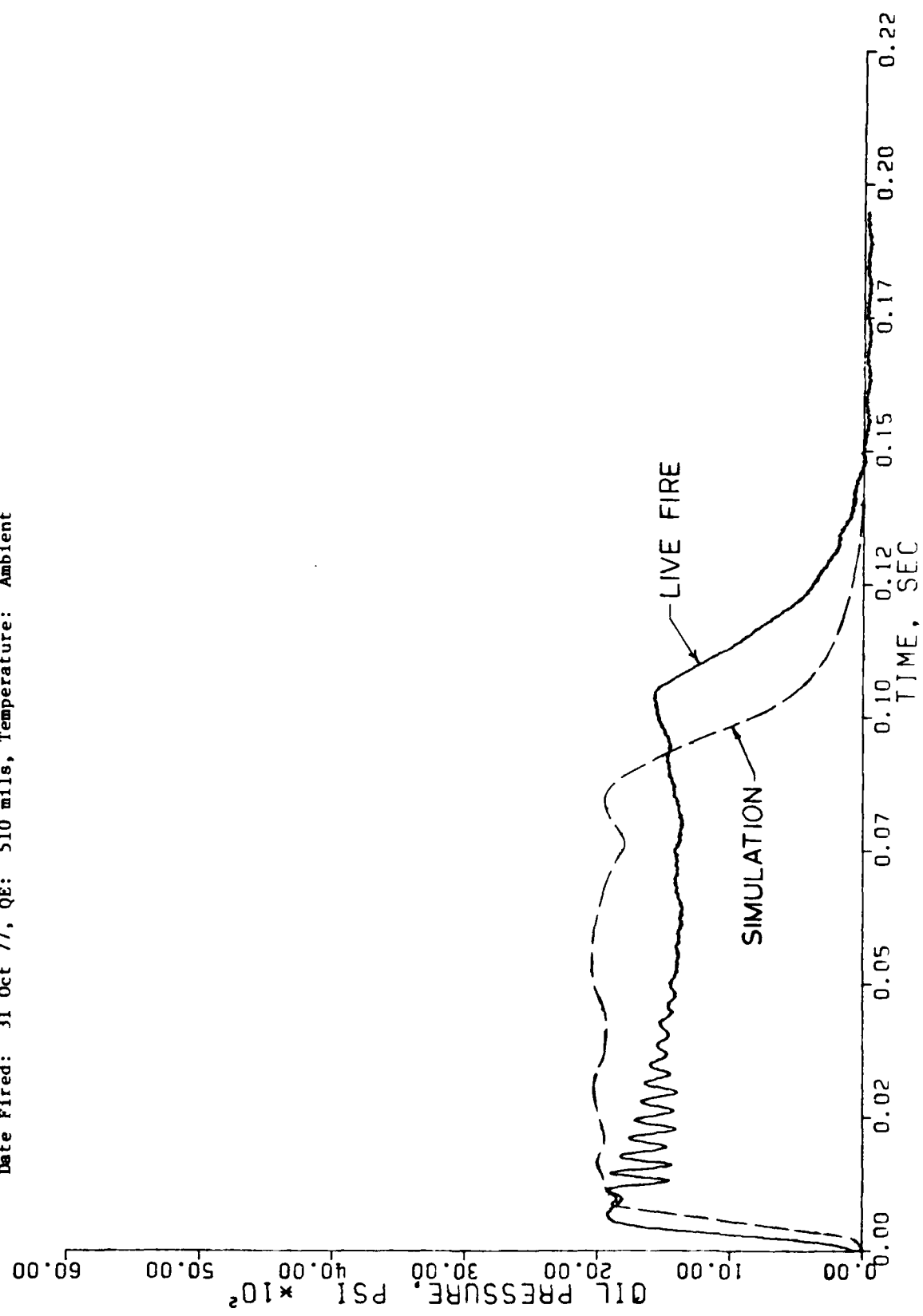


Figure 15. Comparison of recoil brake pressure--SUPER\*SCEPTRE simulation to live fire data

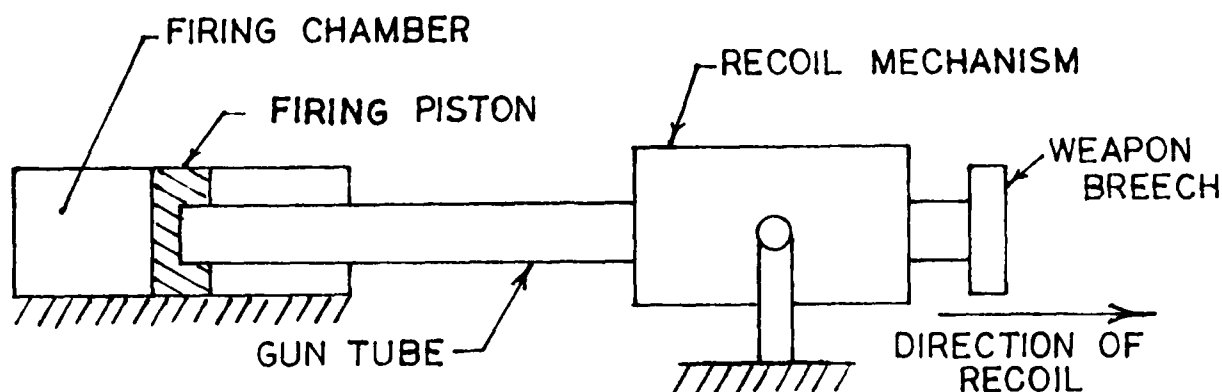


Figure 16. Powder gymnasticator schematic

A firing piston is attached to the gun tube in place of the muzzle brake. This firing piston is placed inside a firing chamber. A pyrotechnic charge is ignited in the firing chamber, driving the recoiling parts rearward, thereby simulating recoil. The advantages of this device over live firings are:

1. Firing ranges are unnecessary
2. Cost for firing each round is significantly reduced

Disadvantages of gymnasticators in general include:

1. Inability to simulate muzzle brake effects
2. Recoil brake oil pressure profiles cannot be exactly matched to live firings

Oil pressure profiles cannot be exactly matched between gymnasticator and live fire situations due to differences in breech force profiles. This can be verified by comparing the design breech force curve (fig. 9), and the gymnasticator equivalent\* (fig. 17). (The smoothed gymnasticator curve discounts oscillations which may be due to electronic noise.) Lowered initial force levels in the gymnasticator curves cause reduced initial velocity of the recoiling parts. This condition, coupled with the fact that orifice area is at a maximum during this period, causes a recoil brake oil pressure "dip." This characteristic is magnified due to the fact that recoil velocity is a squared function in the recoil brake force calculations (eq 8).

Regardless of the disadvantages, gymnasticators are used extensively to proof test recoil mechanisms after assembly. It is the author's opinion that any

---

\* Gymnasticator impulse curves were provided by Aichel Dupont of Rock Island Arsenal, July 1984.

SMOOTHED		GYMNASTICATOR	
TIME (MS)	FORCE (lb)	TIME (MS)	FORCE (lb)
0	0 ( $10^3$ )	0	0 ( $10^3$ )
3.6	1180	3.6	1180
6.0	610	6.0	560
16.0	80	6.7	710
26.0	0	8.0	580
↓	0	9.0	310
		10.0	405
		11.0	380
		12.0	150
		13.5	280
		15.6	12
		17.0	150
		19.0	0
		20.5	90
		22.0	0
		23.5	75
		26.0	0
		↓	0

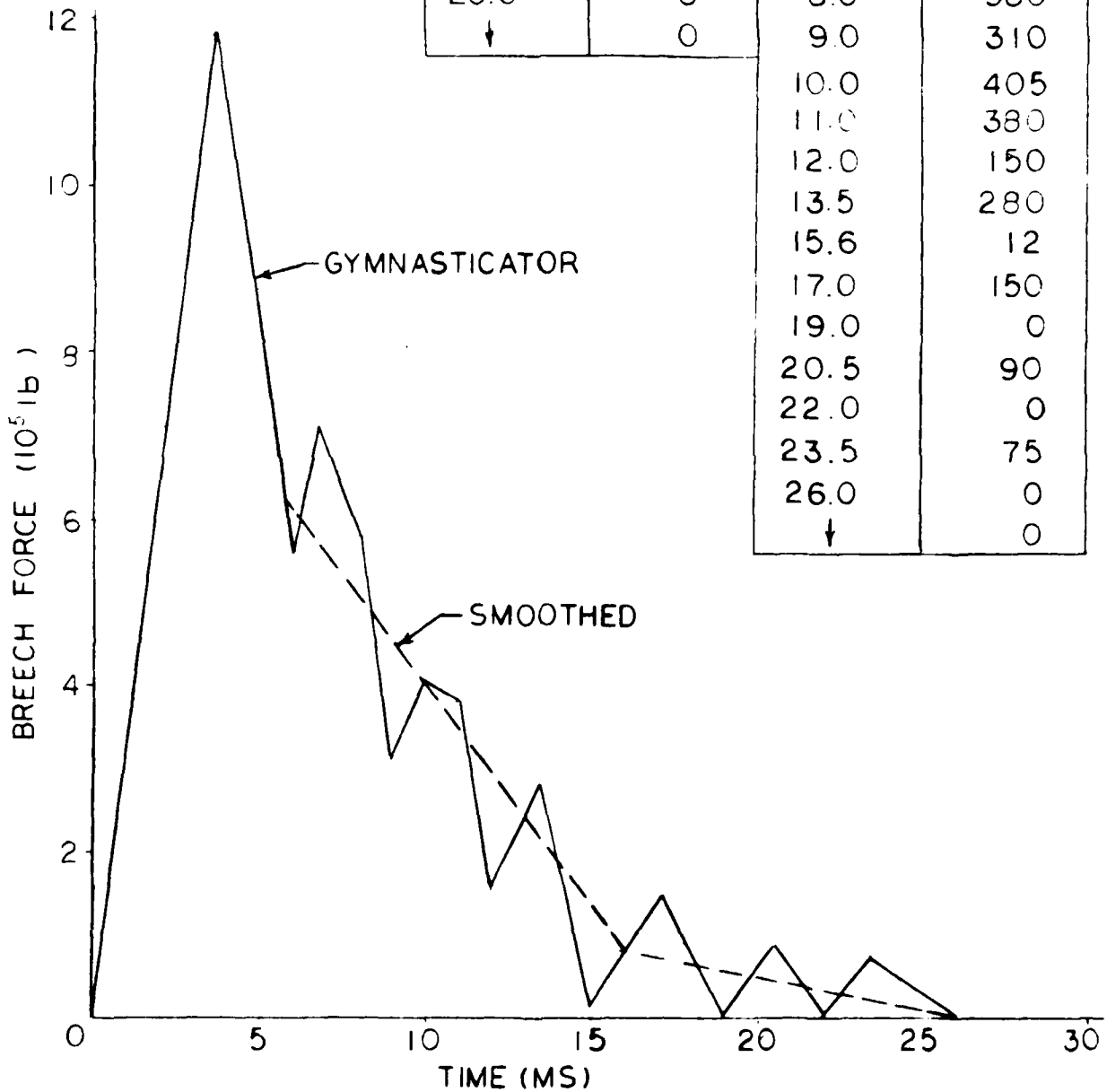


Figure 17. Breach force profile based on recoil response--powder gymnasticator (M203 equivalent)

electronic recoil mechanism test would initially be carried out on a powder gymnasticator. Therefore, the powder gymnasticator curves were used for many simulations. In order to verify that the gymnasticator curves would not cause irrational output in the M178 recoil model, a check run was made. Recoil distance (fig. 18) did not exceed the 36-in. allowable stroke. Peak rodpull (fig. 19), while high at 90,000 lb, was not unrealistic.

## CONTROL ALGORITHMS

### Level 1 Control—Maintain a Preset Rodpull

The initial electronic recoil algorithm was designed to maintain a preselected rodpull. If actual rodpull were less than the preselected value, the bypass servovalve would remain in the closed position. If rodpull were greater than the preset value, the valve would shift to the full open position. The valve did not immediately respond to input signals but operated with a time delay as shown by:

$$\frac{dA_a}{dt} = \frac{1}{\tau} (A_d - A_a) \quad (10)$$

where

$A_a$  = actual servovalve area (in.<sup>2</sup>)

$A_d$  = desired servovalve area (in.<sup>2</sup>)

$A_d = 0$  in.<sup>2</sup> when actual rodpull < desired rodpull

$A_d = 1$  in.<sup>2</sup> when actual rodpull > desired rodpull

$\tau$  = valve time constant (assume 10 ms)

The valve used in the simulation had a flow area of 1.0 in.<sup>2</sup>, which was chosen arbitrarily but appeared to be an adequate size. The 10-ms time constant is only an estimate of what might be possible with a servovalve of this size.

The level 1 control scheme is similar to a recoil device known as a St. Chamond mechanism (ref 1, page 13). The St. Chamond mechanism consists of a pressure relief valve plumbed into the recoil brake. A preset oil pressure is maintained by the opening and closing of a spring loaded poppet valve.

Level 1 control can be visualized as an electronic St. Chamond mechanism. Since the servovalve reacts to rodpull instead of recoil brake pressure, control is improved. This is due to the fact that maintenance of constant rodpull does not equate to a constant brake pressure since there are variations in recuperator and friction forces.

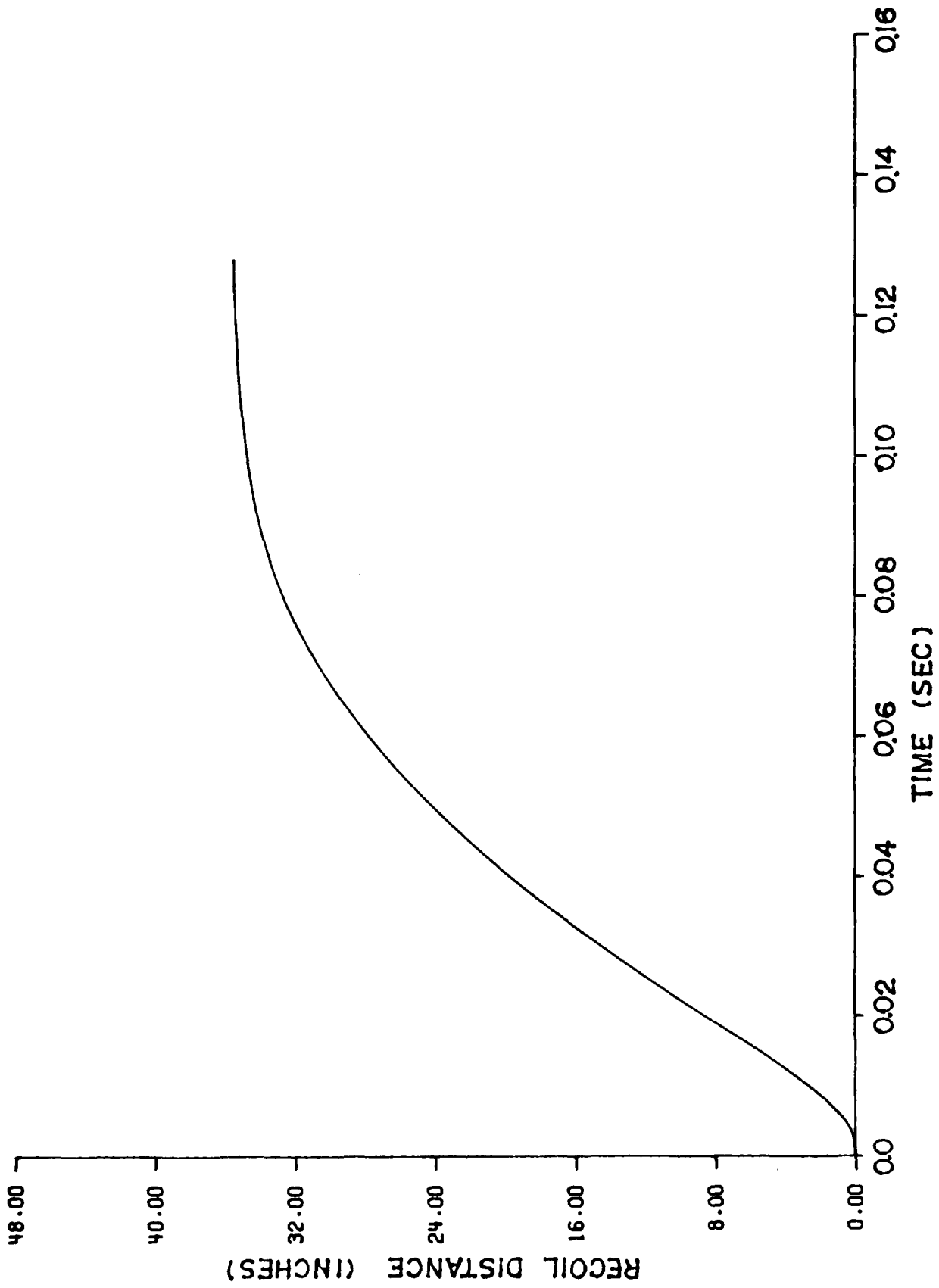


Figure 18. Recoil motion M178 model with gymnast input profile

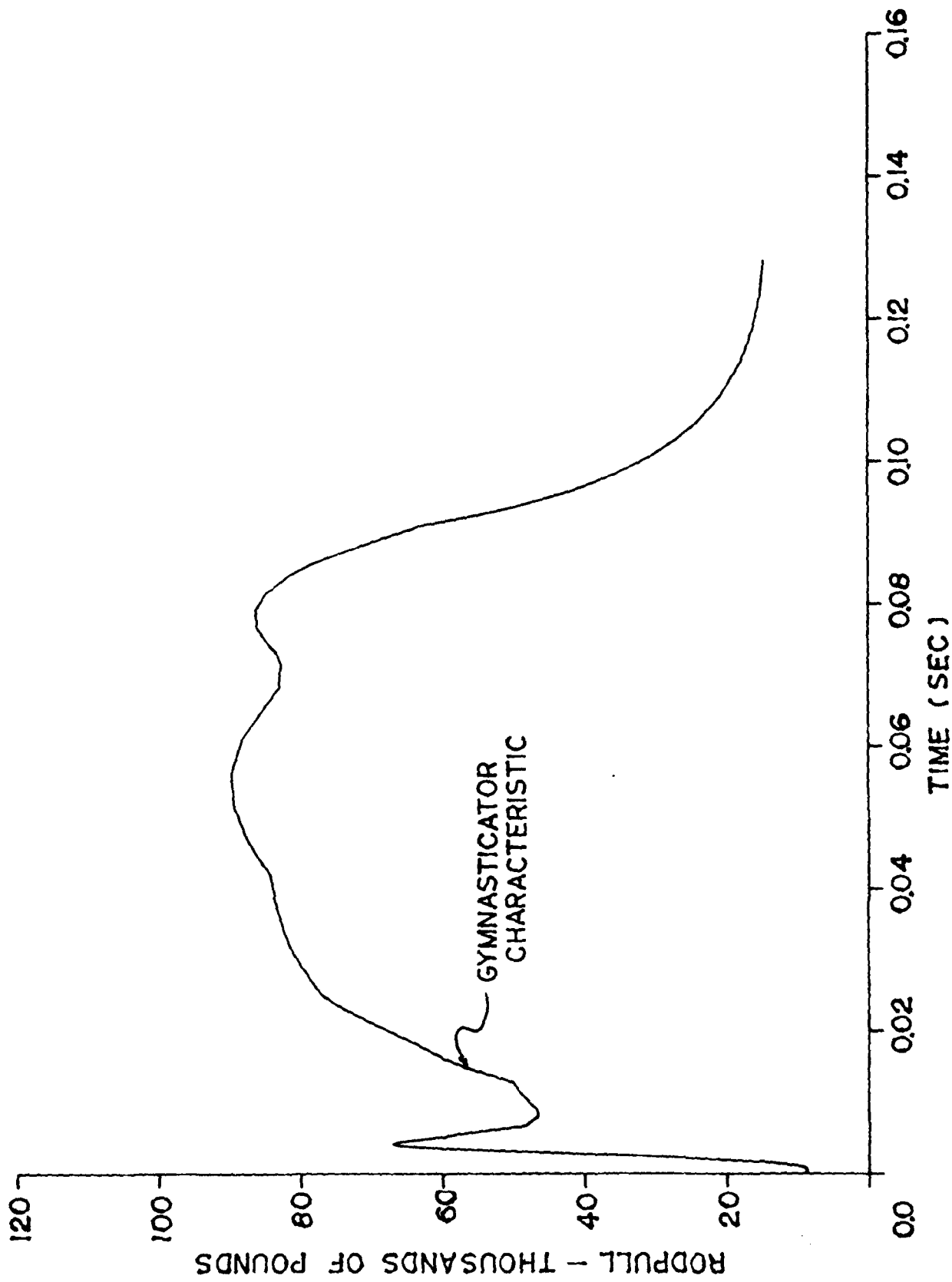


Figure 19. Rodpull profile M178 model with gymnasticator input profile

The control algorithm described above is very simple, yet it has the potential for **true optimization** of each recoil stroke. Assuming that the input impulse is known prior to firing the weapon, a value for rodpull could be mathematically or empirically determined which would cause the recoiling mass to use all available stroke. Thus, an ideal rodpull curve (fig. 6) could be generated for each input impulse.

### Level 2 Control—Compute Rodpull During Recoil

Once it has been demonstrated that a servovalve can maintain a given rodpull (level 1 control), a method to determine the required rodpull dynamically is proposed. This approach has the advantage of not requiring advance notice of what impulse is to be expected since required rodpull is computed during the recoil stroke.

This scheme equates the mechanical energy of the recoiling mass to the amount of work necessary to stop the recoiling parts. This work-energy relationship is established by integrating equation 2 with respect to distance. Recalling equation 2

$$M_r \ddot{X} = B(t) + W_r \sin \theta - K - F_F$$

distance is introduced with the following substitution:

$$\ddot{X} = \frac{dv}{dt} = \frac{dx}{dt} \frac{dv}{dx} = \frac{v dv}{dx} \quad (11)$$

therefore, equation 2 becomes

$$M_r \frac{v dv}{dx} = B(t) + W_r \sin \theta - K - F_F \quad (12)$$

Integration with respect to distance yields

$$\frac{1}{2} M_r v^2 \Big|_1^2 = \int_1^2 B(t) dx + \int_1^2 W_r \sin \theta dx - \int_1^2 K dx - \int_1^2 F_F dx \quad (13)$$

By selecting an initial integration condition at some arbitrary distance (X) where the velocity is V, a final condition at maximum recoil stroke ( $X_{\max}$ ) (where recoil velocity is zero), and assuming that rodpull ( $\tilde{K}$ ) is to be maintained at a constant value, equation 13 becomes

$$\begin{aligned} -\frac{1}{2} M_r v^2 &= \int_X^{X_{\max}} B(t) dx + W_r \sin \theta (X_{\max} - X) \\ &- \tilde{K} (X_{\max} - X) - \int_X^{X_{\max}} F_F dx \end{aligned} \quad (14)$$

This equation can now be solved for the ideal rodpull ( $\tilde{K}$ )

$$\tilde{K} = \frac{1}{X_{\max} - X} \left[ \frac{1}{2} M_r v^2 + \int_X^{X_{\max}} B(t) dt - \int_X^{X_{\max}} F_F dx \right] + W_r \sin \theta \quad (15)$$

The intent of control scheme 2 is to compute equation 15 during weapon recoil. Therefore, it is desirable to simplify the equation to reduce computation time. A comparison of forces used in equation 15 as a function of recoil stroke is depicted in figure 20. It is evident that the friction and weight terms are not large contributors to the work-energy relationship. Realizing that friction tends to reduce rodpull force, while the weight contribution tends to increase required rodpull, it would be prudent to include the weight computation and, to simplify equation 15, neglect friction.

Further simplification of equation 15 can be obtained if the breech force component is ignored. This may appear radical, since the breech force is the largest force applied to the weapon; however, it acts for only a fraction of the total recoil stroke. The computed value would only be correct after  $B(t)$  becomes negligible, however. This approach would require the servovalve to control rodpull at a preset value until the majority of breech force has been applied. This value could be the maximum rodpull the weapon will encounter.

Incorporating these decisions, equation 15 is rewritten:

$$\tilde{K} = \frac{1}{X_{\max} - X} \left[ \frac{1}{2} M_r v^2 \right] + W \sin \theta \quad (16)$$

The obvious question is: At what point during recoil should control transition from the preset rodpull to the calculated rodpull computed by equation 16? This could occur when the acceleration of the recoiling parts changes sign from positive to negative. If the weapon employs a muzzle brake, transition would occur when the muzzle brake activates. If no muzzle brake is present, as is the case with the powder gymnasticator simulation, acceleration will change sign when breech force is reduced to a level below the combined rodpull and frictional forces.

There are both physical and computational problems with equation 16 during the final portion of the recoil process. As recoil ends, velocity and  $(X_{\max} - X)$  approach zero. In order to maintain the high brake force implied by equation 16, the orifice area must be reduced. When the required orifice area is less than leakage flow in the recoil mechanism, the brake force rapidly diminishes. Final stopping is provided by the recuperator and friction forces. This results in the recoiling mass never stopping at precisely the specified  $X_{\max}$  which, in turn, causes equation 16 to become undefined as  $X_{\max}$  is approached. To prevent this, a controlled closure of the servovalve was provided in the control algorithm at a stroke of 2 inches before the desired  $X_{\max}$ . For simplicity, a linear closure of the valve was programmed. (The optimum method to effect closure was not included in this study.)

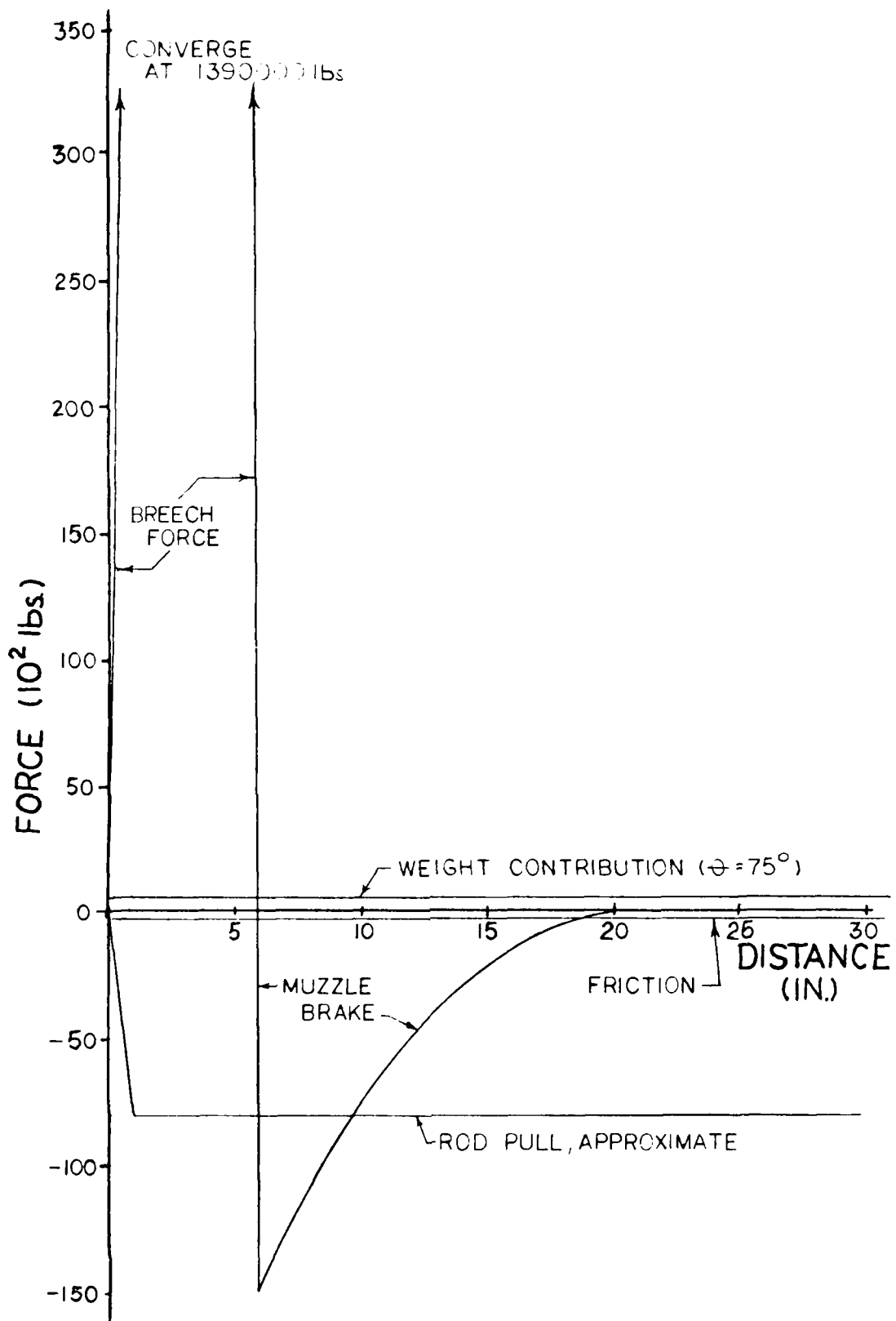


Figure 20. Magnitude of forces in recoil process

For purposes of this study, the preset rodpull was arbitrarily set at 70,000 lb. Transition from preset to the calculated rodpull (eq 16) occurred when the acceleration of the recoiling parts switched from positive to negative. A transition function was incorporated (fig. 21).

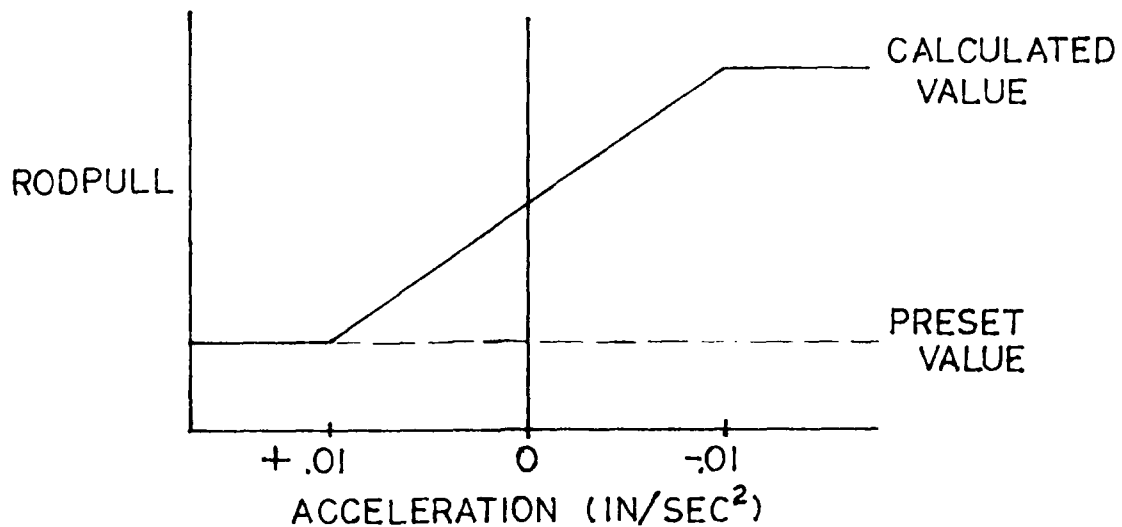


Figure 21. Transition function for calculated rodpull

The selection of the transition function profile is arbitrary. Future studies should investigate the sensitivity of recoil performance to both the value of the acceleration at which transition occurs and the shape of the transition function.

## CONTROL SIMULATIONS

### Level 1 Control--Smoothed Gymnasticator Impulse

A SUPER\*SCEPTRE simulation was run using the St. Chamond approach to recoil control. The smoothed version of the gymnasticator input (fig. 17) was applied to the M178 recoil model at 0 degree weapon elevation. The desired rodpull was set to 75,000 lb. The servovalve was commanded to shift to the full open position when actual rodpull was greater than the desired 75,000 lb using the ramp switching function shown in figure 22.

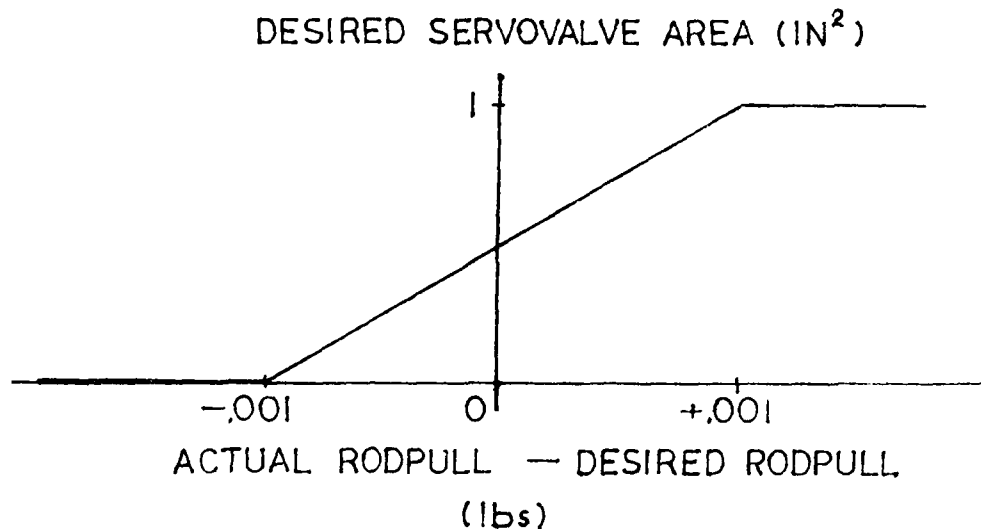


Figure 22. St. Chamond switching function

The error signal boundaries ( $-0.001$  and  $+0.001$ ) were arbitrarily assumed.

The SUPER\*SCEPTRE input deck for level 1 control is listed in appendix C, and selected output curves are shown in figures 23 through 26. It is immediately apparent in figure 23 that the recoil motion exceeds the 36 in. allowable stroke of the M178. This is rational because the original M178 recoil simulation required approximately an 80,000 lb rodpull force to stop the recoiling parts. The simulation does, however, indicate the type of response possible with the St. Chamond control algorithm (fig. 24).

Figure 24 depicts the almost ideal rodpull curve possible with this approach. The initial dip in the profile is due to the gymnasticator characteristics described earlier and is unavoidable if the gymnasticator  $B(t)$  curve is to be used. The OPEN-CLOSE commands to the servovalve are shown in figure 25, while figure 26 shows the actual servovalve area when the time delay is taken into account.

### Level 2 Control--M203 Propelling Charge

A SUPER\*SCEPTRE simulation using the M203 propelling charge with level 2 control was requested. The appropriate input deck is listed in appendix D.

A comparison of the effect of level 2 control on rodpull for the design breech force is shown in figure 27. Since the original M178 recoil mechanism was designed to attenuate this particular impulse, the effect of control is not dramatic; however, some characteristics of the control scheme are demonstrated. Of particular note is the control to the preset rodpull of 70,000 lb, followed by transition to a higher rodpull and, finally, the effect of controlled valve closure.

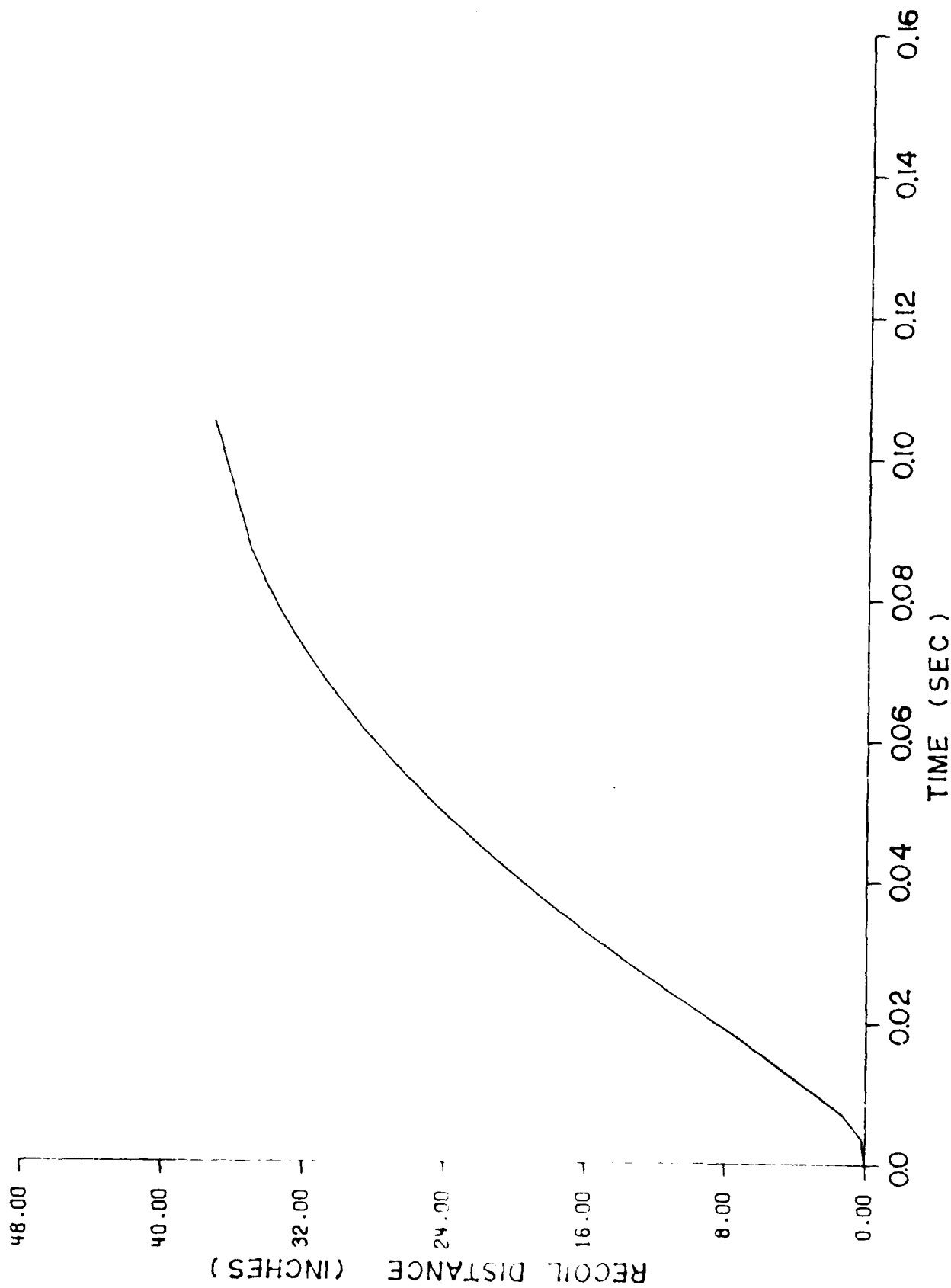


Figure 23. Recoil motion, St. Chamond--75,000 lb desired rodpull

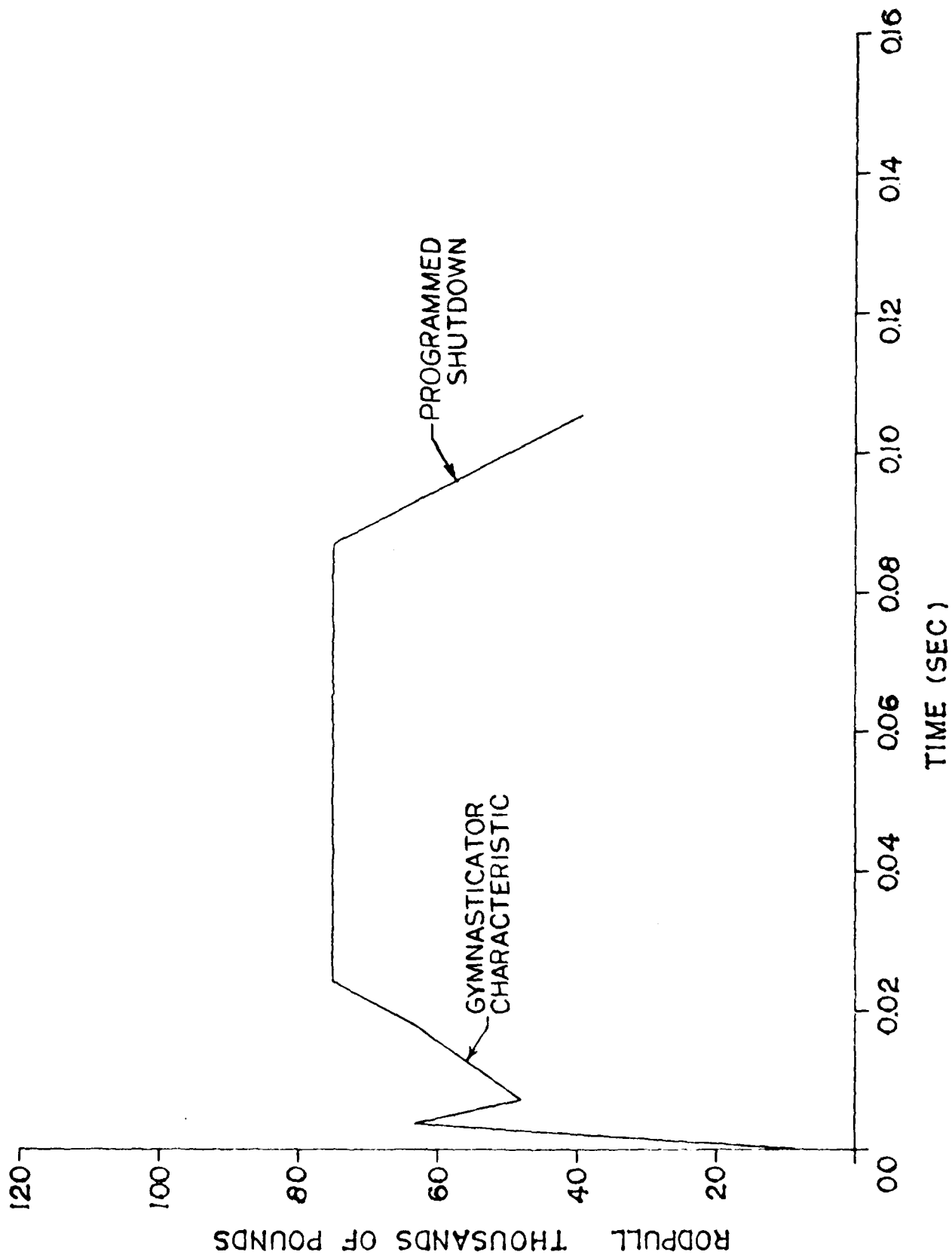


Figure 24. Rodpull profile, St. Chamond--75,000 lb desired rodpull

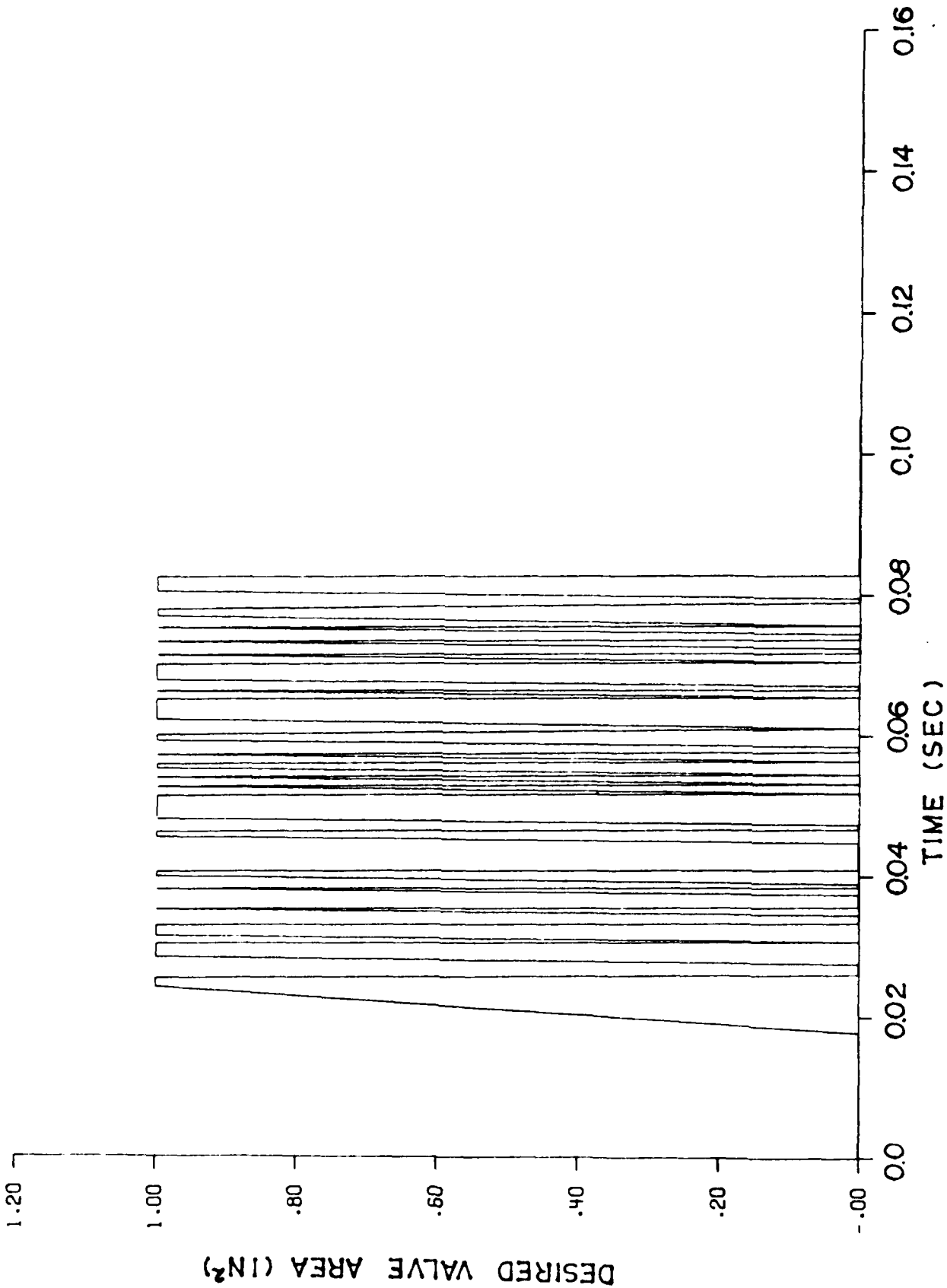


Figure 25. Desired servovalve area, St. Chamond--75,000 lb desired rodpull

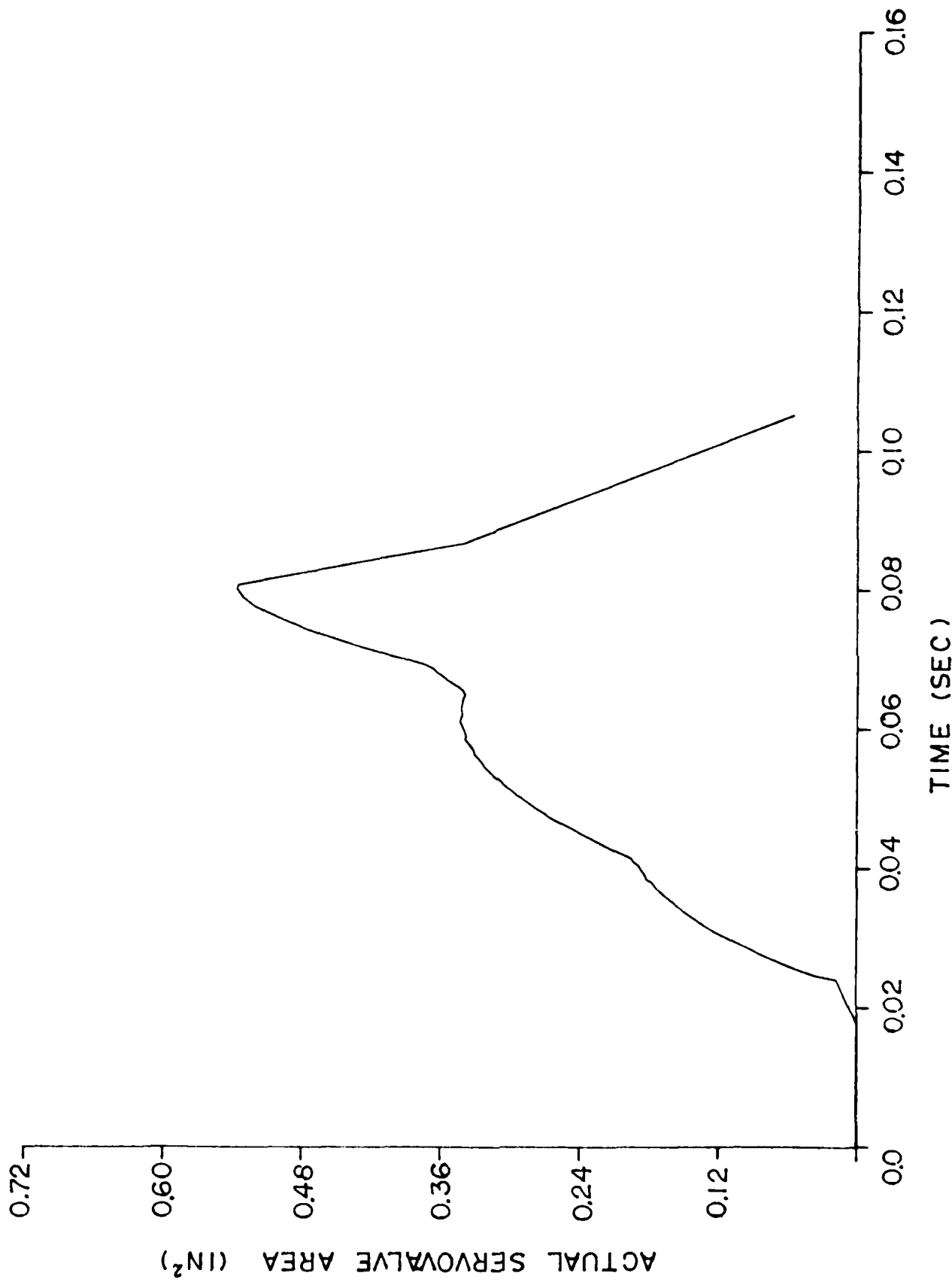


Figure 26. Actual servovalve area, St. Chamond--75,000 lb desired rodpull

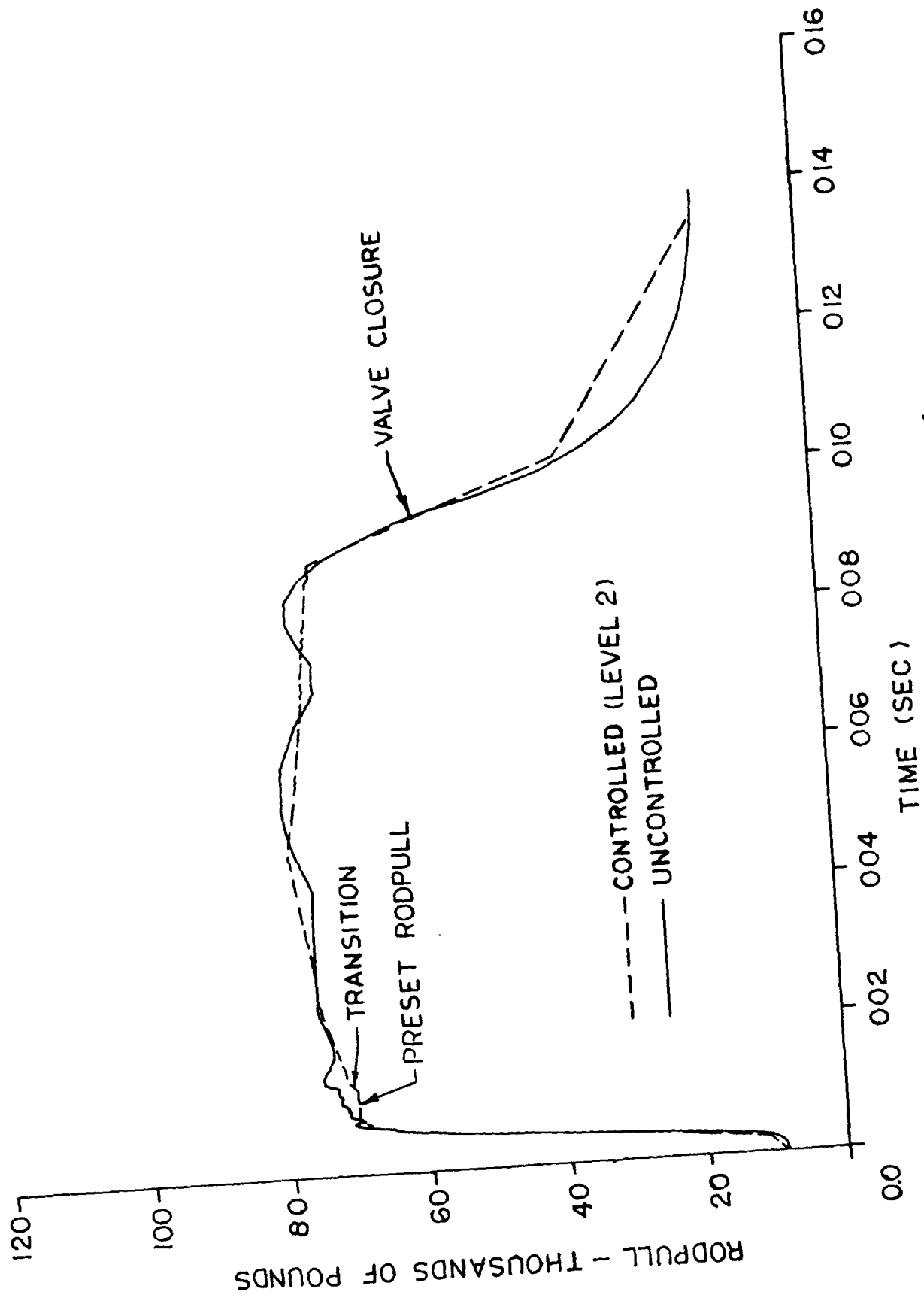


Figure 27. Rodpull comparison--M203 impulse

A greater insight into the action of the control system is shown in figure 28. This graph depicts the relationship between desired rodpull and actual rodpull, with the servovalve position superimposed. Whenever actual rodpull is greater than desired rodpull, the valve position curve has a positive slope. A negative slope indicates actual rodpull is less than desired. Zero slope, found in the initial part of the simulation, indicates the valve has no activity since the actual rodpull has not yet reached the preselected value. When the muzzle brake activates, acceleration becomes negative and the control system then computes rodpull based on equation 16. Since at this point acceleration changes abruptly from positive to negative, it is implicit that recoil velocity peak also. Therefore, desired rodpull also experiences an abrupt peak. After 40 ms the muzzle brake action is exhausted, and the continued slight decrease in desired rodpull is due to the persistent friction force,  $F_f$ .

### **Level 2 Control--Smoothed Gymnasticator Impulse**

A more interesting control problem occurs when the recoil mechanism is exercised by the powder gymnasticator. A SUPER\*SCEPTRE input deck for this condition is presented in appendix D. A comparison of uncontrolled versus controlled rodpull is shown in figure 29. The gymnasticator input is actually a more severe load than live firing. The overall gymnasticator impulse delivered to the recoil mechanism is slightly higher but the initial force is lower. Furthermore, the gymnasticator impulse does not simulate a muzzle brake but delivers lower force levels over a longer period of time.

Consequently the recoiling parts do not achieve as high an initial velocity as the live fire simulation, but this is compensated by higher velocities as recoil stroke continues. The higher velocities cause the uncontrolled recoil brake to apply more rodpull than on an actual firing, since the brake was not designed specifically for this input impulse. However, the servovalve control computes that lower values will be required than the brake is supplying. The valve opens, and rodpull peaks are eliminated.

### **Level 2 Control--Short Recoil Mode (Smoothed Gymnasticator Impulse)**

One of the most dramatic test cases to demonstrate the usefulness of the automatic control process occurs with the recoil mechanism in the short stroke mode. Using the gymnasticator impulse input, the control system is commanded to permit a longer recoil length to occur. Since the short stroke orifice area profile ends at a recoil length of approximately 24 in., any increase in recoil length will be generated exclusively by throttling oil through the servovalve. Therefore, the control system is exercising full control after the 24-in. recoil length is reached. Arbitrarily assuming that 31 in. is available, a simulation was run. The SUPER\*SCEPTRE input deck for this test case is provided in appendix D. Rodpull profiles for both uncontrolled and controlled recoil are shown in figure 30. A slight rise in rodpull is evident at the point where the short stroke profile ends, since the control valve must rapidly adjust to take all remaining flow except leakage. This is a rather severe task, but the system manages to maintain rodpull fairly constant at a level approximately 33% of the uncontrolled amount.

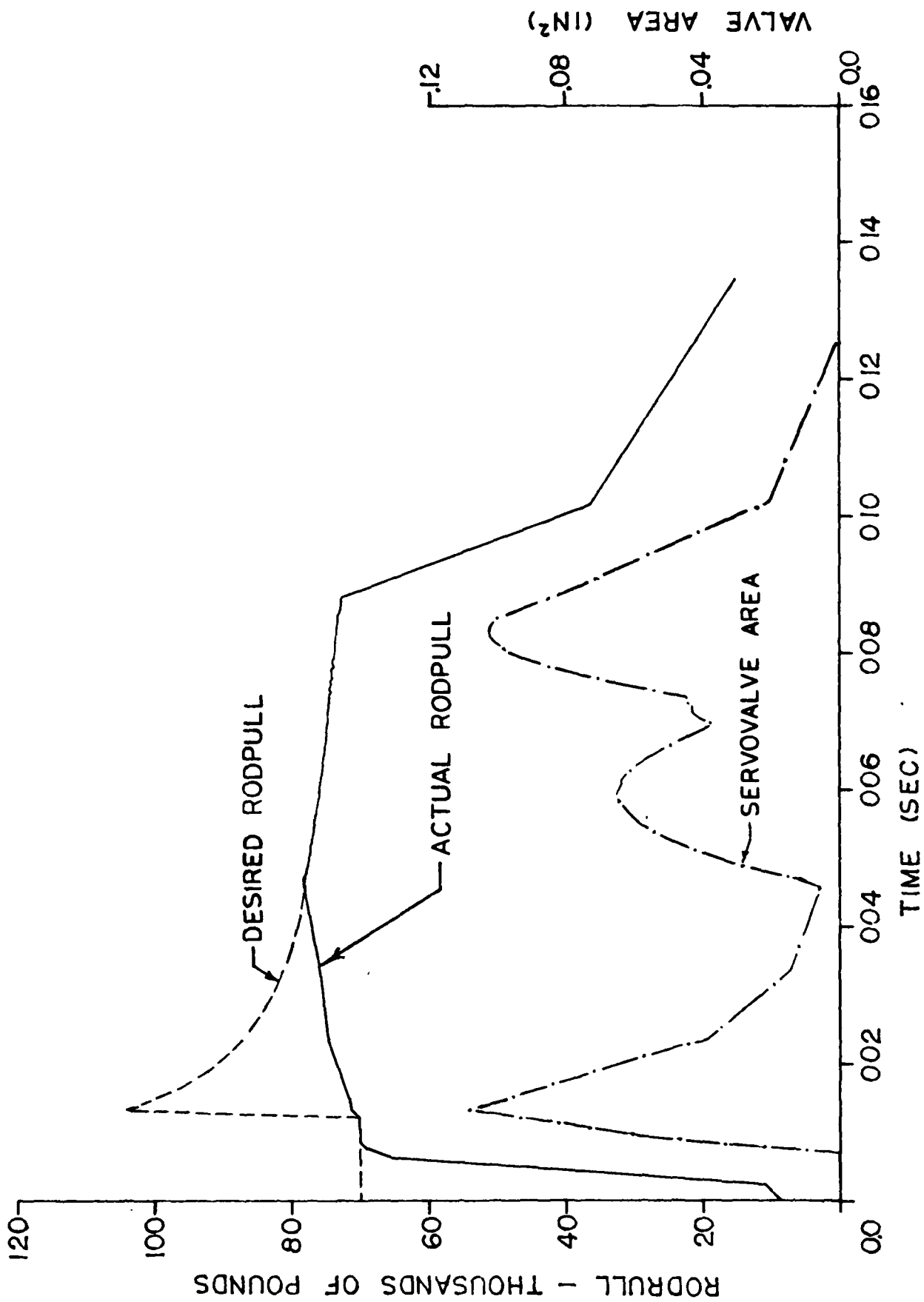


Figure 28. Level 2--control variable relationships

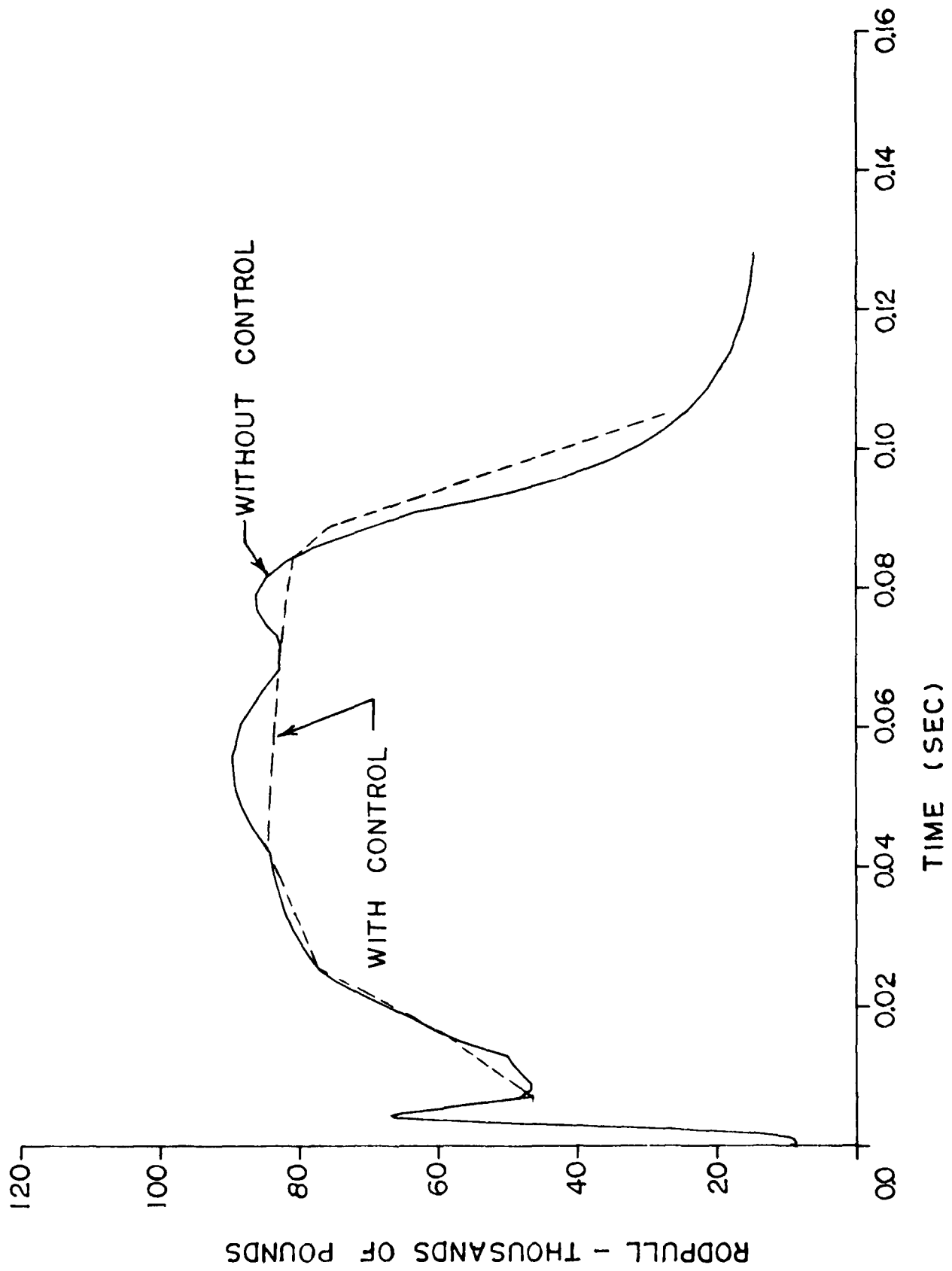


Figure 29. Level 2--controlled and uncontrolled rodpull gymnasticator impulse

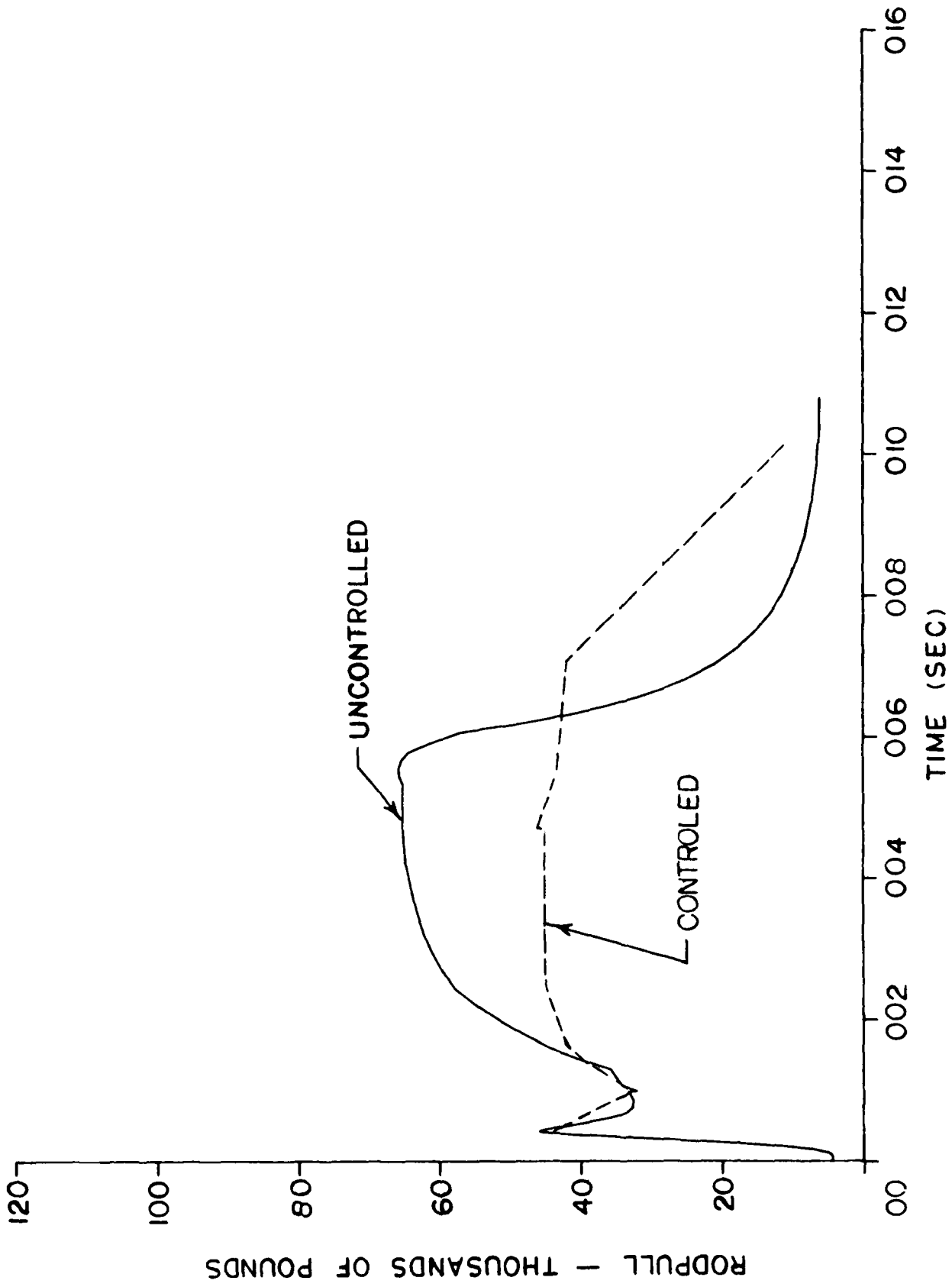


Figure 30. Level 2--rodpull profile, short stroke mode gymnasticator impulse

## FUTURE APPLICATIONS OF MICROPROCESSOR RECOIL CONTROL

The concept of closed-loop feedback control applied to recoil mechanisms has many ramifications. Some areas of interest are described below:

1. Variable Recoil Length--Many artillery recoil mechanisms have provision to shorten recoil stroke for high elevation firings. This is necessary to prevent the recoiling parts from hitting the vehicle floor or, in the case of a towed artillery piece, the ground. The mechanism necessary to accomplish the reduction in stroke adds considerable mechanical complexity to the recoil system. This can be alleviated by providing the microprocessor with an input of weapon elevation. The microprocessor can then perform the trivial trigonometric calculations to determine available recoil length. Rodpull would then be adjusted accordingly.

2. Counter-Recoil Control--The servovalve system used to control the recoil process can be applied to control counter-recoil velocity. Throttling of hydraulic oil can be programmed to insure consistent buffing action and return-to-battery. This eliminates the need for separate counter-recoil control passages.

3. Elimination of Precision Control Orifices--Traditional artillery recoil mechanisms employ control rods or grooves to throttle oil. These orifices are precision machined which makes them costly to manufacture. Furthermore, design of the orifices is often done by tedious iteration with prototype hardware. Precision control orifices can be eliminated by the throttling servovalve. The resulting recoil mechanism would then be mechanically very simple. In order to reduce servovalve size, a very simple fixed throttling orifice might be installed, and the servovalve would provide the fine adjustment.

4. Adaptability to Increased Weapon Impulse--Since recoil mechanisms are designed to attenuate a specific impulse, any significant increase in this impulse (for purposes of increasing projectile range, perhaps) would necessitate a costly mechanical redesign. A microprocessor-controlled recoil mechanism could easily adapt with only a software change, as long as the resultant magnitude of the rodpull is within the maximum allowed for the gun.

5. Lightweight Weapons--Effective lightweight, long-range artillery pieces may become a practical reality with microprocessor servovalve control. If consistent rodpull can be guaranteed, structural safety factors can be reduced significantly. This equates to large weight savings.

The weight saving generated through reduced safety factors is of little value, however, if weapon stability cannot be maintained. An artillery piece must remain rotationally stable throughout the recoil stroke. Practically speaking, this constraint insures that the gun will not jump when fired. While stability is, to a large extent, based on the external configuration of the weapon system, it can constrain the design of the rodpull force profile. Consider the free body diagram of forces acting on the weapon in figure 31.

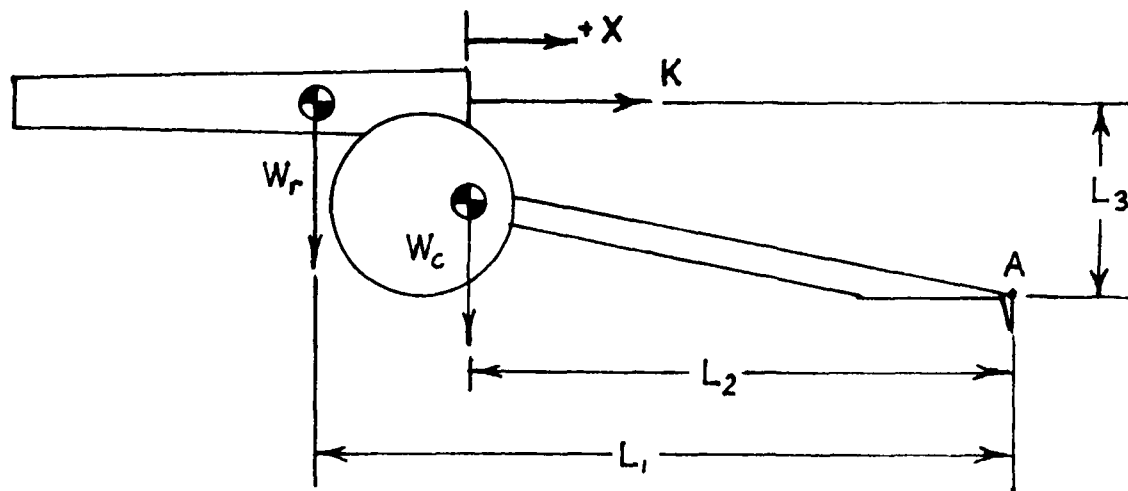


Figure 31. Forces acting on weapon structure

Summing the moments about point A shows that the gun will remain stable as long as the counterclockwise moments from the weights of the recoiling mass and the carriage exceed the clockwise moment from the force that the recoiling mass exerts on the carriage, which is primarily the rodpull. The condition for stability is:

$$K (L_3) < W_r(L_1 - X) + W_c L_2$$

Note that as the recoil progresses to the right, the counterclockwise moment from the recoiling weight decreases due to the moving center of gravity of the recoiling parts; therefore, the stability condition is the most critical at the end of the recoil stroke. While this condition does not override the primary goal of keeping the rodpull force low by making it as constant as possible, it demonstrates that rodpull forces should not increase during the final portion of the stroke. It would be entirely possible for the microprocessor to tailor the rodpull profile to improve stability of a lightweight weapon.

Further reductions in weapon weight through reduced rodpull are possible by applying microprocessor control to the concept of soft recoil. The soft recoil approach reduces rodpull by imparting a forward velocity to the recoiling parts prior to firing. As firing occurs, the moving parts must be stopped from forward motion and driven backwards. Much energy is required to accomplish this, thus reducing overall rodpull. (A more detailed discussion of this approach is provided in reference 5.) Mechanically, this system is very complex since provision must be made for misfire conditions. The microprocessor system could orchestrate the entire process, eliminating much of the heavy mechanical hardware.

Microprocessor recoil control is not the answer to all future recoil mechanisms. It provides a high degree of finesse in controlling rodpull which may not

be necessary or desirable in large artillery weapons where weight and stability are not concerns. However, if precise rodpull control is necessary for any of the reasons mentioned previously, then microprocessor controlled recoil is a viable alternative.

### CONCLUSIONS

This feasibility study demonstrated the viability of microprocessor control for a typical artillery recoil mechanism. Since this effort consists of an add on to an existing system, it is difficult to demonstrate the benefits of control at the very highest breech forces available. This is because the recoil system was actually designed to provide optimum recoil at these levels. Automatic control should smooth out some of the peak stresses which occur at any off-design point such as those which occur when a gymnasticator is used. A level 2 control system should respond well to lower impulses, keeping the stresses low enough to use the entire distance available for recoil. A very dramatic control exercise is seen when the recoil system is in the short mode and the control system is commanded to use a recoil distance longer than the usual short stroke distance.

This study is only a beginning. The work that remains is for the characteristics of an actual servovalve to be placed in the model, then sensitivity studies can be made to determine the best method of controlling the servovalve. Various end of recoil models should be investigated to determine the best method to bring the recoiling mass to a final stop. Finally, a study should be performed to determine the best way to handle the preset value of desired rodpull and to determine if there is a better method of switching over to calculated desired rodpull. The method would have to be satisfactory for both live firing and the gymnasticator simulation.

## REFERENCES

1. "Engineering Design Handbook: Carriages and Mount Series, Recoil Mechanism," AMCP 706-342, U.S. Army Materiel Command, Washington, D.C., September 1963.
2. Jasbir S. Arora and Edward J. Haug, Jr., "A Guide To Design of Artillery Recoil Mechanisms," U.S. Army Armament Research and Development Command, Dover, NJ, September 1977.
3. James C. Bowers, John E. O'Reilly, and Gary A. Shaw, "Users' Manual for Super SUPER-SCEPTRE, A Program for the Analysis of Electrical, Mechanical, Digital, and Control Systems," revision 1, prepared for Picatinny Arsenal, Dover, NJ, May 1975.
4. "Compatiblity Program for the M109 Howitzer/M203 Propelling Charge and Product Improvement Test of M127 Recoil Mechanism Modified for 155-mm M109A1 Howitzer," Firing Record No. M-89550, TECOM Projects No. 2-MD-004-203-011 and 2-WE-200-109-030.
5. Robert E. Seamands, "Exploratory Development of Howitzer, Light, Towed, 105-mm Soft Recoil, XM204," Technical Report RETR 70-179, Weapons Command, Rock Island Arsenal, July 1970.

APPENDIX A  
EQUIVALENT ORIFICE AREA COMPUTATION

# SUPER-SCEPTRE INPUT DECK EQUIVALENT ORIFICE AREA COMPUTATION LONG RECOIL-M178

```

MECHANICAL DESCRIPTION
M109 RECOIL SYSTEM -
TABLE 2 BREECH FORCE FOR DESIGN RUN - OAE = 800 MILS
ORIFICE AREA CALCULATION FOR LONG RECOIL
ELEMENTS
M1,1-2=X1(PWT/PGR)
R1,2-1=TABLE 2 (TIME)
R2,2-1=X2(PWT*SIN(PANG))
R3,1-2=PRDPL
R6,1-2=X7(PMU*PWT*COS(PANG))*(67.15-SM1)/14.15)
DEFINED PARAMETERS
PQAE=800.
PWT=4360
PGR=386.
PIE=X3(4.*ATAN(1.0))
PANG=X4(2.*PIE*PQAE/6400.)
PAR=9.72
PP0=650
PU0=1015.
PN=1.6
PAB=32.98
PUF=.0313
PAE=1.
PMU=0.15
PRDPL=70000
PPAC=2340
PRE=X5(PAR*PP0/(1.-PAR*SM1/PU0))*PN)
PFO=X8(PRDPL-PRE-PPAC)
POR=X9(UM1*SQRT(PUF*PAB**3/2/PGR/PFO))
OUTPUTS
SM1,UM1,R1
POR,PFO,PRE
POR, PLOT(SM1)
FUNCTIONS
TABLE 2
0.,.32300.,.002,184000.,.006,1416000.,.007,1390000
.008,1156000.,.009,809000.,.01,589000.,.011,443000
.012,343000.,.0129,276000.,.013,-148000
.0141,-130000.,.0156,-109000.,.0175,-86000
.0211,-57900.,.024,-42200.,.031,-20400
.0373,-11100.,.0445,-5750.,.0526,-2890.,.0648,-1110
.075,-533.,.0861,-253.,.0981,-120.,.1123,0.,.9,0
RUN CONTROLS
STOP TIME = .15
MAX INTEGRATION PASSES = 1E20
MINIMUM STEP SIZE = 1E-30
COMPUTER TIME LIMIT = 1
TERMINATE IF((UM1.LT.0).AND.(TIME.GT.0.01))
END
$EOR
8
DBEND

```

# TABULAR OUTPUT LONG RECOIL

TRANSIENT ANALYSIS RESULTS  
 139 RECOIL SYSTEM  
 -42 IN 3 SPEED FORCE FOR DESIGN RUN - OAE = 800 MILS  
 CALCULATED AREA CALCULATION

TIME	7.5000E-05	1.6875E-04	3.1875E-04	5.4375E-04	8.4375E-04	1.36875E-03
SPI	-8.2168E-06	-4.8729E-05	-1.2943E-04	-7.0312E-04	-4.9149E-04	-1.9590E-04
UNI	-2.2675E-01	-4.5528E-01	-6.3854E-01	-7.8051E-01	-3.6866E-01	-1.8840E-01
R1	3.7988E+04	4.5997E+04	5.6477E+04	7.3543E+04	9.6298E+04	1.3013E+05
POR	-1.1039E-03	-2.3180E-03	-3.4628E-03	-3.8008E-03	-1.7561E-03	8.9629E-04
PFO	6.1342E+04	6.1342E+04	6.1342E+04	6.1342E+04	6.1342E+04	6.1342E+04
PRE	6.3180E+03	6.3180E+03	6.3179E+03	6.3179E+03	6.3179E+03	6.3179E+03
TIME	2.1187E-03	2.3062E-03	2.6025E-03	3.0562E-03	3.6562E-03	4.7062E-03
SPI	2.1951E-03	5.1240E-03	9.4639E-03	2.0688E-02	4.8341E-02	1.4793E-01
UNI	6.5955E+00	8.3703E+00	1.1304E+01	1.8381E+01	6.1157E+01	1.3289E+02
R1	1.8163E+05	2.2057E+05	2.7832E+05	3.7072E+05	6.9423E+05	1.0175E+06
POR	3.2182E-02	4.0467E-02	5.5044E-02	8.8075E-02	2.9780E-01	6.5363E-01
PFO	6.1341E+04	6.1341E+04	6.1341E+04	6.1340E+04	6.1337E+04	6.1327E+04
PRE	6.3182E+03	6.3182E+03	6.3182E+03	6.3200E+03	6.3226E+03	6.3235E+03
TIME	5.9062E-03	6.0373E-03	6.1125E-03	6.2650E-03	6.4500E-03	6.9937E-03
SPI	3.7690E-01	4.1134E-01	4.3194E-01	4.7515E-01	5.3291E-01	7.2387E-01
UNI	2.5481E+02	2.7020E+02	2.7914E+02	2.9563E+02	3.1917E+02	3.8310E+02
R1	1.3871E+06	1.4150E+06	1.4130E+06	1.4031E+06	1.4016E+06	1.3901E+06
POR	1.2404E+00	1.3161E+00	1.3596E+00	1.4465E+00	1.5547E+00	1.8604E+00
PFO	6.1305E+04	6.1300E+04	6.1300E+04	6.1295E+04	6.1290E+04	6.1271E+04
PRE	6.3546E+03	6.3580E+03	6.3600E+03	6.3642E+03	6.3798E+03	6.3887E+03
TIME	7.0687E-03	7.1812E-03	7.3312E-03	7.5937E-03	8.0812E-03	8.2312E-03
SPI	7.5293E-01	7.9774E-01	8.5971E-01	9.7467E-01	1.1135E-01	1.2810E-01
UNI	3.9183E+02	4.0469E+02	4.2143E+02	4.4910E+02	4.8000E+02	5.1952E+02
R1	1.3739E+06	1.3475E+06	1.3124E+06	1.2510E+06	1.1808E+06	1.0776E+06
POR	1.9090E+00	1.9717E+00	2.0534E+00	2.1910E+00	2.3397E+00	2.4948E+00
PFO	6.1268E+04	6.1264E+04	6.1257E+04	6.1246E+04	6.1237E+04	6.1216E+04
PRE	6.3915E+03	6.3960E+03	6.4021E+03	6.4134E+03	6.4364E+03	6.4402E+03
TIME	8.5312E-03	8.9065E-03	9.0775E-03	9.1150E-03	9.2625E-03	9.7500E-03
SPI	1.4385E+00	1.6452E+00	1.7200E+00	1.7632E+00	1.8507E+00	2.1441E+00
UNI	5.3720E+02	5.6503E+02	5.7373E+02	5.7853E+02	5.8781E+02	6.1454E+02
R1	9.7156E+05	8.4153E+05	8.0975E+05	7.8450E+05	7.5123E+05	6.4000E+05
POR	2.6182E+00	2.7543E+00	2.7975E+00	2.8210E+00	2.8669E+00	2.9952E+00
PFO	6.1202E+04	6.1179E+04	6.1171E+04	6.1167E+04	6.1158E+04	6.1147E+04
PRE	6.4597E+03	6.4806E+03	6.4881E+03	6.4935E+03	6.5013E+03	6.5126E+03
TIME	1.0012E-02	1.0163E-02	1.0387E-02	1.0637E-02	1.1025E-02	1.1400E-02
SPI	2.3024E+00	2.4010E+00	2.5457E+00	2.7406E+00	2.9640E+00	3.2655E+00
UNI	6.3437E+02	6.3437E+02	6.3392E+02	6.3328E+02	6.3289E+02	6.3255E+02
R1	5.8717E+05	5.6527E+05	5.3242E+05	4.8825E+05	4.4050E+05	4.0300E+05
POR	3.0618E+00	3.0949E+00	3.1419E+00	3.1972E+00	3.2817E+00	3.3157E+00
PFO	6.1112E+04	6.1102E+04	6.1087E+04	6.1073E+04	6.1041E+04	6.1017E+04
PRE	6.5479E+03	6.5576E+03	6.5724E+03	6.5826E+03	6.6150E+03	6.6423E+03

PAGE NUMBER = 6 TOTAL PAGES OF OUTPUT = 17

PAGE = --- (RIGHT JUSTIFIED)

# TABULAR OUTPUT - CONTINUED

## LONG RECOIL

TRANSIENT ANALYSIS RESULTS  
 125 RECOIL SYSTEM  
 43.5 B BREACH FORCE FOR DESIGN RUN - OAE = 800 MILS  
 CRITICAL AREA CALCULATION

TIME	1.1700E-02	1.20750E-02	1.23750E-02	1.29000E-02	1.30031E-02	1.30219E-02	1.30547E-02
SM1	3.68128E+00	3.89145E+00	4.25388E+00	4.52377E+00	4.33762E+00	4.35101E+00	4.37443E+00
UM1	6.97115E+02	7.03948E+02	7.14479E+02	7.14479E+02	7.14479E+02	7.14479E+02	7.13384E+02
R1	3.73000E+05	3.73000E+05	3.15083E+05	3.40480E+05	-1.47949E+05	-1.47642E+05	-1.47105E+05
POR	3.35775E+00	3.40480E+00	3.43883E+00	3.49139E+00	3.49110E+00	3.48938E+00	3.48638E+00
PFO	6.09361E+04						
PRE	6.66391E+03	6.69142E+03	6.71382E+03	6.73380E+03	6.76177E+03	6.76321E+03	6.76575E+03
TIME	1.30022E-02	1.31672E-02	1.32609E-02	1.34109E-02	1.36359E-02	1.39359E-02	1.44609E-02
SM1	4.40117E+00	4.45456E+00	4.52115E+00	4.62737E+00	4.78590E+00	4.99583E+00	5.35938E+00
UM1	7.12688E+02	7.11241E+02	7.09470E+02	7.06662E+02	7.02510E+02	6.97890E+02	6.87905E+02
R1	-1.46391E+05	-1.45264E+05	-1.43739E+05	-1.41276E+05	-1.37594E+05	-1.32885E+05	-1.24947E+05
POR	3.48296E+00	3.47616E+00	3.46779E+00	3.45431E+00	3.43450E+00	3.40855E+00	3.34841E+00
PFO	6.08914E+04	6.08556E+04	6.08783E+04	6.08668E+04	6.08435E+04	6.08255E+04	6.07863E+04
PRE	6.76864E+03	6.77443E+03	6.78165E+03	6.79321E+03	6.81051E+03	6.83353E+03	6.87370E+03
TIME	1.50609E-02	1.62609E-02	1.74609E-02	1.89609E-02	1.88109E-02	2.04489E-02	2.12109E-02
SM1	5.76907E+00	6.57097E+00	7.35121E+00	7.73379E+00	8.20288E+00	8.94489E+00	9.57080E+00
UM1	6.78292E+02	6.58933E+02	6.41706E+02	6.35900E+02	6.23293E+02	6.08923E+02	5.90622E+02
R1	-1.16547E+05	-1.08999E+05	-8.16216E+04	-8.16216E+04	-7.57674E+04	-6.94007E+04	-5.90622E+02
PCR	3.31681E+00	3.22700E+00	3.14475E+00	3.10613E+00	3.05922E+00	2.98882E+00	2.92292E+00
PFO	6.07406E+04	6.06496E+04	6.05593E+04	6.05142E+04	6.04581E+04	6.03683E+04	6.03096E+04
PRE	6.93432E+03	7.01038E+03	7.10075E+03	7.14576E+03	7.20186E+03	7.29133E+03	7.38045E+03
TIME	2.24109E-02	2.40609E-02	2.46609E-02	2.55609E-02	2.67609E-02	2.88609E-02	3.09609E-02
SM1	1.03732E+01	1.13195E+01	1.16564E+01	1.21564E+01	1.28107E+01	1.39246E+01	1.59011E+01
UM1	5.82012E+02	5.65200E+02	5.59365E+02	5.58004E+02	5.39737E+02	5.21330E+02	5.04145E+02
R1	-5.08029E+04	-4.20102E+04	-4.01417E+04	-3.73388E+04	-3.36017E+04	-2.70617E+04	-2.05217E+04
POR	2.86093E+00	2.78110E+00	2.75341E+00	2.71276E+00	2.66031E+00	2.57280E+00	2.49120E+00
PFO	6.01907E+04	6.00639E+04	6.00245E+04	5.99584E+04	5.98702E+04	5.97162E+04	5.95637E+04
PRE	7.46331E+03	7.59114E+03	7.63535E+03	7.70161E+03	7.78980E+03	7.94377E+03	8.09733E+03
TIME	3.15609E-02	3.23109E-02	3.35109E-02	3.53109E-02	3.74109E-02	3.86109E-02	4.04109E-02
SM1	1.53021E+01	1.56745E+01	1.62614E+01	1.71213E+01	1.80946E+01	1.86368E+01	1.94313E+01
UM1	4.99438E+02	4.93620E+02	4.8445E+02	4.71900E+02	4.56037E+02	4.47625E+02	4.35304E+02
R1	-1.95719E+04	-1.84648E+04	-1.66934E+04	-1.46362E+04	-1.10176E+04	-1.01253E+04	-8.78840E+03
POR	2.46884E+00	2.44121E+00	2.39779E+00	2.33408E+00	2.26235E+00	2.22330E+00	2.16322E+00
PFO	5.95189E+04	5.94641E+04	5.94574E+04	5.94574E+04	5.90934E+04	5.90066E+04	5.88769E+04
PRE	8.14114E+03	8.19587E+03	8.28333E+03	8.41426E+03	8.56566E+03	8.65335E+03	8.79314E+03
TIME	4.28109E-02	4.70109E-02	5.18109E-02	5.42109E-02	5.72109E-02	6.20109E-02	6.52109E-02
SM1	2.04563E+01	2.21578E+01	2.39624E+01	2.48098E+01	2.58191E+01	2.73149E+01	2.87440E+01
UM1	1.18980E+02	1.91408E+02	3.60652E+02	3.45532E+02	3.26748E+02	2.96955E+02	2.74816E+02
R1	-7.00507E+03	-4.86342E+03	-3.16861E+03	-2.54932E+03	-2.21726E+03	-1.91607E+03	-1.64131E+03
POR	2.08543E+00	1.95315E+00	1.80486E+00	1.71635E+00	1.64035E+00	1.49482E+00	1.36065E+00
PFO	5.87047E+04	5.84065E+04	5.80725E+04	5.79084E+04	5.77075E+04	5.73966E+04	5.71736E+04
PRE	8.95331E+03	9.25340E+03	9.58778E+03	9.76158E+03	9.95251E+03	1.02634E+04	1.04864E+04

PAGE NUMBER = 7 TOTAL PAGES OF OUTPUT = 17

SPACE = --- (RIGHT JUSTIFIED)

# TABULAR OUTPUT - CONTINUED

## LONG RECOIL

**TRANSIENT ANALYSIS RESULTS**

LONG RECOIL SYSTEM -  
 CASE 3 SHEET P FORCE FOR DESIGN RUN - OAE = 800 MILS  
 CRITICAL AREA CALCULATION

TITE	6.80109E-02	7.22109E-02	7.70109E-02	8.18109E-02	8.66109E-02	9.14109E-02	9.62109E-02
SM1	2.89859E+01	3.00245E+01	3.10799E+01	3.19955E+01	3.27714E+01	3.34089E+01	3.39955E+01
UM1	2.60119E+02	2.34478E+02	2.05293E+02	1.76182E+02	1.47135E+02	1.18132E+02	8.93592E+01
R1	-9.28362E+02	-6.90773E+02	-4.82274E+02	-3.61193E+02	-2.47337E+02	-1.34137E+02	-1.40037E+02
POR	1.31358E+00	1.18658E+00	1.04120E+00	8.95345E-01	7.49042E-01	6.02283E-01	4.55107E-01
PFO	5.70304E+04	5.67920E+04	5.65407E+04	5.63150E+04	5.61178E+04	5.59519E+04	5.58193E+04
PRE	1.06296E+04	1.08680E+04	1.11193E+04	1.13450E+04	1.15422E+04	1.17082E+04	1.18407E+04
TIME	1.01011E-01	1.05811E-01	1.06111E-01	1.06111E-01	1.06111E-01	1.06111E-01	1.06111E-01
SM1	3.42640E+01	3.44836E+01	3.45644E+01	3.45644E+01	3.45644E+01	3.45644E+01	3.45644E+01
UM1	6.02140E+01	3.12904E+01	2.38610E+00	2.38610E+00	2.38610E+00	2.38610E+00	2.38610E+00
R1	-9.54005E+01	-5.48371E+01	-1.42738E+01	-1.42738E+01	-1.42738E+01	-1.42738E+01	-1.42738E+01
POR	3.07625E-01	1.59945E-01	1.21993E-02	1.21993E-02	1.21993E-02	1.21993E-02	1.21993E-02
PFO	5.57224E+04	5.56624E+04	5.56408E+04	5.56408E+04	5.56408E+04	5.56408E+04	5.56408E+04
PRE	1.19376E+04	1.19976E+04	1.20198E+04	1.20198E+04	1.20198E+04	1.20198E+04	1.20198E+04

PAGE NUMBER = 8 TOTAL PAGES OF OUTPUT = 17

PAGE = ---- (RIGHT JUSTIFIED)

SUPER-SCEPTRE INPUT DECK  
EQUIVALANT ORIFICE AREA COMPUTATION  
SHORT RECOIL - M178

```

MECHANICAL DESCRIPTION
M109 RECOIL SYSTEM -
TABLE 2 BREACH FORCE FOR DESIGN RUN - QAE = 1333.33 MILS
ORIFICE AREA CALCULATION FOR SHORT RECOIL
ELEMENTS
M1,1-2=X1(PUT/PGR)
R1,2-1=TABLE 2 (TIME)
R2,2-1=X2(PUT*SIN(PANG))
R3,1-2=PRDPL
R6,1-2=X7(PMU*PUT*COS(PANG))*(67.15-SM1)/14.15)
DEFINED PARAMETERS
QAE=1333.33
PUT=4360
PGR=386.
PIE=X3(4.*ATAN(1.0))
PANG=X4(2.*PIE*QAE/6400.)
PAR=9.72
PP0=650
PU0=1015.
PN=1.6
PAB=32.98
PUF=.0313
PAE=1.
PMU=0.15
PRDPL=100000
PPAC=2340
PRE=X5(PAR*PP0/(1.-PAR*SM1/PU0))*PN)
PFO=X8(PRDPL-PRE-PPAC)
POR=X9(UM1*SQRT(PUF*PAB**3/2/PGR/PFO))
OUTPUTS
SM1,UM1,R1
POR,PFO,PRE
POR, PLOT(SM1)
FUNCTIONS
TABLE 2
0.,.32300,.002,184000,.006,1416000,.007,1390000
.008,1156000,.009,809000,.01,589000,.011,443000
.012,343000,.0129,276000,.013,-148000
.0141,-130000,.0156,-109000,.0175,-86000
.0211,-57900,.024,-42200,.031,-20400
.0373,-11100,.0445,-5750,.0526,-2890,.0648,-1110
.075,-533,.0861,-253,.0981,-120,.1123,0,.9,0
RUN CONTROLS
STOP TIME = .15
MAX INTEGRATION PASSES = 1E20
MINIMUM STEP SIZE = 1E-30
COMPUTER TIME LIMIT = 1
TERMINATE IF((UM1.LT.0).AND.(TIME.GT.0.01))
END
*EOR
8
DBEND

```

# TABULAR OUTPUT SHORT RECOIL

TRANSIENT ANALYSIS RESULTS  
 1-D SYSTEM -  
 TABULAR OUTPUT FOR DESIGN RUN - OAE - 1333.33 MILS  
 CASE - AREA CALCULATION FOR SHORT RECOIL

TIME	2.1875E-03	2.3025E-03	2.6065E-03	3.1870E-04	5.4375E-04	8.4375E-04	1.3687E-03
SRI	-2.5219E-03	-1.3451E-03	1.2016E-03	-2.5260E-04	-6.6254E-04	-1.3570E-03	4.7754E-03
UMI	1.8068E+00	3.1561E+00	1.1747E+01	-1.4743E+00	-2.1034E+00	-2.4134E+00	1.5016E+00
R1	1.8163E+05	2.2857E+05	7.7075E+05	5.6472E+04	7.3543E+04	9.6284E+04	1.3620E+05
POR	7.2096E-03	2.2718E-02	4.6875E-02	-5.8830E-03	-8.3932E-03	-9.5936E-03	5.9936E+05
PFO	9.1342E+04	9.1342E+04	9.1341E+04	9.1342E+04	9.1342E+04	9.1342E+04	9.1342E+04
PRE	6.3180E+03	6.3179E+03	6.3178E+03	6.3178E+03	6.3179E+03	6.3178E+03	6.3177E+03
TIME	1.9687E-03	2.1187E-03	2.6065E-03	3.1870E-04	5.4375E-04	8.4375E-04	1.3687E-03
SRI	-2.5219E-03	-1.3451E-03	1.2016E-03	-2.5260E-04	-6.6254E-04	-1.3570E-03	4.7754E-03
UMI	1.8068E+00	3.1561E+00	1.1747E+01	-1.4743E+00	-2.1034E+00	-2.4134E+00	1.5016E+00
R1	1.8163E+05	2.2857E+05	7.7075E+05	5.6472E+04	7.3543E+04	9.6284E+04	1.3620E+05
POR	7.2096E-03	2.2718E-02	4.6875E-02	-5.8830E-03	-8.3932E-03	-9.5936E-03	5.9936E+05
PFO	9.1342E+04	9.1342E+04	9.1341E+04	9.1342E+04	9.1342E+04	9.1342E+04	9.1342E+04
PRE	6.3180E+03	6.3179E+03	6.3178E+03	6.3178E+03	6.3179E+03	6.3178E+03	6.3177E+03
TIME	5.9065E-03	6.0770E-03	6.2625E-03	6.2625E-03	6.4500E-03	6.7500E-03	6.9937E-03
SRI	3.3467E-01	3.6700E-01	4.2743E-01	4.8230E-01	5.7854E-01	6.6437E-01	6.6437E-01
UMI	2.5522E+02	2.6426E+02	2.8172E+02	3.0347E+02	3.3830E+02	3.8001E+02	3.6603E+02
R1	1.4150E+06	1.4150E+06	1.4091E+06	1.4043E+06	1.3955E+06	1.3901E+06	1.3901E+06
POR	9.5908E-01	1.0198E+00	1.1242E+00	1.2125E+00	1.3454E+00	1.5354E+00	1.4611E+00
PFO	9.1305E+04	9.1305E+04	9.1304E+04	9.1295E+04	9.1295E+04	9.1277E+04	9.1277E+04
PRE	6.3505E+03	6.3536E+03	6.3590E+03	6.3649E+03	6.3741E+03	6.3828E+03	6.3828E+03
TIME	7.0687E-03	7.1812E-03	7.3325E-03	7.5937E-03	7.8937E-03	8.0825E-03	8.2315E-03
SRI	6.9215E-01	7.3500E-01	7.9427E-01	8.6392E-01	9.4377E-01	1.0286E-01	1.0986E+00
UMI	3.7462E+02	3.8721E+02	4.0359E+02	4.2114E+02	4.6087E+02	4.7817E+02	4.9182E+02
R1	1.3739E+06	1.3475E+06	1.3111E+06	1.2510E+06	1.1808E+06	1.1278E+06	1.0757E+06
POR	1.4954E+00	1.5457E+00	1.6116E+00	1.7212E+00	1.8400E+00	1.9140E+00	1.9637E+00
PFO	9.1274E+04	9.1274E+04	9.1264E+04	9.1253E+04	9.1240E+04	9.1231E+04	9.1222E+04
PRE	6.3855E+03	6.3898E+03	6.3956E+03	6.4063E+03	6.4197E+03	6.4285E+03	6.4357E+03
TIME	8.5312E-03	8.9062E-03	9.0375E-03	9.1125E-03	9.2250E-03	9.4500E-03	9.7500E-03
SRI	1.3498E+00	1.5488E+00	1.6287E+00	1.6622E+00	1.7463E+00	1.8533E+00	2.0284E+00
UMI	5.1644E+02	5.4339E+02	5.5173E+02	5.5635E+02	5.6527E+02	5.7598E+02	5.9214E+02
R1	9.7165E+05	8.4153E+05	8.0075E+05	7.8420E+05	7.5125E+05	7.1000E+05	6.4400E+05
POR	2.0622E+00	2.1599E+00	2.2053E+00	2.2227E+00	2.2577E+00	2.2991E+00	2.3617E+00
PFO	9.1209E+04	9.1189E+04	9.1181E+04	9.1177E+04	9.1169E+04	9.1158E+04	9.1146E+04
PRE	6.4509E+03	6.4708E+03	6.4823E+03	6.4823E+03	6.4908E+03	6.5016E+03	6.5194E+03
TIME	1.0012E-02	1.0162E-02	1.0387E-02	1.0687E-02	1.1025E-02	1.1175E-02	1.1400E-02
SRI	2.1852E+00	2.2762E+00	2.4144E+00	2.6017E+00	2.8161E+00	2.9156E+00	3.0582E+00
UMI	6.9325E+02	6.9635E+02	6.1844E+02	6.2961E+02	6.4061E+02	6.4585E+02	6.5141E+02
R1	5.8715E+05	5.6527E+05	5.3425E+05	4.8865E+05	4.4050E+05	4.2550E+05	4.0700E+05
POR	2.4100E+00	2.4356E+00	2.4718E+00	2.5160E+00	2.5602E+00	2.6037E+00	2.6472E+00
PFO	9.1124E+04	9.1116E+04	9.1110E+04	9.1108E+04	9.1105E+04	9.1103E+04	9.1103E+04
PRE	6.5354E+03	6.5447E+03	6.5559E+03	6.5787E+03	6.6004E+03	6.6105E+03	6.6255E+03

PAGE NUMBER - 8 TOTAL PAGES OF OUTPUT - 17

PAGE # --- (RIGHT JUSTIFIED)

# TABULAR OUTPUT - CONTINUED

## SHORT RECOIL

TRANSIENT ANALYSIS RESULTS  
 1109 0E-02 SYSTEM  
 TABULAR FORCE FOR DESIGN RUN - ONE • 1333.33 MILS  
 ORIGIN AREA CALCULATION FOR SHORT RECOIL

TIME	1.1700E-02	1.20750E-02	1.23750E-02	1.29000E-02	1.30031E-02	1.30219E-02	1.30547E-02
SY	3.2593E+00	3.5036E+00	3.7051E+00	4.0613E+00	4.1310E+00	4.1466E+00	4.1670E+00
UM	6.6716E+02	6.7716E+02	6.73817E+02	6.8306E+02	6.82709E+02	6.82303E+02	6.81594E+02
R	3.7400E+05	3.37417E+05	3.15083E+05	2.7600E+05	-1.47948E+05	-1.47642E+05	-1.4710E+05
POR	2.6349E+00	2.66957E+00	2.69427E+00	2.7318E+00	2.73051E+00	2.7283E+00	2.7261E+00
PFO	9.0974E+04	9.0966E+04	9.0966E+04	9.0928E+04	9.0920E+04	9.09150E+04	9.09166E+04
PRE	6.74637E+03	6.67661E+03	6.69395E+03	6.7320E+03	6.73959E+03	6.74096E+03	6.74337E+03
TIME	1.30922E-02	1.31672E-02	1.32609E-02	1.34109E-02	1.36359E-02	1.39359E-02	1.44609E-02
SM	4.1925E+00	4.2435E+00	4.30715E+00	4.4085E+00	4.55962E+00	4.7594E+00	5.10487E+00
JM	6.80787E+02	6.79177E+02	6.7717E+02	6.7400E+02	6.69301E+02	6.63148E+02	6.52681E+02
R	-1.46491E+05	-1.45264E+05	-1.43730E+05	-1.41276E+05	-1.37594E+05	-1.32685E+05	-1.24947E+05
POR	2.72292E+00	2.71657E+00	2.70867E+00	2.69613E+00	2.67757E+00	2.6537E+00	2.61194E+00
PFO	9.09139E+04	9.09084E+04	9.09015E+04	9.0890E+04	9.08742E+04	9.0854E+04	9.08145E+04
PRE	6.74612E+03	6.75161E+03	6.75848E+03	6.76944E+03	6.78583E+03	6.80762E+03	6.84554E+03
TIME	1.50609E-02	1.62609E-02	1.74609E-02	1.80609E-02	1.88109E-02	2.00109E-02	2.12109E-02
SM	5.49299E+00	6.24911E+00	6.98004E+00	7.37663E+00	7.77142E+00	8.45714E+00	9.1190E+00
JM	6.41139E+02	6.1935E+02	5.90147E+02	5.89563E+02	5.77930E+02	5.6017E+02	5.3328E+02
R	-1.16547E+05	-1.09999E+05	-8.16547E+04	-8.18216E+04	-7.57674E+04	-6.64007E+04	-5.72994E+04
POR	2.56636E+00	2.48034E+00	2.40051E+00	2.3626E+00	2.31669E+00	2.24634E+00	2.17999E+00
PFO	9.07714E+04	9.05864E+04	9.06035E+04	9.05610E+04	9.05934E+04	9.04279E+04	9.03473E+04
PRE	6.88856E+03	6.97364E+03	7.05752E+03	7.09904E+03	7.15956E+03	7.23213E+03	7.31267E+03
TIME	2.24109E-02	2.40609E-02	2.46609E-02	2.56609E-02	2.67609E-02	2.88609E-02	3.09609E-02
SM	1.0871E+01	1.06141E+01	1.09158E+01	1.13601E+01	1.19377E+01	1.29089E+01	1.38319E+01
JM	5.2322E+02	5.06467E+02	4.99161E+02	4.89388E+02	4.74373E+02	4.5089E+02	4.28452E+02
R	-5.08029E+04	-4.20102E+04	-4.01417E+04	-3.73388E+04	-3.36917E+04	-2.70617E+04	-2.05217E+04
POR	2.11667E+00	2.03415E+00	2.00524E+00	1.95259E+00	1.90708E+00	1.81364E+00	1.72494E+00
PFO	9.02678E+04	9.01600E+04	9.01212E+04	9.00636E+04	8.99875E+04	8.9858E+04	8.97292E+04
PRE	7.39222E+03	7.50001E+03	7.53877E+03	7.58645E+03	7.67250E+03	7.8039E+03	7.93078E+03
TIME	3.15609E-02	3.23109E-02	3.35109E-02	3.5109E-02	3.74109E-02	3.86109E-02	4.04109E-02
SM	1.40871E+01	1.4009E+01	1.48912E+01	1.55995E+01	1.63860E+01	1.68165E+01	1.74368E+01
JM	4.23267E+02	4.14602E+02	4.02491E+02	3.84679E+02	3.64435E+02	3.5301E+02	3.36204E+02
R	-1.97719E+04	-1.84648E+04	-1.66934E+04	-1.49362E+04	-1.10176E+04	-1.01259E+04	-8.28840E+03
POR	1.70038E+00	1.66993E+00	1.62179E+00	1.55091E+00	1.47026E+00	1.42493E+00	1.35759E+00
PFO	8.96933E+04	8.96489E+04	8.96786E+04	8.94752E+04	8.93579E+04	8.9295E+04	8.91965E+04
PRE	7.96666E+03	8.01114E+03	8.08144E+03	8.18400E+03	8.30210E+03	8.36747E+03	8.46315E+03
TIME	4.2109E-02	4.70109E-02	5.18109E-02	5.42109E-02	5.72109E-02	6.20109E-02	6.56109E-02
SM	1.82170E+01	1.94560E+01	2.06785E+01	2.12134E+01	2.18111E+01	2.2602E+01	2.30680E+01
JM	3.14048E+02	2.76083E+02	2.33431E+02	2.1235E+02	1.86122E+02	1.4435E+02	1.13294E+02
R	-7.09507E+03	-4.86342E+03	-3.1686E+03	-2.6549E+03	-2.1226E+03	-1.5163E+03	-1.06413E+03
POR	1.2590E+00	1.1158E+00	0.9546E+00	8.609E-01	7.5456E-01	5.8593E-01	4.595E-01
PFO	8.9740E+04	8.8828E+04	8.6666E+04	8.5749E+04	8.4686E+04	8.3256E+04	8.240E+04
PRE	8.8603E+03	8.7872E+03	8.5933E+03	8.4604E+03	8.2844E+03	7.9344E+03	7.41970E+03

PAGE NUMBER • 7 TOTAL PAGES OF OUTPUT • 17

PAGE • (RIGHT JUSTIFIED)

# TABULAR OUTPUT - CONTINUED

## SHORT RECOIL

TRANSIENT ANALYSIS RESULTS  
 SHORT RECOIL SYSTEM -  
 148.23 INCH FORCE FOR DESIGN RUN - OAE • 1333.33 MILS  
 COMPLETE WPEM CALCULATION FOR SHORT RECOIL

TIME	6.8010E-02	7.2210E-02	7.7010E-02
S/A	2.3315E+01	2.3622E+01	2.3806E+01
V/I	9.2618E+01	5.6503E+01	1.5338E+01
A	-9.2836E+02	-6.0073E+02	-4.8227E+02
PCR	3.7611E-01	2.2953E-01	6.2318E-02
PFC	8.8194E+04	8.8135E+04	8.8103E+04
PRE	9.4656E+03	9.5244E+03	9.5570E+03

PAGE NUMBER • 8 TOTAL PAGES OF OUTPUT • 17

PAGE • --- (RIGHT JUSTIFIED)

APPENDIX B  
M178 RECOIL MECHANISM MODEL

# SUPER-SCEPTRE INPUT DECK M178 RECOIL MECHANISM MODEL

## MECHANICAL DESCRIPTION

M109 RECOIL SYSTEM -  
TABLE 2 BREECH FORCE FOR DESIGN RUN - QAE = 800 MILS  
FIRING WITH KNOWN ORIFACE AREA  
TABLE 1 HAS DUPONT GYMMER DATA  
TABLE 4 HAS SIMPLIFIED GYMMER DATA

## ELEMENTS

M1,1-2=X1(PUT/PGR)  
R1,2-1=TABLE 2 (TIME)  
R2,2-1=X2(PUTXSIN(PANG))  
R3,1-2=PRDPL  
R6,1-2=X7(PMU\*PUTXCOS(PANG)\*(67.15-SM1)/14.15)

## DEFINED PARAMETERS

PQAE=800.  
PUT=4360  
PGR=386.  
PIE=X3(4.\*ATAN(1.0))  
PANG=X4(2.\*PIE\*PQAE/6400.)  
PAR=9.72  
PP0=650  
PU0=1015.  
PN=1.6  
PAB=32.98  
PUF=.0313  
PAE=TABLE 3 (SM1)  
PMU=0.15  
PPAC=2340  
PRE=X5(PAR\*PP0/(1.-PAR\*SM1/PU0)\*PN)  
PBR=X8(PAB\*X13\*UM1\*X2\*PUF/PAE\*X2/2./PGR)  
PRDPL=X9(PRE+PPAC+PBR)  
PRESS=X10(PBR/PAB)

## OUTPUTS

SM1,UM1,R1  
PRESS,PRDPL,PRE  
PAE, PLOT(SM1)

## FUNCTIONS

### TABLE 1

-1.,0,0,0,0,0038,1180000,006,610000,016,80000,026,0.

### TABLE 4

-1.,0,0,0,0,0036,1180000,0060,560000,0067,710000  
.0080,580000,009,310000,01,405000,0110,380000  
.012,150000,0135,280000,0156,12000,017,150000,019,0  
.0205,90000,022,0,0235,75000,026,0

### TABLE 2

0.,32300,002,184000,006,1416000,007,1390000  
.008,1156000,009,809000,01,589000,011,443000  
.012,343000,0129,276000,013,-148000  
.0141,-130000,0156,-109000,0175,-86000  
.0211,-57900,024,-42200,031,-20400  
.0373,-11100,0445,-5750,0526,-2890,0648,-1110  
.075,-533,0861,-253,0981,-120,1123,0,9,0

### TABLE 3

-10.,0.5,0.,0.5,53,1.55,1.11,2.34,1.65,2.75,2.14,3.00  
3.06,3.28,4.26,3.49,4.63,3.45,5.35,3.36,7.35,3.19  
11.3,2.78,15.3,2.47,20.5,2.09,30.0,1.19,31.1,1.04  
33.4,0.602,34.0,0.50,40.0,0.50

## RUN CONTROLS

STOP TIME = .15  
MAX INTEGRATION PASSES = 1E20  
MINIMUM STEP SIZE = 1E-30  
COMPUTER TIME LIMIT = 1  
TERMINATE IF((UM1.LT.0).AND.(TIME.GT.0.01))  
END  
Xeor  
8  
DBEND

# TABULAR OUTPUT M178 MODEL

STRESS/STRAIN ANALYSIS RESULTS  
 22 NODS - SYSTEM  
 TABLE 3 STRESS FORCE FOR DESIGN RUN - ONE - 800 MILS  
 FINISH - 174 KNOWN STRIPFACE AREA  
 TABLE 1 HAS SUPPORT MEMBER DATA  
 TABLE 2 HAS SIMPLIFIED MEMBER DATA

TIME	9.3750E-05	2.4375E-04	4.6875E-04	8.4375E-04	1.5187E-03	2.8031E-03	5.0625E-03	8.9375E-03	1.5187E-03	2.8031E-03	5.0625E-03	8.9375E-03	1.5187E-03	2.8031E-03	5.0625E-03	8.9375E-03	1.5187E-03	2.8031E-03	5.0625E-03	8.9375E-03	1.5187E-03	2.8031E-03	5.0625E-03	8.9375E-03	
SRI	9.9873E-06	7.0840E-06	3.5107E-04	2.5107E-04	1.4024E-03	8.2385E-02	5.2555E-01	2.5255E-01	1.4024E-03	8.2385E-02	5.2555E-01	2.5255E-01	1.4024E-03	8.2385E-02	5.2555E-01	2.5255E-01	1.4024E-03	8.2385E-02	5.2555E-01	2.5255E-01	1.4024E-03	8.2385E-02	5.2555E-01	2.5255E-01	
U1	3.3192E-01	7.2764E-01	1.7643E+00	4.4363E+00	1.0206E+01	2.3963E+01	5.5719E+01	1.3878E+02	3.0206E+01	7.2764E+01	1.7643E+02	4.4363E+02	1.0206E+03	2.3963E+03	5.5719E+03	1.3878E+04	3.0206E+04	7.2764E+04	1.7643E+05	4.4363E+05	1.0206E+06	2.3963E+06	5.5719E+06	1.3878E+07	3.0206E+07
R1	3.2300E+04	9.9410E+04	6.0788E+04	3.9410E+04	2.4847E+04	1.5933E+06	1.0993E+06	1.8238E+06	9.9410E+04	6.0788E+04	3.9410E+04	2.4847E+04	1.5933E+06	1.0993E+06	1.8238E+06	1.5933E+06	1.0993E+06	6.0788E+04	3.9410E+04	2.4847E+04	1.5933E+06	1.0993E+06	1.8238E+06	1.5933E+06	
PRESS	0.6500E+03	9.4877E-03	3.3372E-02	5.4140E-01	3.1052E+00	1.4593E+03	1.4593E+03	1.4593E+03	3.1052E+00	5.4140E-01	3.3372E-02	9.4877E-03	9.4877E-03	3.3372E-02	5.4140E-01	3.1052E+00	1.4593E+03	1.4593E+03	1.4593E+03	3.1052E+00	5.4140E-01	3.3372E-02	9.4877E-03	9.4877E-03	
PRDPL	8.6500E+03	8.6500E+03	8.6500E+03	8.6500E+03	8.6500E+03	8.6500E+03	8.6500E+03	8.6500E+03	8.6500E+03	8.6500E+03	8.6500E+03	8.6500E+03	8.6500E+03												
PNE	5.0000E-01	5.0000E-01	5.0000E-01	5.0000E-01	5.0000E-01	5.0000E-01	5.0000E-01	5.0000E-01	5.0000E-01	5.0000E-01	5.0000E-01	5.0000E-01	5.0000E-01												
TIME	2.2312E-03	2.6625E-03	3.2062E-03	3.8604E-03	4.6250E-03	5.5000E-03	6.4875E-03	7.5875E-03	8.8000E-03	1.0125E-02	1.1562E-02	1.3125E-02	1.4812E-02	1.6625E-02	1.8562E-02	2.0625E-02	2.2812E-02	2.5125E-02	2.7562E-02	3.0125E-02	3.2812E-02	3.5625E-02	3.8562E-02	4.1625E-02	
SRI	1.7999E-02	2.7801E-02	3.8604E-02	5.0406E-02	6.3208E-02	7.7010E-02	9.1812E-02	1.0761E-01	1.2473E-01	1.4335E-01	1.6347E-01	1.8509E-01	2.0831E-01	2.3313E-01	2.5955E-01	2.8767E-01	3.1749E-01	3.4901E-01	3.8223E-01	4.1715E-01	4.5367E-01	4.9179E-01	5.3161E-01	5.7323E-01	
U1	2.1999E+01	3.7019E+01	5.5555E+01	7.7667E+01	1.0333E+02	1.3250E+02	1.6528E+02	2.0167E+02	2.4167E+02	2.8533E+02	3.3267E+02	3.8367E+02	4.3833E+02	4.9667E+02	5.5867E+02	6.2433E+02	6.9367E+02	7.6667E+02	8.4333E+02	9.2367E+02	1.0073E+03	1.0943E+03	1.1843E+03	1.2773E+03	
R1	7.4955E+01	1.4570E+02	3.7323E+02	8.0928E+02	1.4116E+03	2.0928E+03	2.8319E+03	3.6208E+03	4.4593E+03	5.3478E+03	6.2858E+03	7.2733E+03	8.3108E+03	9.3983E+03	1.0535E+04	1.1728E+04	1.2973E+04	1.4270E+04	1.5613E+04	1.7003E+04	1.8440E+04	1.9923E+04	2.1450E+04	2.3023E+04	
PRESS	1.7154E+03	1.4991E+04	1.3499E+04	1.1168E+04	8.7828E+03	6.3208E+03	3.8231E+03	1.3499E+03	8.7828E+03	6.3208E+03	3.8231E+03	1.3499E+03	8.7828E+03	6.3208E+03	3.8231E+03	1.3499E+03	8.7828E+03	6.3208E+03	3.8231E+03	1.3499E+03	8.7828E+03	6.3208E+03	3.8231E+03	1.3499E+03	
PRDPL	6.5283E+03	6.7536E+04	7.0079E+04	7.2883E+04	7.5936E+04	7.9240E+04	8.2793E+04	8.6596E+04	9.0649E+04	9.4952E+04	9.9505E+04	1.04308E+05	1.09361E+05	1.14714E+05	1.20367E+05	1.26320E+05	1.32573E+05	1.39126E+05	1.45979E+05	1.53132E+05	1.60585E+05	1.68338E+05	1.76391E+05	1.84744E+05	
PNE	6.3697E+03	6.3756E+03	6.3871E+03	6.3944E+03	6.4079E+03	6.4184E+03	6.4258E+03	6.4303E+03	6.4328E+03	6.4333E+03	6.4328E+03	6.4303E+03	6.4258E+03	6.4184E+03	6.4079E+03	6.3944E+03	6.3871E+03	6.3756E+03	6.3697E+03	6.3697E+03	6.3697E+03	6.3697E+03	6.3697E+03	6.3697E+03	6.3697E+03
TIME	7.8937E-03	8.1175E-03	8.3812E-03	8.6859E-03	9.0316E-03	9.4183E-03	9.8460E-03	1.0315E-02	1.0808E-02	1.1331E-02	1.1884E-02	1.2467E-02	1.3080E-02	1.3723E-02	1.4396E-02	1.5099E-02	1.5832E-02	1.6595E-02	1.7388E-02	1.8211E-02	1.9064E-02	1.9947E-02	2.0860E-02	2.1803E-02	
SRI	1.2417E+00	1.3572E+00	1.4795E+00	1.6086E+00	1.7443E+00	1.8866E+00	2.0355E+00	2.1908E+00	2.3525E+00	2.5206E+00	2.6951E+00	2.8760E+00	3.0633E+00	3.2570E+00	3.4571E+00	3.6636E+00	3.8765E+00	4.0958E+00	4.3215E+00	4.5536E+00	4.7921E+00	5.0370E+00	5.2883E+00	5.5460E+00	
U1	5.0810E+02	5.2414E+02	5.4735E+02	5.7644E+02	6.1143E+02	6.5242E+02	6.9941E+02	7.5240E+02	8.1139E+02	8.7638E+02	9.4737E+02	1.02436E+03	1.10655E+03	1.19434E+03	1.28773E+03	1.38672E+03	1.49131E+03	1.60150E+03	1.71729E+03	1.83868E+03	1.96567E+03	2.09826E+03	2.23645E+03	2.38024E+03	
R1	1.1800E+06	1.1147E+06	1.0237E+06	9.0681E+05	7.7475E+05	6.2819E+05	4.7713E+05	3.2157E+05	1.6151E+05	8.6985E+04	4.5639E+04	2.3813E+04	1.2407E+04	6.2531E+03	3.1905E+03	1.6129E+03	8.0649E+02	4.0323E+02	2.0161E+02	1.0080E+02	5.0400E+01	2.5200E+01	1.2600E+01	6.3000E+00	
PRESS	1.8711E+03	1.8711E+03	1.8711E+03	1.8711E+03	1.8711E+03	1.8711E+03	1.8711E+03	1.8711E+03	1.8711E+03	1.8711E+03	1.8711E+03	1.8711E+03	1.8711E+03												
PRDPL	7.0490E+04	7.1325E+04	7.2150E+04	7.2975E+04	7.3800E+04	7.4625E+04	7.5450E+04	7.6275E+04	7.7100E+04	7.7925E+04	7.8750E+04	7.9575E+04	8.0400E+04	8.1225E+04	8.2050E+04	8.2875E+04	8.3700E+04	8.4525E+04	8.5350E+04	8.6175E+04	8.7000E+04	8.7825E+04	8.8650E+04	8.9475E+04	
PNE	6.4400E+03	6.4565E+03	6.4730E+03	6.4895E+03	6.5060E+03	6.5225E+03	6.5390E+03	6.5555E+03	6.5720E+03	6.5885E+03	6.6050E+03	6.6215E+03	6.6380E+03	6.6545E+03	6.6710E+03	6.6875E+03	6.7040E+03	6.7205E+03	6.7370E+03	6.7535E+03	6.7700E+03	6.7865E+03	6.8030E+03	6.8195E+03	
TIME	9.8750E-03	1.0012E-02	1.0154E-02	1.0296E-02	1.0438E-02	1.0580E-02	1.0722E-02	1.0864E-02	1.1006E-02	1.1148E-02	1.1290E-02	1.1432E-02	1.1574E-02	1.1716E-02	1.1858E-02	1.2000E-02	1.2142E-02	1.2284E-02	1.2426E-02	1.2568E-02	1.2710E-02	1.2852E-02	1.2994E-02	1.3136E-02	
SRI	2.2623E+00	2.4023E+00	2.5423E+00	2.6823E+00	2.8223E+00	2.9623E+00	3.1023E+00	3.2423E+00	3.3823E+00	3.5223E+00	3.6623E+00	3.8023E+00	3.9423E+00	4.0823E+00	4.2223E+00	4.3623E+00	4.5023E+00	4.6423E+00	4.7823E+00	4.9223E+00	5.0623E+00	5.2023E+00	5.3423E+00	5.4823E+00	
U1	6.3336E+02	6.4966E+02	6.6596E+02	6.8226E+02	6.9856E+02	7.1486E+02	7.3116E+02	7.4746E+02	7.6376E+02	7.8006E+02	7.9636E+02	8.1266E+02	8.2896E+02	8.4526E+02	8.6156E+02	8.7786E+02	8.9416E+02	9.1046E+02	9.2676E+02	9.4306E+02	9.5936E+02	9.7566E+02	9.9196E+02	1.00826E+03	
R1	6.0600E+05	5.8715E+05	5.6830E+05	5.4945E+05	5.3060E+05	5.1175E+05	4.9290E+05	4.7405E+05	4.5520E+05	4.3635E+05	4.1750E+05	3.9865E+05	3.7980E+05	3.6095E+05	3.4210E+05	3.2325E+05	3.0440E+05	2.8555E+05	2.6670E+05	2.4785E+05	2.2900E+05	2.1015E+05	1.9130E+05	1.7245E+05	
PRESS	1.8161E+03	1.8161E+03	1.8161E+03	1.8161E+03	1.8161E+03	1.8161E+03	1.8161E+03	1.8161E+03	1.8161E+03	1.8161E+03	1.8161E+03	1.8161E+03	1.8161E+03												
PRDPL	7.8870E+04	7.8870E+04	7.8870E+04	7.8870E+04	7.8870E+04	7.8870E+04	7.8870E+04	7.8870E+04	7.8870E+04	7.8870E+04	7.8870E+04	7.8870E+04	7.8870E+04												
PNE	6.8437E+03	6.8437E+03	6.8437E+03	6.8437E+03	6.8437E+03	6.8437E+03	6.8437E+03	6.8437E+03	6.8437E+03	6.8437E+03	6.8437E+03	6.8437E+03	6.8437E+03												
TIME	3.0304E+00	3.1410E+00	3.2516E+00	3.3622E+00	3.4728E+00	3.5834E+00	3.6940E+00	3.8046E+00	3.9152E+00	4.0258E+00	4.1364E+00	4.2470E+00	4.3576E+00	4.4682E+00	4.5788E+00	4.6894E+00	4.8000E+00	4.9106E+00	5.0212E+00	5.1318E+00	5.2424E+00	5.3530E+00	5.4636E+00	5.5742E+00	

PAGE NUMBER = 6 TOTAL PAGES OF OUTPUT = 19  
 PAGE = (RIGHT JUSTIFIED)



# TABULAR OUTPUT - CONTINUED

## M178 MODEL

TRANSIENT ANALYSIS RESULTS  
 11.25 RECON SYSTEM  
 9-2-53 BREACH FORCE FOR DESIGN RUN - ONE - 800 MILS  
 FRACTURE - WITH INJURY ORIFACE AREA  
 TABLE 1 HAS INPUT CYMNER DATA  
 TABLE 4 HAS SIMPLIFIED CYMNER DATA

TIME	6.95109E-02	7.10109E-02	7.37109E-02	7.67109E-02	7.97109E-02	8.27109E-02	8.57109E-02
SFI	3.00839E+01	3.03839E+01	3.06839E+01	3.10000E+01	3.21551E+01	3.56501E+01	3.30839E+01
UFI	2.42200E+02	2.31000E+02	2.14313E+02	1.94555E+02	1.70544E+02	1.54094E+02	1.35866E+02
R1	-8.42600E+02	-7.58066E+02	-6.66920E+02	-4.88041E+02	-4.14166E+02	-3.38490E+02	-2.02144E+02
PRESS	1.82424E+03	1.82709E+03	1.81785E+03	1.87769E+03	1.91900E+03	1.98974E+03	1.84156E+03
PRDPL	7.37255E+04	7.35697E+04	7.33890E+04	7.55128E+04	7.70250E+04	7.69345E+04	7.46982E+04
PRE	1.06931E+04	1.09525E+04	1.09965E+04	1.12466E+04	1.13851E+04	1.15116E+04	1.18366E+04
PAE	1.18001E+00	1.13706E+00	1.05556E+00	9.44792E-01	8.39078E-01	7.44803E-01	6.61980E-01
TIME	8.87109E-02	9.17109E-02	9.44109E-02	9.62109E-02	9.92109E-02	1.02211E-01	1.05211E-01
SFI	3.34625E+01	3.37832E+01	3.40332E+01	3.41788E+01	3.43024E+01	3.45758E+01	3.47343E+01
UFI	1.16385E+02	9.90377E+01	8.50268E+01	7.69827E+01	6.58443E+01	5.67590E+01	4.91360E+01
R1	-2.24062E+02	-1.90812E+02	-1.60887E+02	-1.40937E+02	-1.10612E+02	-8.52597E+01	-5.99076E+01
PRESS	1.70810E+03	1.50240E+03	1.27526E+03	1.04538E+03	7.64758E+02	5.68274E+02	4.25800E+02
PRDPL	7.03956E+04	6.37006E+04	5.62731E+04	4.87311E+04	3.95344E+04	3.21047E+04	2.84232E+04
PRE	1.17226E+04	1.18084E+04	1.18750E+04	1.19145E+04	1.19726E+04	1.20230E+04	1.20668E+04
PAE	5.91371E-01	5.36531E-01	5.00000E-01	5.00000E-01	5.00000E-01	5.00000E-01	5.00000E-01
TIME	1.02211E-01	1.14211E-01	1.20211E-01	1.20211E-01	1.22211E-01	1.20211E-01	1.20211E-01
SFI	3.48717E+01	3.50933E+01	3.52561E+01	3.53691E+01	3.54378E+01	3.54662E+01	3.54732E+01
UFI	4.25071E+01	3.17209E+01	2.28005E+01	1.50363E+01	7.95353E+00	1.20616E+00	0.
R1	-3.45555E+01	0.	0.	0.	0.	0.	0.
PRESS	3.19233E+02	1.77581E+02	9.17019E+01	3.98814E+01	1.11586E+01	2.56624E-01	2.56624E-01
PRDPL	2.49000E+04	2.03036E+04	1.75771E+04	1.50000E+04	1.49723E+04	1.48206E+04	1.48206E+04
PRE	1.21049E+04	1.21649E+04	1.22127E+04	1.22447E+04	1.22643E+04	1.22720E+04	1.22720E+04
PAE	5.00000E-01						

PAGE NUMBER = 8 TOTAL PAGES OF OUTPUT = 19

PAGE = --- (RIGHT JUSTIFIED)

APPENDIX C

ST. CHAMOND RECOIL MECHANISM MODEL.

# SUPER-SCEPTRE INPUT DECK

## St. CHAMOND

100=MECHANICAL DESCRIPTION  
110=M109 RECOIL SYSTEM -  
120=QAE = 0 MILS  
130=FIRING WITH KNOWN ORIFACE AREA  
140=AND WITH AUTOMATIC CONTROL UALUE  
150=JITH LEVEL 1 CONTROL ONLY (ST CHAMOND)  
160=SET PSRDPL TO DESIRED MAXIMUM RODPULL  
170=USING SMOOTHER DUPONT DATA FOR BREECH FORCE  
180=ELEMENTS  
190=M1,1-2=X1(PUT/PGR)  
200=R1,2-1=TABLE 1 (TIME)  
210=R2,2-1=X2(PUTXSIN(PANG))  
220=R3,1-2=PRDPL  
230=R6,1-2=X7(PMU\*PUT\*COS(PANG)\*(67.15-SM1)/14.15)  
240=DEFINED PARAMETERS  
250=PQAE=0.  
260=PUT=4360  
270=PGR=386.  
280=PIE=X3(4.\*ATAN(1.0))  
290=PANG=X4(2.\*PIE\*PQAE/6400.)  
300=PAR=9.72  
310=PP0=650  
320=PU0=1015.  
330=PN=1.6  
340=PAB=32.98  
350=PUF=.0313  
360=PA0=TABLE 3 (SM1)  
370=PE=X12(PRDPL-PDRDPL)  
380=PSRDPL=70000  
390=PDRDPL=X13(PSRDPL)  
400=PAT=TABLE 4 (PE)  
410=PAD=X17(PAT)  
420=PTAU=.01  
430=DPAA=X16((PAD-PAA)/PTAU)  
440=PAA=0.  
450=PON=1  
460=PAE=X15(PA0+PON\*PAA)  
470=PMU=0.15  
480=PPAC=2340  
490=PRE=X5(PAR\*PP0/(1.-PAR\*SM1/PU0)\*PN)  
500=PSR=X8(PAB\*X3\*UM1\*X2\*PUF/PAE\*X2/2./PGR)  
510=PRDPL=X9(PRE+PPAC+PBR)  
520=PRESS=X10(PBR/PAB)  
530=OUTPUTS  
540=SM1,PDRDPL,PRDPL,PAA,PAD  
550=PRESS

..

# St. CHAMOND, INPUT DECK - CONTINUED

```

520=FUNCTIONS
570=TABLE 1
520=-.1,0,0,0,.0036,1180000,.006,610000,.016,80000,.026,0
590=.9,0
600=TABLE 2
610=0,.32300,.002,184000,.006,1416000,.007,1390000
620=.008,1156000,.009,809000,.01,589000,.011,443000
630=.012,343000,.0129,276000,.013,-148000
640=.0141,-130000,.0156,-109000,.0175,-86000
650=.0211,-57900,.024,-42200,.031,-20400
660=.0373,-11100,.0445,-5750,.0526,-2890,.0648,-1110
670=.075,-533,.0861,-253,.0981,-120,.1123,0,.9,0
680=TABLE 3
690=-10,.05,0,.05,.53,1.55,1.11,2.34,1.65,2.75,2.14,3.00
700=3.06,3.28,4.26,3.49,4.63,3.45,5.35,3.36,7.35,3.19
710=11.3,2.78,15.3,2.47,20.5,2.09,30.0,1.19,31.1,1.04
720=33.4,0.602,34.0,0.50,40.0,0.50
730=TABLE 4
740=-100000,0,-.001,0,.001,1,100000,1.
750=TABLE 5
760=-10000,0,10000,0.
770=TABLE 6
780=-1,0,0,0,.0036,1180000,.006,560000,.0067,710000
790=.008,580000,.009,310000,.01,405000,.011,380000
800=.012,150000,.0135,280000,.0156,12000,.017,150000
810=.019,0,.0205,900000,.022,0,.0235,75000,.026,0
820=.9,0.
830=TABLE 7
840=-100,0,2,0,2,1,100,1
850=RUN CONTROLS
860=STOP TIME = .15
870=MAX INTEGRATION PASSES = 1E20
880=MINIMUM STEP SIZE = 1E-30
890=COMPUTER TIME LIMIT = 1
900=TERMINATE IF((UMI.LT.-1).AND.(TIME.GT.0.01))
910=MECHANICAL RERUN DESCRIPTION
920=DEFINED PARAMETERS
930=PSRDPL=75000
940=MECHANICAL RERUN DESCRIPTION
950=DEFINED PARAMETERS
960=PSRDPL=80000
970=MECHANICAL RERUN DESCRIPTION
980=DEFINED PARAMETERS
990=PSRDPL=90000
1000=END
1010=IEOR
1020=S
1030= DBEND

```

APPENDIX D  
FULL AUTOMATIC CONTROL MODELS

# SUPER-SCEPTRE INPUT DECK AUTOMATIC CONTROL - M203 IMPULSE

```

MECHANICAL DESCRIPTION
M173 RECOIL MECHANISM
PIPEING WITH KNOWN ORIFACE AREA (LONG NOSE)
AUTOMATIC CONTROL-FULL LEVEL2
ELEVATION - 45 DEGREES
USE M203 CHARGE DATA (TABLE 2)
ELEMENTS
M1,1-2*X1(PUT/PGR)
R1,2-1*TABLE 2 (TIME)
R3,2-1*X2(PUT&SIN(PANG))
R3,1-2*PRDPL
R6,1-2*X7(PMU&PUT&COS(PANG))*((67.15-SM1)/14.15)
DEFINED PARAMETERS
PQAE=800.
PUT=4360
PGR=386.
PIE=X3(4.*ATAN(1.0))
PANG=X4(2.*PIE&PQAE/6400)
PAR=9.72
PP0=650
PUO=1015.
PN=1.6
PAB=32.98
PUF=.0313
PAO=TABLE 3 (SM1)
PE=X12(PRDPL-PDRDPL)
PSRDPL=70000
PSWITCH=TABLE 5 (AM1)
PXLEFT=X18(PX-SM1)
PSU2=TABLE 7 (PXLEFT)
PCRDPL=X14(PUT&UM1&UM1/PGR/2/PXLEFT+PUT&SIN(PANG))
PSX=35.
PDRDPL=X13(((1-PSWITCH)&PSRDPL+PSWITCH&PCRDPL)
PAT=TABLE 4 (PE)
PAD=X17(PAT&PSU2)
PTAU=.01
DPAA=X16((PAD-PAA)/PTAU)
PAA=0.
PON=1
PAE=X15(PAO+PON&PAA)
PMU=0.15
PPAC=2340
PRE=X5(PAR&PP0/(1.-PAR&SM1/PUO)&PN)
PBR=X8(PAB&X3&UM1&X2&PUF/PAE&X2/2./PGR)
PRDPL=X9(PRE+PPAC+PBR)
PRESS=X10(PBR/PAB)
OUTPUTS
SM1,UM1,R1
PRESS,PRDPL,PRE
PAA,PAD
PSWITCH,PDRDPL,PCRDPL
FUNCTIONS
TABLE 2
0.,.32300.,.002,184000.,.006,1416000.,.007,1390000
.008,1156000.,.009,899000.,.01,589000.,.011,443000
.012,343000.,.0129,276000.,.013,-148000
.0141,-130000.,.0156,-109000.,.0175,-86000
.0211,-57000.,.024,-42200.,.031,-20400
.0373,-11100.,.0445,-5750.,.0526,-2890.,.0648,-1110
.075,-533.,.0861,-253.,.0981,-120.,.1123,0.,.0.0
TABLE 3
-10.,0.5,0.,0.5,.53,1.55,1.11,2.34,1.85,2.76,2.14,3.00
3.00,3.28,4.28,3.40,4.63,3.45,5.35,3.36,7.36,3.19
11.3,2.78,15.3,2.47,20.5,2.09,30.0,1.19,31.1,1.04
33.4,0.602,34.0,0.5,40.0,0.50
TABLE 4
-100000,0,-.001,0.,.001,1.,100000,1.
TABLE 5
-10000,1.,-.01,1.,.01,0,10000,0
TABLE 7
-100,0,1,0,2,1,100,1
RUN CONTROLS
CALCOMP PLOTS
XPLOT DIMENSION = 8.
YPLOT DIMENSION = 6.
STOP TIME=.15
MAX INTEGRATION PASSES=1E20
MINIMUM STEP SIZE=1E-30
COMPUTER TIME LIMIT=1
TERMINATE IF((UM1.LT.-1).AND.(TIME.GT.0.01))
MECHANICAL RERUN DESCRIPTION
DEFINED PARAMETERS
PON=0
END
$EOR
&
DBEND

```

# SUPER-SCEPTRE INPUT DECK AUTOMATIC CONTROL GYMNASTICATOR IMPULSE (LONG STROKE)

```

MECHANICAL DESCRIPTION
R173 RECOIL MECHANISM
FIRING WITH KNOWN ORIFACE AREA (LONG MODE)
AUTOMATIC CONTROL-FULL LEVEL2
ELUATION - 0
USE SMOOTHED GYMMER DATA (TABLE 1)
ELEMENTS
M1,1-2=X1(PUT/PGR)
R1,2-1=TABLE 1 (TIME)
R2,2-1=X2(PUT*SIN(PANG))
R3,1-2=PRDPL
R6,1-2=X7(PMU*PUT*COS(PANG))*((67.15-SM1)/14.15)
DEFINED PARAMETERS
PQAE=0.
PUT=4360
PGR=386.
PIE=X3(4.1ATAN(1.0))
PANG=X4(2.3PIE*PQAE/6400)
PAR=9.72
PP0=650
PUO=1015.
PN=1.6
PAB=32.08
PUF=.0313
PAO=TABLE 3 (SM1)
PE=X12(PRDPL-PDRDPL)
PSRDPL=70000
PSWITCH=TABLE 5 (AM1)
PXLEFT=X18(PSX-SM1)
PSU2=TABLE 7 (PXLEFT)
PCRDPL=X14(PUT*SUM1*UM1/PGR/2/PXLEFT+PUT*SIN(PANG))
PSX=35.
PCRDPL=X13((1-PSWITCH)*PSRDPL+PSWITCH*PCRDPL)
PAT=TABLE 4 (PE)
PAD=X17(PAT*PSU2)
PTAU=.01
DPAA=X16((PAD-PAA)/PTAU)
PAA=0.
PON=1
PAE=X15(PAO+PON*PAA)
PMU=0.15
PPAC=2340
PRE=X5(PAR*PP0/(1.-PAR*SM1/PUO))*PN)
PBR=X8(PAB*3*UM1*32*PUF/PAE*2./PGR)
PRDPL=X9(PRE+PPAC+PBR)
PRESS=X10(PBR/PAB)
OUTPUTS
SM1,UM1,R1
PRESS,PRDPL,PRE
PAA,PAD
PSWITCH,PDRDPL,PCRDPL
FUNCTIONS
TABLE 1
-.1,0,0,0,.0036,110000,.006,610000,.010,80000,.026,0
.0,0
.0373,-11100,.0445,-5750,.0526,-2890,.0648,-1110
TABLE 3
-10.,0.5,0.,0.5,.53,1.55,1.11,2.34,1.65,2.75,2.14,3.00
3.06,3.88,4.26,3.49,4.03,3.45,5.35,3.38,7.35,3.19
11.3,2.78,15.3,2.47,20.5,2.09,30.0,1.10,31.1,1.04
33.4,0.802,34.0,0.5,40.0,0.50
TABLE 4
-100000,0,-.001,0,.001,1.,100000,1.
TABLE 5
-10000,1.,-.01,1.,.01,0,10000,0
TABLE 7
-100,0,1,0,2,1,100,1
RUN CONTROLS
CALCOMP PLOTS
XPLOT DIMENSION = 8.
YPLOT DIMENSION = 6.
STOP TIME=.15
MAX INTEGRATION PASSES=1E20
MINIMUM STEP SIZE=1E-30
COMPUTER TIME LIMIT=1
TERMINATE IF((UM1.LT.-1).AND.(TIME.GT.0.01))
MECHANICAL RERUN DESCRIPTION
DEFINED PARAMETERS
PON=0
END
XEOR
8
DBEND

```

# SUPER-SCEPTRE INPUT DECK AUTOMATIC CONTROL GYMNASTICATOR IMPULSE (SHORT STROKE)

```

MECHANICAL DESCRIPTION
N179 RECOIL MECHANISM
PIPING WITH KNOWN ORIFACE AREA (SHORT MODE)
AUTOMATIC CONTROL-FULL LEVEL2
ELEVATION - 3
USE SMOOTHED GYMER DATA (TABLE 1)
31 IN. ALLOWABLE RECOIL
ELEMENTS
R1.1-2=X1(PUT/PGR)
R1.2-1=TABLE 1 (TIME)
R2.2-1=X2(PUTXSIN(PANG))
R3.1-2=PRDPL
R6.1-2=X7(PMUxPUTxCOS(PANG)x(67.15-SM1)/14.15)
DEFINED PARAMETERS
PQAE=0
PUT=4360
PGR=386.
PIE=X3(4.XATAN(1.0))
PANG=X4(2.XPIEXPOAE/6400)
FAR=5.72
PPQ=650
PUC=1015.
PN=1.6
PAB=32.98
PUF=.0313
PAO=TABLE 6 (SM1)
PE=X12(PRDPL-PDRDPL)
PSRDPL=90000
PSWITCH=TABLE 5 (AM1)
PXLEFT=X18(PX-SM1)
PSW2=TABLE 7 (PXLEFT)
PCRDPL=X14(PUTxUM1xUM1/PGR/2/PXLEFT+PUTXSIN(PANG))
PSX=30.2
PDRDPL=X13((1-PSWITCH)xPSRDPL+PSWITCHxPCRDPL)
PAT=TABLE 4 (PE)
PAD=X17(PATxPSW2)
PTAU=.01
DPAA=X16((PAD-PAA)/PTAU)
PAA=0.
PON=1
PAE=X15(PAO+PONxPAA)
PMU=0.15
PPAC=2340
PRE=X5(PARxPPQ/(1.-PARxSM1/PUC)xPN)
PBR=X8(PABxUM1xUM1x2xPUF/PAE/2./PGR)
PRDPL=X9(PRE+PPAC+PBR)
PRESS=X10(PBR/PAB)
OUTPUTS
SM1,UM1,R1
PRESS,PRDPL,PRE
PAA,PAD
PSWITCH,PDRDPL,PCRDPL
FUNCTIONS
TABLE 1
-.1,0.0,0.,.0036,1180000,0.008,610000,0.016,200000,0.028,0
0.0
TABLE 4
-100000,0,-.001,0,0.001,1,100000,1.
TABLE 5
-10000,1,-.01,1,0.01,0,10000,0
TABLE 7
-100,0,1,0.2,1,100,1
TABLE 6

```

# SUPER-SCEPTRE INPUT DECK

- CONTINUED -

```
-10.,0.5,0.,0.5.,00120101.,5.,009325.,5  
.33447,.95908,.387,1.0198,.3885,1.08473,.42744,1.1244,.4823,  
.5785,1.3495,.8644,1.4813,.89215,1.495,.735,1.5457,.7943,1.0  
.9039,1.7212,1.0378,1.84,1.120,1.9104,1.1008,1.064  
1.350,2.06227,1.5488,2.1099,1.821,2.2035,1.082,2.2220  
1.746,2.2577,1.853,2.2999,2.028,2.3617,2.105,2.4101  
2.276,2.4356,2.414,2.4718,2.062,2.5100,2.810,2.5802  
2.913,2.5782,3.058,2.8037,3.255,2.6350,3.504,2.8806  
3.705,2.8543,4.061,2.7318,4.132,2.7385,4.145,2.7889  
4.176,2.7261,4.193,2.7229,4.244,2.7166,4.307,2.7087  
4.409,2.8961,4.560,2.6776,4.759,2.8533,5.105,2.8119  
5.493,2.5664,6.248,2.4893,6.980,2.4005,7.337,2.3827  
7.774,2.3167,8.457,2.2463,9.119,2.1799,9.761,2.1167  
10.61,2.0382,10.92,2.0052,11.36,1.9828,11.94,1.9071  
12.91,1.8136,13.83,1.7249,14.09,1.7004,14.40,1.6699  
14.89,1.6218,15.60,1.5509,16.39,1.4793,16.82,1.4249  
17.44,1.3576,18.22,1.2690,19.46,1.1169,20.62,.8454  
21.21,.8695,21.81,.7546,22.60,.5859,23.07,.5,40.00,.5  
RUN CONTROLS  
CALCOMP PLOTS  
XPLOT DIMENSION = 8.  
YPLOT DIMENSION = 6.  
STOP TIME = .15  
MAX INTEGRATION PASSES = 1E20  
MINIMUM STEP SIZE = 1E-30  
COMPUTER TIME LIMIT = 1  
TERMINATE IF ((UM1.LT.-1).AND.(TIME.GT.0.01))  
MECHANICAL RERUN DESCRIPTION  
DEFINED PARAMETERS  
PON = 0  
END
```

### SUPER\*SCEPTRE SYMBOLS

M1	Mass of the recoiling parts (slugs)
R1	Breech force ( $lb_f$ )
R2	Weight force component ( $lb_f$ )
R3	Rodpull ( $lb_f$ )
R6	Sliding friction ( $lb_f$ )
PQAE	Angle of elevation (mils)
PWT	Weight of recoiling parts ( $lb_f$ )
PGR	Gravitational constant ( $in./s^2$ )
PIE	$\pi$ (constant)
PANG	Angle of elevation (radians)
PAR	Area of recuperator piston ( $in.^2$ )
PPO	Initial pressure of recuperator (psi)
PVO	Initial volume of recuperator ( $in.^3$ )
PN	Polytropic exponent for recuperator gas
PAB	Total area of brake pistons ( $in.^2$ )
PWF	Weight density of fluid ( $lb/in.^3$ )
PAO	Equivalent orifice area ( $in.^3$ )
PE	Error between actual and desired rodpull
PSRDPL	Initial value, desired rodpull ( $lb_f$ )
PSWITCH	Switching function
PXLEFT	Amount recoil distance remaining (in.)
PSW2	End of recoil control function
PCRDPL	Calculated desired rodpull ( $lb_f$ )
PSX	Maximum recoil length (in.)
PDRDRL	Desired rodpull ( $lb_f$ )

PAT	Servo valve desired area (in. <sup>2</sup> )
PAD	Desired servo valve area with end of recoil control function
PTAU	Servo valve time constant (sec)
DPAA	Differential equation for actual valve area
PAA	Initial value of valve area (in. <sup>2</sup> )
PON	Flag for automatic control (1 = on)
PAE	Total brake orifice area (in. <sup>2</sup> )
PMU	Coefficient of friction
PPAC	Packing friction force (lb <sub>f</sub> )
PRE	Recuperator force (lb <sub>f</sub> )
PBR	Brake force (lb <sub>f</sub> )
PRDPL	Total rod pull (lb <sub>f</sub> )
PRESS	Brake hydraulic pressure (lb/in. <sup>2</sup> )
SM1	Recoil distance (in.)
VM1	Recoil velocity (in./s)
AM1	Recoil acceleration (in./s <sup>2</sup> )
Table 1	Smoothed gymnasticator data
Table 2	M203 charge breech force profile
Table 3	Long recoil-existing orifice area versus recoil distance
Table 4	Servo valve area desired versus error (PE)
Table 5	Switching function versus acceleration
Table 6	Short recoil-existing orifice area versus recoil distance
Table 7	End of recoil control function versus distance left

DISTRIBUTION LIST

Commander  
Armament Research and Development Center  
U.S. Army Armament, Munitions  
and Chemical Command  
ATTN: SMCAR-TSS (5)  
SMCAR-LC  
SMCAR-LCA  
SMCAR-LCE  
SMCAR-LCM  
SMCAR-LCN  
SMCAR-LCS  
SMCAR-LCU  
SMCAR-LCW (15)  
Dover, NJ 07801-5001

Administrator  
Defense Technical Information Center  
ATTN: Accessions Division (12)  
Cameron Station  
Alexandria, VA 22314

Director  
U.S. Army Materiel Systems  
Analysis Activity  
ATTN: DRXSY-MP  
Aberdeen Proving Ground, MD 21005-5066

Commander  
Chemical Research and Development Center  
U.S. Army Armament, Munitions  
and Chemical Command  
ATTN: SMCCR-SPS-IL  
Aberdeen Proving Ground, MD 21010-5423

Commander  
Chemical Research and Development Center  
U.S. Army Armament, Munitions  
and Chemical Command  
ATTN: SMCCR-RSP-A  
Aberdeen Proving Ground, MD 21010-5423

Director  
Ballistic Research Laboratory  
ATTN: AMXBR-OD-ST  
Aberdeen Proving Ground, MD 21005-5066

Chief  
Benet Weapons Laboratory, LCWSL  
Armament Research and Development Center  
U.S. Army Armament, Munitions  
and Chemical Command  
ATTN: SMCAR-LCB-TL  
Watervliet, NY 12189-5000

Commander  
U.S. Army Armament, Munitions  
and Chemical Command  
ATTN: AMSMC-LEP-L  
Rock Island, IL 61299-6000

Director  
U.S. Army TRADOC Systems  
Analysis Activity  
ATTN: ATAA-SL  
White Sands Missile Range, NM 88002

Assistant Secretary of the Army  
Research and Development  
ATTN: Department for Science  
and Technology  
The Pentagon  
Washington, DC 20315

Commander  
U.S. Army Materiel Command  
ATTN: AMCDE-SG  
5001 Eisenhower Avenue  
Alexandria, VA 22304

Commander  
U.S. Army Electronics Command  
ATTN: Technical Library  
Ft. Monmouth, NJ 07703

Commander  
U.S. Army Mobility Equipment Research  
and Development Command  
ATTN: Technical Library  
Ft. Belvoir, VA 22060

Commander  
U.S. Army Tank-Automotive Research  
and Development Command  
ATTN: DRSTA-TSL, Tech Library  
Warren, MI 48090

Commander  
U.S. Military Academy  
ATTN: MADN-F, Dept of Engineering (10)  
West Point, NY 10996-1779

Commander  
U.S. Army Missile Command  
ATTN: Documents Section, Bldg 4484  
Redstone Arsenal, AL 35898

Commander  
Rock Island Arsenal  
ATTN: SMCRI-ENM, Mat Sci Div  
Rock Island, IL 61299-5000

Commander  
HQ, U.S. Army Aviation School  
ATTN: Office of the Librarian  
Ft. Rucker, AL 36362

Commander  
U.S. Army Foreign Science  
and Technology Center  
ATTN: DRXST-SD  
220 7th Street, N.E.  
Charlottesville, VA 22901

Commander  
U.S. Army Materials and Mechanics  
Research Center  
ATTN: DRXMR-PL, Tech Library (2)  
Watertown, MA 02172

Commander  
U.S. Army Research Office  
ATTN: Chief IPO  
P.O. Box 12211  
Research Triangle Park, NC 27709

Commander  
Harry Diamond Laboratories  
ATTN: Technical Library  
2800 Powder Mill Road  
Adelphia, MD 20783

Director  
U.S. Naval Research Laboratory  
ATTN: Director, Mech Div  
Code 26-27 (DOC Library)  
Washington, DC 20375

Mechanical Properties Data Center  
Battelle Columbus Laboratory  
505 King Avenue  
Columbus, OH 43201

Commander  
Naval Surface Weapons Center  
ATTN: Technical Library  
Code X212  
Dahlgren, VA 22448